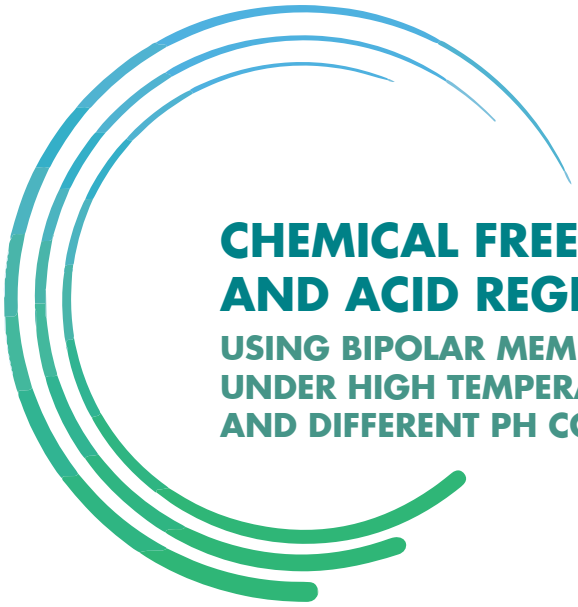

CHEMICAL FREE AMMONIUM RECOVERY AND ACID REGENERATION

USING BIPOLAR MEMBRANE ELECTRODIALYSIS UNDER HIGH TEMPERATURE, HIGH CONCENTRATION AND DIFFERENT PH CONDITIONS

Master Thesis

Eline van Berlo

April, 2021

Chemical free ammonium recovery and acid regeneration using bipolar membrane electrodialysis under high temperature, high concentration and different pH conditions

Showing the potential of BPMED technology for ammonium and sulfate removal, in situ generation of sulfuric acid and production of ammonium hydroxide, creating opportunities for sustainable nitrogen (re-)use in the industrial cycle

by

Eline Maria Clazina van Berlo

to obtain the degree of Master of Science in Civil Engineering
at the Delft University of Technology,
to be defended publicly on Friday April 23, 2021 at 11:00 AM.

Student number:	4498216	
Project duration:	September 1, 2020 – April 23, 2021	
Thesis committee:	Dr. Ir. Henri Spanjers	TU Delft, chair
	Prof. Dr. Ir. Jules van Lier	TU Delft
	Dr. Ir. David Vermaas	TU Delft
	Ir. Dhavissen Narayen	TU Delft, daily supervisor

TU Delft

Abstract

The abundant presence of nitrogen in natural waters can be a threat to both humans and environment. Therefore, municipal and industrial wastewater streams need to be treated before their disposal in the environment. Currently used biological and physical-chemical treatment methods have drawbacks such as high greenhouse gas emissions, high energy use and high use of chemicals. This research used bipolar membrane electrodialysis (BPMED) as a technology for the removal of ammonium sulfate ($(NH_4)_2SO_4$) from industrial wastewaters with extreme characteristics. The industrial stripper/scrubber system removing nitrogen from industrial waters creates an ammonium sulfate rich water stream with a pH of 2, a temperature of 70 °C and concentrations up to 250 g/L. The study investigated the influence of a low pH, high concentration and high temperature on the removal of ammonium (NH_4^+) and sulfate (SO_4^{2-}) from wastewater and in situ generation of sulfuric acid and production of ammonium hydroxide.

Key performance parameters to measure the influence of these extreme conditions were the efficiency of nitrogen removal in the form of ammonium (NH_4^+ **current efficiency** and NH_4^+ **removal efficiency**) and sulfate removal (SO_4^{2-} **removal efficiency**). More key performance parameters were the consumed energy for this removal in the form of **electrochemical energy consumption**, the **purity** of the generated acid and base and the **final** NH_4^+ **concentration in the base** and the SO_4^{2-} **concentration in the acid**.

Model wastewater with a pH between 2 and 10, a concentration between 50 - 250 g/L ammonium sulfate $(NH_4)_2SO_4$ and with a temperature between 20 °C and 40 °C was treated with BPMED. The influence of pH, concentration and temperature was researched independently in experiments of 180 minutes, after which the removal efficiency and the quality of the produced acid and base were assessed.

First, the BPMED functionality at different diluate pH was assessed. The electrochemical energy consumption for NH_4^+ transportation decreased with increasing pH of wastewater within the acidic range with a pH between 2 and 5. The NH_4^+ current efficiency increased with increasing pH, with a NH_4^+ current efficiency of 54% for wastewater with pH 5. The purity of the generated sulfuric acid reduced slightly to 86%, while the purity of the ammonium hydroxide improved to 96%. The removal efficiency of both ammonium and sulfate increased with pH, with 95% ammonium removal (13 g ammonium removed from original diluate) and 92% sulfate removal (33.4 g sulfate removed from original diluate) for pH 5. The better performance with increasing pH for the pH range between pH 2 and 5 can be explained by a reduced competition between H^+ ions and NH_4^+ ions with increasing pH, resulting in a smaller energy use for a higher ammonium removal. Sulfate removal improved with increasing concentration due to the smaller fraction of SO_4^{2-} present in the HSO_4^- form for pH 5, since HSO_4^- is experiencing less electrical driving force to leave the diluate than SO_4^{2-}.

In the high pH range between pH 6 and 10, an increasing pH showed a decrease in electrochemical energy consumption for NH_4^+ transportation as well as a marked increase in NH_4^+ current efficiency. The sulfuric acid purity declined to 77%, while the purity of the produced base slightly raised to 97%. The efficiency of ammonium removal decreased to 80% (51.9 g) and the sulfate removal increased to 99% (36 g). The higher ammonium removal with higher pH was because of 1) less competition between NH_4^+ and H^+ at pH 10, 2) a higher concentration gradient between diluate and base resulting in dissolved ammonia diffusion and 3) more ammonia volatilization resulting in losses at pH 10. Looking into theoretical explanations for the increased sulfate removal at higher pH is recommended for future research. Enhanced water splitting resulted in a higher energy consumption for higher pH.

Secondly, the influence of diluate concentration on BPMED treatment was investigated. With rising initial ammonium sulfate ($(NH_4)_2SO_4$) concentration, the electrochemical energy consumption for transport of NH_4^+ decreased, while the NH_4^+ current efficiency increased to 74% for 250 g/L $(NH_4)_2SO_4$ wastewater. The purity of both acid and base decreased with higher concentrations to a 83% acid and a 90% base for 250 g/L $(NH_4)_2SO_4$. The amount of ammonium removed increased with concentration, with 12.9 g ammonium removal (94%) for 50 g/L $(NH_4)_2SO_4$ synthetic wastewater and 17.8 g (26%) ammonium removal for 250 g/L $(NH_4)_2SO_4$. Sulfate removal dropped with increasing wastewater concentrations, with 34.4 g (95%) sulfate removal for 50 g/L $(NH_4)_2SO_4$ and 21.7 g removal for 250 g/L $(NH_4)_2SO_4$. The higher ammonium removal finds its origin in the increasing ammonia diffusion and co-ion leakage. The smaller sulfate removal with increasing concentration could be influenced by the low activity of sulfatesalts or due to ion pair formation, but the exact reasoning behind the increased sulfate removal remains uncertain.

Lastly, the effect of temperature on the BPMED functionality was researched. A lower electrochemical energy consumption for NH_4^+ removal was observed with increasing wastewater temperature. The NH_4^+ current efficiency elevated slightly to 61% for wastewater of 40°C. Both acid and base purity showed a decrease with increasing temperature, with a produced acid of 85% for 20°C and acid of 79% for 40°C. The purity of the base decreased with a purity of 97% for 20°C to 91% purity for 40°C. The removal of both ammonium and sulfate increased with increasing temperature, with the highest removal of ammonium (90% - 12.2 g) and sulfate (94% - 34.2 g) at 40°C. With higher temperature, higher ammonia diffusion was observed, explaining the improved NH_4^+ removal and the lowered purity of both acid and base. The smaller proton leakage from acid to diluate at higher temperature resulted in less competition between NH_4^+ and H^+ for removal, which could explain the higher sulfate removal with higher temperature. The higher ammonium removal due to less proton leakage at 40°C forced SO_4^{2-} ions to leave the diluate too.

The possibility to treat ammonium sulfate rich waters with extreme characteristics by BPMED is successfully demonstrated. Industrial wastewater streams with acidic pH, high concentrations up to 250 g/L and high temperatures up to 40°C could be treated on laboratory scale with only limited energy use. The functionality of BPMED under these extreme conditions makes this technology an interesting alternative for current treatment technologies treating nitrogen-rich streams. The high purity acid can be internally used in the stripper/scrubber system, creating a chemical free, circular nitrogen removal process. The produced ammonium hydroxide can be economically attractive for selling for the production of fertilizer or can be used in another application in the chemical industry. BPMED is a functional method even under extreme conditions and could create opportunities in other wastewater treatment processes with extreme characteristics.

Graphical Abstract

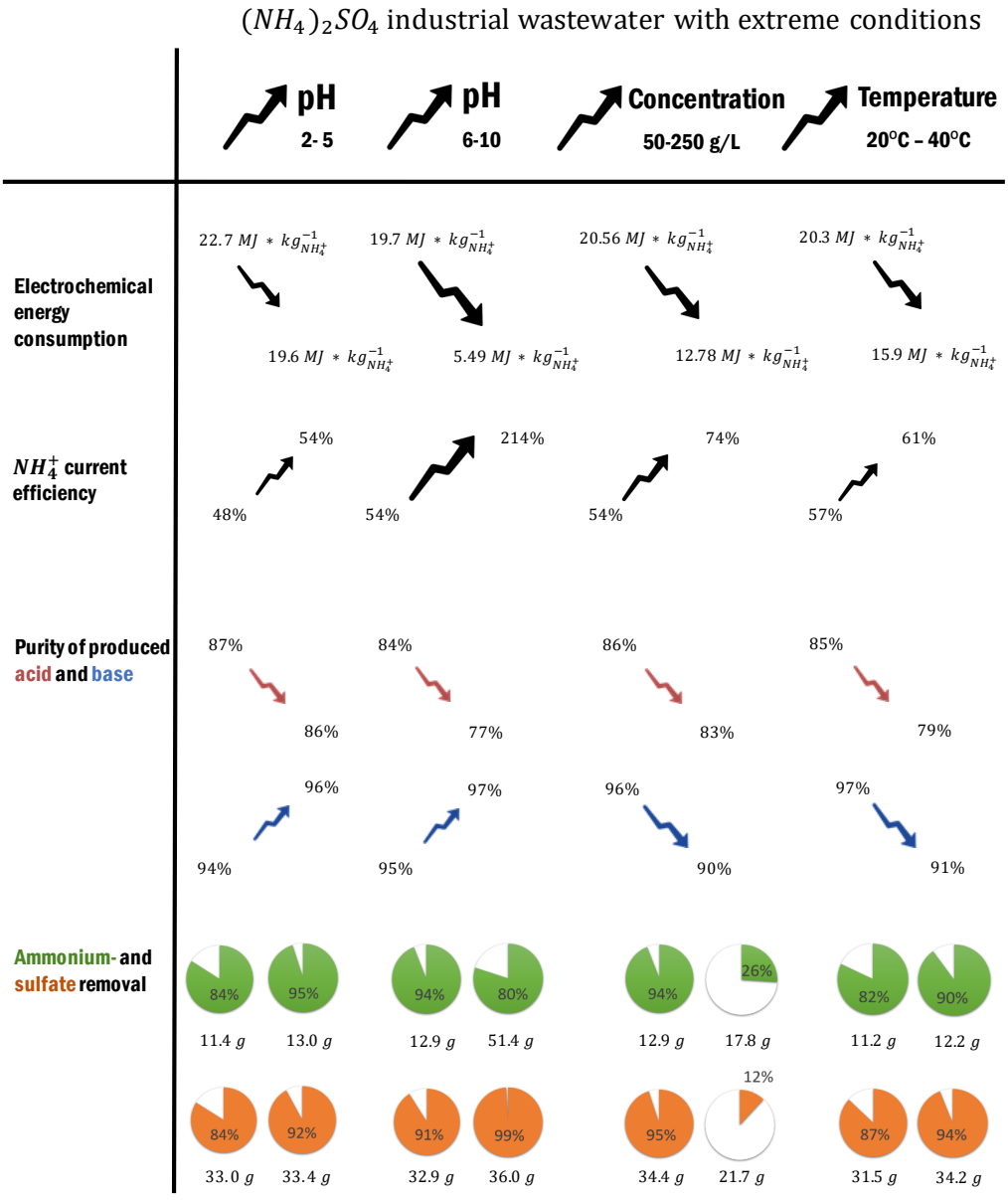

Acknowledgements

There have been a lot of people that supported me during the process of writing this thesis without whom it would never have been as much fun! I would like to thank you all!

First of all, I wish to thank my daily supervisor Dhavissen Narayen for his help and encouragement during my thesis. For answering all my questions and always being patient with me, but also for your guidance during this exploration of the new world of research. I would like to express my gratitude towards Dr. Ir. HenRi Spanjers, chair of my committee, for your guidance during my graduation process and for always providing help and feedback when I needed it. I would also like to thank the other members of my committee. Thanks Prof. Dr. Ir. Jules van Lier and Dr. Ir David Vermaas for making time for me and for providing useful comments, suggestions and motivation!.

Besides that, I would like to express my gratitude towards the whole Waterlab community (and visitors). The coffeebreaks and lunches during which one of us had to run to take a sample were unforgettable. For me it felt like a really supportive environment, both during good but also during more difficult times. Tobias, thanks for your help at the start and for being involved during all phases of my thesis. Thank you Ben, for the beautiful paintings in my lab book. Thank you Armand and Patricia for your technical support.

Of course my gratitude goes to the proofreaders of my report, during different stages of writing it; Thank you Asiman Dash, Jente and Roos for your useful comments and advice. Thank you Romee, for helping me with the visuals!

Besides academic guidance, I was so lucky to have a great group of people that helped me through this thesis on a social level. All amazing people I met at the masters Environmental Engineering and Watermanagement made the last 2.5 years to an unforgettable period of my life. My roommates of Huize Gsus were always there to provide good food, company, skating sessions, the bongo and parties to distract me (in a positive way) from my computer. Thank you so much for offering a listening ear!

Thank you Jeanne, for the unlimited borrels, thank you Stijn, for always putting a smile on my face and thank you Waifies, Diehard Farmachicks+1, Knapperds and Alpha for the support and fun during the past 7 months! Marit, I know you were struggling sometimes as well, but you were always ready for a call or a walk, thanks! Thank you Roos, for being my parasite and chasing me during my whole (career) path :). It wouldn't have been the same without you! Looking forward to many more adventures to come!

Dankjewel lieve Wessel, voor je positiviteit en al het leuke (onverwachtse) vermaak!

Lieve papa en mama, Bas en Thijs, bedankt voor jullie oneindige support! Ook tijdens deze thesis was het zo fijn om te weten dat er thuis altijd een een lekker bordje eten, vers gebakken taart of opbeurende woorden voor mij klaar stonden, of gewoon even uitwaaien tijdens een fietstocht! Ik hoop dat ik jullie trots heb gemaakt!

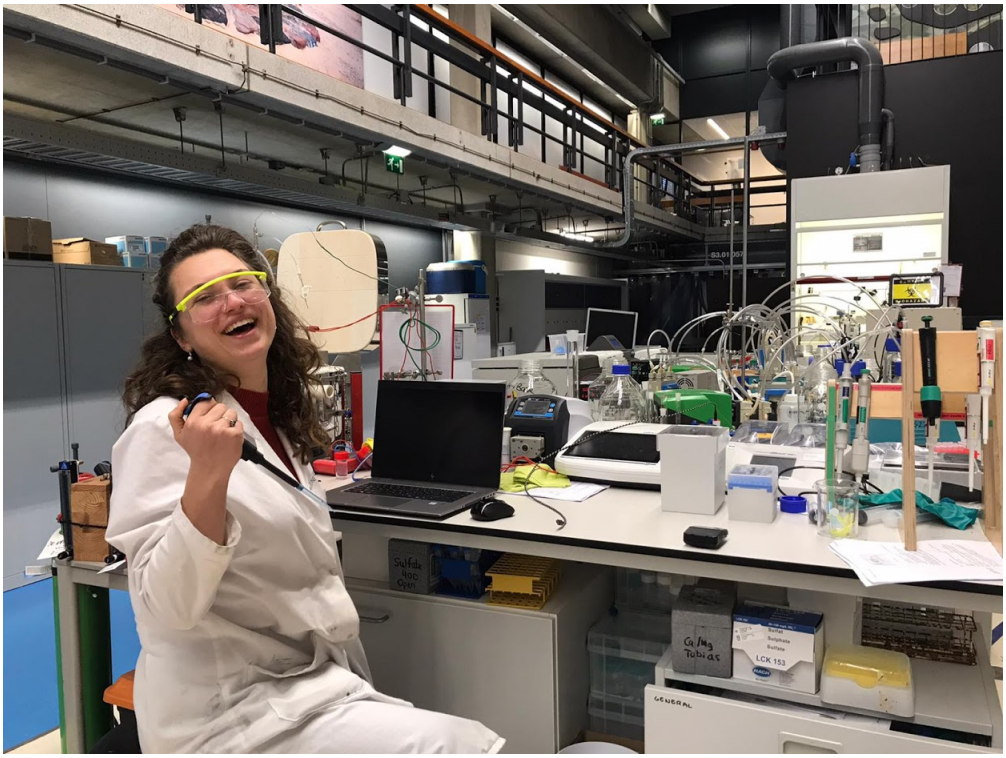

Figure 0.1: Me having fun in my natural habitat!

Nomenclature

Salts and ions

NH_3	Ammonia
NH_4^+	Ammonium
NH_4OH	Ammonium hydroxide
$(NH_4)_2SO_4$	Ammonium sulfate
OH^-	Hydroxide ion
NO_x	Nitrogen oxides
NO_3^-	Nitrate
N_2O	Nitrous oxide
H^+	Proton
Na_2SO_4	Sodium sulfate
SO_4^{2-}	Sulfate
H_2SO4	Sulfuric acid

Symbols and abbreviations

α	Membrane permselectivity
a	Activity
A	Effective membrane surface area
AEM	Anion Exchange Membrane
$AEEM$	Anion Exchange End Membrane
$BPMED$	Bipolar Membrane Electrodialysis
C	Concentration (mol/L or g/L)
CEM	Cation Exchange Membrane
$CEEM$	Cation Exchange End Membrane
CP	Concentration Polarization
D	Diffusion coefficient ($m^2 \cdot s^{-1}$)
DBL	Diffusive boundary layer
$\eta_{NH_4^+}$	NH_4^+ Current efficiency (unitless)
EC	Electrical Conductivity ($\mu S \cdot cm^{-1}$)
E_e	Electrochemical energy consumption (J $\cdot g{-}N^{-1}$)
ED	Electrodialysis
F	Faraday constant ($= 96.485\ C \cdot mol^{-1}$)
γ	Activity coefficient (-)
i	Electrical current density ($A \cdot m^{-2}$)
$I_{\Delta t}$	Average electric current during each time interval ($A = C \cdot s^{-1}$)
IEM	Ion Exchange Membrane
J	Ion flux ($mol \cdot m^{-2} \cdot min$)
LCD	Limiting current density ($A \cdot m^{-2}$)
M	Mass (kg)
N	number of cell triplets in the BPMED membrane stack (unitless, in this case N = 10)
$n_{NH_4^+}$	Amount of NH_4^+ transported (depleted) from the diluate (mol)
$m_{NH_4^+}$	amount of transported NH_4^+ from diluate (g-N)
P	Permselectivity
ϕ	Electrochemical potential (V)
R	Universal gas constant ($J \cdot K^{-1} \cdot mol$)

R	Resistance (Ω)
$SOFC$	Solid oxide fuel cell
Δt	Time interval (seconds or minutes)
T	Temperature (K)
$U_{\Delta t}$	Average electric potential during each time interval (V)
V	Volume (L)
$WWTP$	Wastewater treatment plant
x	distance (m)
z	Ion valence (1 for NH_4^+)

Contents

List of Figures

List of Tables

1 Introduction

1.1 Nitrogen in the Environment - Problem or Opportunity

1.1.1 The problem of nitrogen in the environment

Nitrogen (N) is the fourth most abundant element in cellular biomass and it comprises, in the form of N_2, about 78% of earth's atmosphere [5, 6]. Naturally, only small amounts of fixed nitrogen (N_2 converted into ammonia (NH_3), ammonium (NH_4^+), nitrate (NO_3) or another nitrogen oxide) are present on planet earth, since nitrogen largely remains locked in the atmosphere [7]. Until the discovery of the Haber-Bosch process in 1909, nearly all the reactive nitrogen in the biosphere was fixed and recycled by nitrogen-fixing soil bacteria like *Rhozobium*, working together with plant roots to fixate nitrogen for nourishing the soil and thereby making nitrogen available to the rest of life. This resulted in a balanced nitrogen cycle on earth [2, 5, 8]. The Haber-Bosch process is the industrial fixation of N_2 into ammonia (NH_3). Since fixed nitrogen is crucial for the growth of plants, it is often supplied in the form of ammonia (NH_3) as a fertilizer. These synthetic fertilizers enable farmers to transform infertile lands into fertile fields which resulted in a quadrupled productivity of agricultural crops, resulting in a global population rise from 1.6 billion to 6 billion in the 20th century [5, 8, 9].

The excessive use of fertilizers containing NH_3 to provide food security for the growing world population, the production of reactive nitrogen during the combustion of fossil fuels and other reactive nitrogen producing processes result in the injection of NH_3 in the environment at an accelerating pace [8]. Industrial production of reactive nitrogen was about 43 Tg (million tons) per year in 2008, of which 75% was used as fertilizer and 25% was used in the chemical industry [10]. Currently, the release of nitrogen in the environment by human activity is under a heavy debate, since it can lead to environmental and health issues. Measures in the Netherlands to lower ammonia emissions by farmers and construction companies have led to protests [9]. Half of the produced NH_3 eventually ends up in the environment, which is associated with threats to water quality, air quality, greenhouse gas balance, ecosystems and biodiversity and soil quality [10]. Harmful algal blooms and eutrophication, coastal dead zones and acidification of soils could lead to an increased loss of trace nutrients and to the release of heavy metals from the ground into the drinking water sources [11] [8].

Additionally, increasing amounts of nitrous oxide are released into the atmosphere because of excessive fertilizer use. Nitrous oxide is produced during biological wastewater treatment, contributing to global warming. Nitrous oxide has a more than 300-fold greater potential for global warming effects than carbon dioxide, with an actual impact of N_2O on global warming that has been estimated up to 10% of total greenhouse gas emissions [12, 13]. Lately, the loss of biodiversity and the linkage to several human diseases like methemoglobinemia in infants and several cancers because of high nitrate concentrations in water are of rising concern [7, 8, 11]. The overall environmental costs of all nitrogen losses in Europa are estimated at €70 - €320 billion per year at current rates which outweighs the direct economic benefits of nitrogen in agriculture. The highest costs for society due to nitrogen emissions are associated with loss of air quality and water quality [10].

1.1.2 Opportunities with nitrogen

To prevent negative side effects for human and environmental health, but to keep in mind global population growth and the industrial, agricultural and economical benefits of NH_3 use, it is extremely important that wastewater both from industries and municipalities is treated before being released back

into the environment. Fortunately, the recovery of Total Ammoniacal Nitrogen TAN (dissolved NH_3 and NH_4^+) from wastewater creates enormous potential for reuse of NH_3. NH_3 is one of the most used inorganic chemicals in the world. This chemical is already widely used in industrial applications; NH_3 is used in the application as fertilizer, providing reliable food supply to malnourished regions [8]. This application of NH_3 use accounts for 80% of the global NH_3 consumption. It is also used in the production of acrylonitrile for acrylic fibers and plastics, hexamethylenediamine for nylon 66, caprolactam for nylon 6, isocyanates for polyurethanes and hydrazine, and various amines and nitriles. Additionally, TAN can be recovered from residual waters and the NH_3 can be used for the generation of electrical and thermal energy in a solid oxide fuel cell (SOFC) [14, 15]. During 2020–25, world apparent consumption of ammonia is forecasted to grow by about 12.9% [16]. The global ammonia supply/demand balance is expected to move toward a surplus, as future capacity additions will continue to outpace consumption. Ammonia capacity is increasing primarily in areas where the availability and cost of natural gas are lower, the United States and the Middle East in particular. This comes together with the expected population growth, resulting in increasing demand for fertilizer to assure food production. Science and understanding on how nitrogen can be converted into a form that is useful to government, industry and society is is one of the key challenges of this time [10].

1.2 Current Nitrogen Removal from Industrial and Municipal Wastewaters

Industrial and municipal wastewaters containing ammoniacal nitrogen are treated before discharge, which prevents environmental and human damage. In this section, the conventional way of treating this ammonium rich waters is discussed.

1.2.1 Biological nitrogen removal

There are several treatment options for the removal of TAN from wastewater streams of which one is biological treatment. Biological treatment for nitrogen removal is traditionally performed by the energy intensive nitrification-denitrification process, which converts ammonia aerobically to nitrate (nitrification) and in the second step nitrates are converted to N_2O or N_2 under anoxic conditions (denitrification) [17, 18]:

Nitrification:

$$NH_4^+ \longrightarrow NO_2 \longrightarrow NO_3^- \tag{1}$$

Denitrification:

$$NO_3^- \longrightarrow NO_2 \longrightarrow NO \longrightarrow N_2O \longrightarrow N_2 \tag{2}$$

With the recently developed anammox biological treatment, nitrogen is removed by the following reaction [12]:

$$NH_4^+ + NO_2 \longleftrightarrow N_2 + 2H_2O \tag{3}$$

During heterotrophic denitrification, N_2O can be emitted [12, 19].

1.2.2 Physiochemical nitrogen removal

In addition to biological treatment, physiochemical treatment can be performed to remove TAN from wastewater. Physiochemical methods can be based on the ionexchange principle and electrodialysis membranes. Physiochemical treatment has lower undesirable emissions compared to biological treatment, but on the contrary needs the addition of substantial amounts of salts for regeneration [2, 20]. One example of a physiochemical water treatment method is the stripper/scrubber system which is widely used in industrial and municipal wastewater treatment [20]. This system is currently used to remove components which are harmful to the environment, like NH_3, from waste (air) streams and thereby producing an ammonium sulfate waste stream.

1.2.3 Electrodialysis with bipolar membranes - current applications

In this thesis, the use of BPMED for the treatment of ammonium sulfate rich wastewaters with extreme characteristics was investigated. The oldest industrial application of BPMED is the recovery of HF (Hydrogen fluoride) and HNO_3 (nitric acid) from a stream generated by a pickling bath in a steel plant [21]. BPMED is often used as an alternative method to electrolysis for the generation of H^+ and OH^- ions, and it can be used to generate acids and bases from salts without the production of oxygen and hydrogen gases [21]. The configuration of the bipolar membrane electrodialysis process depends on the application. The technology is currently used to produce acids and bases from a concentrated salt stream such as Na_2SO_4, for the recovery of concentrated acids like H_2SO_4 and $NaOH$ [21, 22]. Bipolar membranes are not only used in environmental control, but can also be used in chemical processing. A promising application is the recovery of organic acids from fermentations [23].

1.2.4 Electrodialysis for (sulfuric) acid and (ammonium hydroxide) base production

Treating an ammonium sulfate waste stream from the stripper/scrubber process with the physiochemical treatment BPMED is of interest, since this combination could in theory be able to sustainably remove NH_4^+ from industrial reject waters and simultaneously produce acid that can be reused in the stripper/scrubber system. The BPMED technology makes it possible to change the solution pH in situ by only using electrical energy, without the addition of chemicals [22, 24]. Sulfuric acid (H_2SO4) is currently often added to the scrubber for changing its pH. The combination of the stripper/scrubber system and BPMED for the removal of ammonium sulfate $(NH_4)_2SO_4$) from reject waters could have both positive financial and sustainable implications(Figure 1.1. Sulfuric acid has a higher market value than ammonium sulfate, which asks for a smaller use of sulfuric acid to make the system profitable. A circular system can be designed, in which sulfuric acid produced from the BPMED technology can be re-used in the stripper/scrubber system to lower the pH. With this fusion of technologies, the addition of external/additional chemicals is prevented and a circular loop can be created for the removal of ammonium salts from industrial and municipal wastewaters and the creation of a valuable ammonium rich stream.

Sulfuric acid and ammonia generation by BPMED was performed before by Zhang et al. [25] . They found that it was feasible to regenerate sulfuric acid and ammonia and they described the water and ion transport trough anion exchange membranes with empirical models [25]. The paper of Nowak et al. describes the possibility of conversion of waste sodium sulfate to sulfuric acid and sodium hydroxide by bipolar membrane electrodialysis [26].

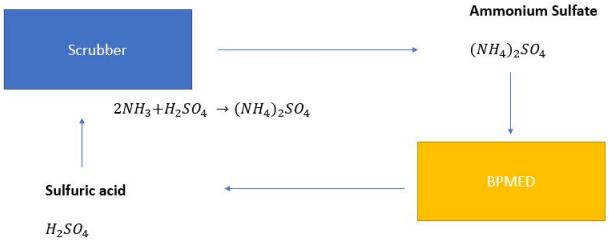

Figure 1.1: Simplistic representation of the theoretical scrubber/BPMED combination. The produced ammonium hydroxide (not shown in this figure) can be used for selling purposes.

1.3 NoChemNAR Project/ Industrial Relevance

This Master's thesis project looks into one aspect of the bigger NoChemNAR project and should therefore be treated confidentially. NoChemNAR stands for Chemical Free Ammonium Recovery. The NoChemNAR project has the goal to develop a combination of a stripper/scrubber technology and the BPMED technology for the treatment of reject waters under environmentally friendly and sustainable conditions. The focus will be on the use of BPMED to convert ammonium sulfate to ammonium hydroxide, by which sulfuric acid is created which can be re-used in the scrubber, see Figure 1.2. This potential system results in two benefits; ammonium sulfate is removed from wastewater and expenditures on sulfuric acid addition for the scrubbers are reduced/prevented. The eventual, broader focus of the developed technology is on the cheaper production of renewable energy. The NoChemNAR project is a cooperation between TU Delft and Nijhuis Industries and several additional organizations and companies which together combine knowledge, resources and services to reach their common goal [27].

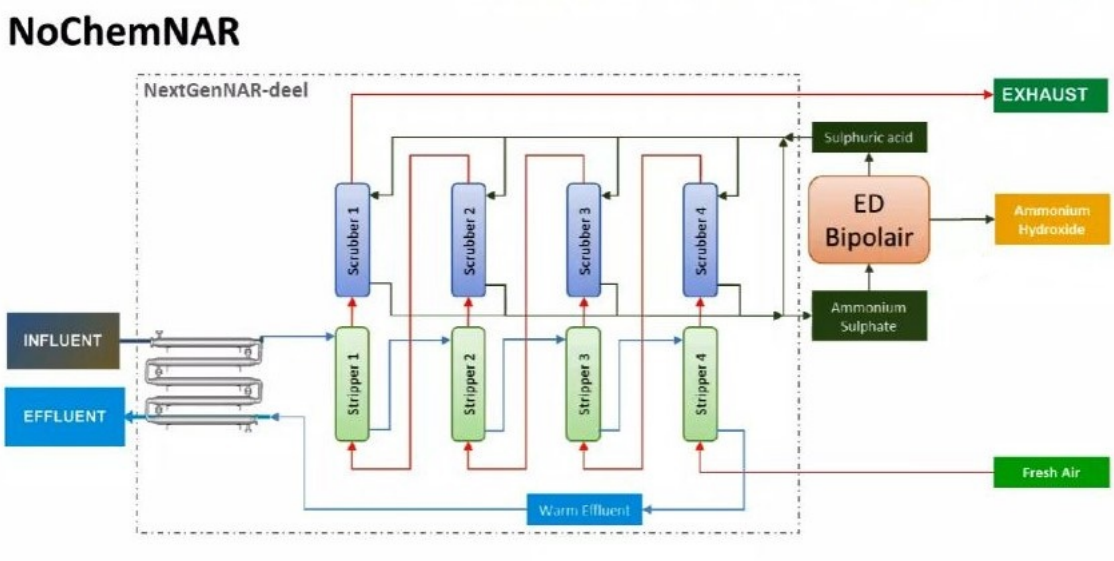

Figure 1.2: Goal of the NoChemNAR project, creating a circular system of a stripper/scrubber with BPMED technology for the removal of nitrogen from industrial waters. The ammonium sulfate BPMED feed water is considered to be very pure without other components dissolved.

1.3.1 The value of sulfuric acid

Committing to the NoChemNAR mission to create a circular system for ammonium recovery, the generated sulfuric acid can be used in situ (Figure 1.1). This circular loop of sulfuric acid would prevent the purchase and therefore expenses on additional sulfuric acid. The current market price for sulfuric acid is between 210 $ and 335 $ per ton, depending on the purity [28]. However, the price is expected to increase, because of increasing demand. The global sulfuric acid market was found to be 10.22 $ billion in 2020 and is expected to grow up to a 12.36 $ billion market in 2027, mostly due to population growth, needing an increase in fertilizers to ensure food security [29]. Therefore, the NoChemNAR would become even more relevant in the future, creating a circular sulfuric acid loop.

1.3.2 The value of ammonium hydroxide

Ammonium hydroxide is ammonia dissolved in water and therefore its second name is Aqua Ammonia [30]. Ammonium hydroxide finds its application across different industries such as the chemical, food and beverage, personal care and pharmaceutical industry [31]. It is often used as a cleaning agent in households and industry, but it can also be used in the manufacturing of products such as fertilizer, plastic, rayon and rubber [32]. The ammonia market in general is expected to follow a rising trend due to the growing fertilizer growth [33]. The aqua ammonia market will reach a 591.4 $ million market size by 2025, from 556 $ million in 2019 [34]. Ammonia solution/ammonium hydroxide with a purity between 20-28% has a price of 180-240 $ per ton [35].

1.4 Knowledge gaps in BPMED Treatment of Ammonium Sulfate Streams

The BPMED technology is known for being economically attractive and it has multiple interesting industrial applications [21]. However, large-scale technical use of bipolar membranes has been rather limited by the availability of efficient membranes [4]. On top of that, treatment of ammonium sulfate streams with non-industrial characteristics with BPMED was only little researched before [25]. Scrubber/stripper effluent ammonium sulfate rich streams were not found to be treated before with the BPMED technology. This section guides you through the existing knowledge and the still present knowledge gaps on influence of pH, concentration and temperature on the functionality of BPMED.

1.4.1 Optimum pH for BPMED technology

The scrubber effluent is known to have a pH in a range between pH 2 and 3. The BPMED technique currently used for ammonium recovery is however only known to function between a pH of 7.9 and 9.8 [36]. Therefore, the functioning of BPMED for treatment of wastewater with low pH is of interest. In literature, very limited information can be found on the influence of pH on the functioning of the BPMED system. Chen et al. stated that it is not wise to operate the BPMED at very high pH in the coupled system of BPMED and MFC (microbial fuel cell), due to the functional group degradation of the bipolar membrane and the limitation of electroosmosis and co-ion/counter-ion migration [37, 38]. Ben Ali et al. used a salt solution of NH_4NO_3 acidified to pH<3, which was necessary to avoid blocking the AW membranes (Anion exchange membrane - Solvay). The research concluded that the main factors affecting the current efficiency are acid and ammonia concentrations [39]. In conclusion, the influence of pH on the functioning of the BPMED system for ammonium removal is unknown and therefore investigated in this research.

1.4.2 Influence of concentration on BPMED treatment

The industrial effluent of the stripper scrubber system can contain ammonium sulfate concentrations up to 250 g/L. Ammonium removal with BPMED from water streams has been researched before, although this research worked with diluate streams containing 1.5 g/L ammonium [36]. However, the influence of higher concentrations of ammonium was not researched before [25]. Besides the unknown effect of high ammonium concentrations on the BPMED functionality, on the effect of treatment of sulfate waters even less research is performed. Kroupa et al. describes about the recovery of sulfuric acid with a purity ranging between 71.9% and 83.3% from treatment of sodium sulfate containing water by electrodialysis with heterogeneous bipolar membranes [40]. Sulfate itself does not directly threat the environment, since sulfate is a chemically inert, non-volatile and nontoxic compound [41]. However, under anaerobic conditions it can be biochemically converted to H_2S. On top of that, high sulfate concentrations can cause an imbalance in the natural sulfur cycle [42]. Sulfate's ionic radius is 0.242 nm, which is relatively large compared to e.g. protons with a radius of 0.84-0.87 fm [43]. Consequently, more difficulties might be expected with sulfate passing the membranes than for smaller ions. This could lead to a higher energy consumption of the BPMED. The functionality of BPMED for treating ammonium sulfate solutions up to 40 g/L ammonium sulfate was tested before and found to be feasible, but on higher concentrations, to the best of our knowledge, no research was performed [25]. In this research, ammonium sulfate concentrations up to 250 g/L are treated with BPMED and its functionality is evaluated.

1.4.3 Influence of temperature on BPMED

Currently, the water leaving the stripper/scrubber system has a temperature of about 70 °C (363K). However, previous research done on the NH_4^+ current efficiency with BPMED from reject streams was done at room temperature [36]. It is known that the temperature has an influence on the form in which ammoniacal nitrogen can be present in the water [36]. Additionally, it was found that the operating temperature is of influence on the physico-chemical properties of the membrane and on its lifetime [44]. Kroupa et al. researched the influence of temperature on the feasibility of BPMED for the recovery of sodium sulfate to sulfuric acid. It was found that the lowest power consumption was obtained for the highest BPMED operating temperature [40]. This indicates that the mobility of ions, which increases with temperature, has a dominant effect on the decrease in the resistance faced during the process [40]. So the temperature of the wastewater is found to have an influence on the energy consumption by BPMED. Raucq et al. stated that for BPMED an increase in temperature lead to an increase of the current efficiency [45]. However, it remains unclear what the influence of temperature on the current efficiency of NH_4^+ ions is. The influence of temperature on the NH_4^+ current efficiency is of interest since in municipal treatment facilities, seasonal temperature variations might occur. Additionally, the temperature of the ammonium sulfate in industrial environments can be adjusted easily. The scrubber effluent of 70°C could be adjusted to the temperature reaching the highest efficiencies and the lowest total energy usage, creating economic and sustainable interest for industrial companies.

1.5 Research Approach

The process of ammonium sulfate removal from stripper/scrubber installation reject streams with BPMED is found to be a high potential process for the recovery of ammonia from reject waters and the production of dissolved ammonia. This is a high potential process since no addition of chemicals is needed due to in situ generation of sulfuric acid and it is expected to be energetically competitive with currently used ammonium removal treatment systems [36]. Treating effluent from the stripper/scrubber with BPMED could therefore create a circular system. The use of BPMED technology for treatment of

industrial ammonium sulfate rich wastewater streams is not yet optimized, but could be contributing to the creation of a more environmentally friendly ammonium removal system. The primary objective of this research was to evaluate and optimize the BPMED technology for treatment of ammonium sulfate rich industrial wastewaters by looking into the influence of pH, temperature and concentration on the BPMED functionality. The main research question being addressed through this research is:

What is the influence of high temperature, high concentration and pH on the ammonium and sulfate removal efficiency and the purity of the generated sulfuric acid and ammonium hydroxide by scrubber effluent treatment with Bipolar Membrane Electrodialysis?

1.6 Approach and Research Sub Questions

Based on the research gaps found in literature, several sub questions were investigated during this thesis:

Research sub question 1: *What is the influence of pH on BPMED treatment of ammonium sulfate-rich scrubber effluent?*

Research sub question 2: *What is the influence of the ammonium sulfate concentration on BPMED treatment of ammonium sulfate-rich scrubber effluent?*

Research sub question 3: *What is the influence of temperature on BPMED treatment of ammonium sulfate-rich scrubber effluent?*

The BPMED technology and its advantages and disadvantages are evaluated in Chapter 2. The experimental set-up and methodology are explained in Chapter 3. Results from these experiments are presented in Chapter 4 and discussed in Chapter 5. Eventually, a conclusion is drawn in Chapter 6, together with some recommendations for further research and implementation.

2 Theoretical Framework

2.1 Stripper/Scrubber System

In industrial applications, the stripper/scrubber system is currently used to remove components which are harmful to the environment, like NH_3, from waste (air) streams. Stripping is a physical separation process for removing solute(s) from a loaded solvent or extract. Scrubbing is the operation of removing contaminants (impurities) from an extract [46]. In the scrubber, the ammonia (NH_3) is removed from the air by reaction with sulfuric acid (H_2SO_4) in water to form ammonium sulfate $(NH_4)_2SO_4$ with the following reaction:

$$2NH_3 + H_2SO4 \longleftrightarrow (NH_4)_2SO_4 \tag{4}$$

Traditionally, the term "scrubber" has referred to pollution control devices that use liquid to wash unwanted pollutants from a gas stream. Recently, the term has also been used to describe systems that inject a dry reagent or slurry into a dirty exhaust stream to wash out acid gases [47]. Scrubbers are one of the primary devices that control gaseous emissions, especially acid gases [1].

For this thesis, the removal of ammonium by the stripping/scrubbing combination is considered (Figure 2.1). This treatment is widely used on industrial scale and has been proven to successfully remove nitrogen from different waste waters, e.g. pig slurry, landfill leachate and wastewaters from the production of mineral fertilizers. The efficiency of the stripping/scrubbing depends on several main factors: pH, temperature, ratio of air to liquid volume, and liquid characteristics [47, 48, 49]. Prior to entering the stripper scrubber/system, the substrate has to be heated and/or the pH should be raised. In a wet environment the gaseous ammonia (NH_3) is in equilibrium with ammonium (NH_4^+). A higher temperature and/or a higher pH shift the equilibrium towards the ammonia side. The substrate is pumped into the first stripper, where air is blown through the substrate in counter-current flow mode. Ammonia (NH_3) is captured by the air. Prior to the scrubber system, an acid has to be added to the feed solution to lower the pH [1]. In this research, the acid required for lowering the pH is sulfuric acid.

The stripper/scrubber system produces a $(NH_4)_2SO_4$ waste stream. Dependent on the type of system, this stream can have different (extreme) characteristics, like a very low pH, high concentration and/or high temperature. Currently this stream is often used as soil fertilizer but it can also find its application as flame retardant [50].

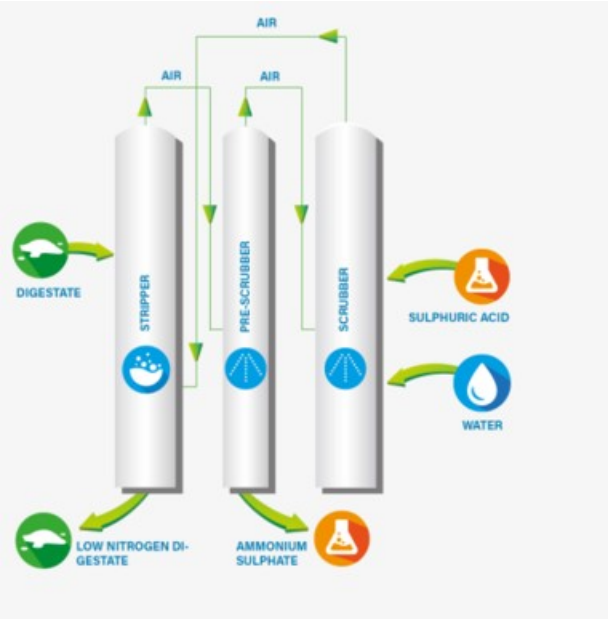

Figure 2.1: Visualization of the stripper/scrubber system as used for treatment of industrial waterstreams. Retrieved from Byoflex.nl [1]

2.2 (Bipolar Membrane) Electrodialysis Fundamentals

Electrodialysis is the principle behind the functioning of the BPMED. To fully understand the phenomena happening, first the fundamentals of ion exchange and electrodialysis have to be explored.

2.2.1 Fundamentals of ion exchange

ion exchange membranes are the fundamental principle behind BPMED. ion exchange is about coupling the transport of electrical charges with a transport of mass through a permselective membrane due to an externally applied or internally generated electrical potential gradient [4]. The most important properties of ion exchange membranes include:

- high permselectivity (preferential permeation of certain ionic species through ion exchange membranes)
- low electrical resistance
- good mechanical and form stability
- high chemical and thermal stability

There are two types of ion exchange membranes: cation exchange membranes which contain negatively charged groups fixed to the polymer matrix, and anion exchange membranes which contain positively charged groups fixed to the polymer matrix. Selectivity of the ion exchange membranes results from the exclusion of similarly charged ions as the membrane (co-ions) from the membrane phase [4, 51]. Cation exchange membranes are permeable for cations and more or less impermeable for anions, whereas anion exchange membranes are permeable to anions and more or less impermeable for cations [4].

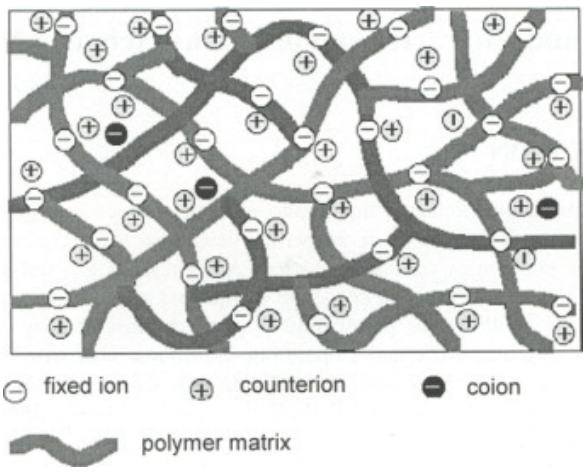

Figure 2.2: Schematic drawing illustrating the structure of a cation exchange membrane. Species with the same charge as the fixed membrane charges are referred to as co-ions, which cannot pass the membrane due to repulsion. Counterions can pass the membrane due to attractive forces. For an anion exchange membrane, the charges in this figure are opposite. Image retrieved from Strathmann et al. [2].

2.2.2 Electrodialysis

Electrodialysis (ED) is an electrochemical membrane separation process based on the concept of ion exchange membranes, separating according to the electric charges of the particles. Ionic (electrically charged) species are transported from one solution to another by crossing one or more selective permeability membranes, under the influence of a direct electrical current. In electrodialysis, the driving force for the transport of components from the wastewater to the receiving solution is an electrical potential difference across a membrane separating the two solutions [2, 4].

In an electrolytic cell (one used for electrolysis), the anode is positively charged and the cathode is negatively charged. By providing a salt feed solution to the ED, positively charged cations migrate towards the cathode and negatively charged anions migrate to the anode under influence of the applied electrical potential. The membranes are selective for the type of ion: the negatively charged ions pass through the anion exchange membrane and the positively charged ions pass through the cation exchange membrane (Figure 2.2). In case of a cation exchange membrane with fixed negative ions, mobile cations (counterions) can pass the membrane since they have opposite charge from the membrane. Mobile anions are referred to as co-ions, which are (ideally) excluded from the polymer matrix since their repulsion because of the identical electrical charge. This type of exclusion is called Donnan exclusion [4, 52].

The anion- and cationselective membranes are alternately organized in an electrodialysis membrane stack (Figure 2.6). This results in a cation and anion stream (concentrate) and a stream depleted from ions, called the diluate solution [4]. An actual electrodialysis membrane can be built up by a few hundred of these membranes.

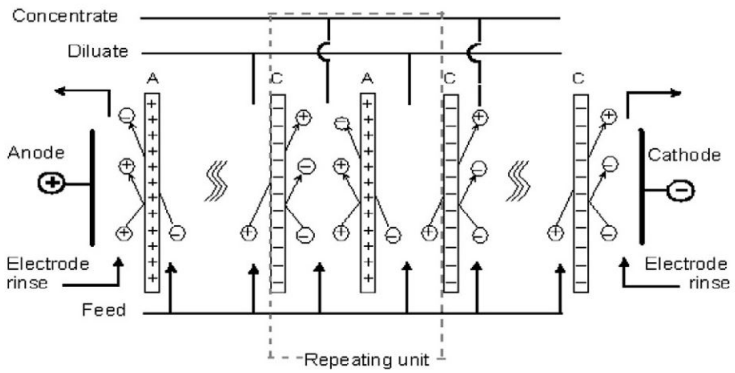

Figure 2.3: Schematic diagram illustrating the principle of electrodialysis [2]

The separation in electrodialysis is the result of differences in the transport numbers of ions in the solution and in the ion exchange membranes. The ion transport number (t), also called the transference number, is the fraction of the total electrical current carried (I) in an electrolyte by a given ionic species i [52]:

$$t_i = \frac{I_i}{I_{tot}} \tag{5}$$

The current supplied to the cell is being carried in the solution by charged ions, in this case cations and anions. In ion exchange membranes, the current is carried mainly by the counterions which have a transference number close to 1.

2.2.3 Applications of Electrodialysis

The earliest studies with ED focused on the demineralization of brackish sea water to produce drinking water [53, 54]. Pre-concentration of sea water for the production of table salt is the largest application of electrodialysis in the field of brine concentration [4]. Electrodialysis is also used for further concentration after reverse osmosis to minimize environmental pollution. However by improvements in membrane properties, like better selectivity and lower electrical resistance, the electrodialysis membrane technology is of interest for many more applications in the food, drug, chemical and biotechnological industries [55, 56].

2.3 BPMED Technology

The Bipolar Membrane Electrodialysis (BPMED) technology is an extension of the ED technology, in which additional bipolar membranes are added which make the production of separate acids and bases possible. More detailed electrochemical characteristics and phenomena present during operation of (BPM)ED will be discussed in this chapter.

2.3.1 Electrodialysis with bipolar membranes - Fundamentals

Technological details

Electrodialysis can be used in combination with bipolar membranes. BPMED is a membrane separation technique which can be used for the production of acids and bases separately. BPMED is favourable over the standard electrodialysis because of its ability to change the pH in situ by only using electrical energy, i.e. without the addition of chemicals [22, 24]. The concentrate produced during conventional

ED is further separated into an acid and a base, which will for the scope of this research be indicated as 'acid' and 'base' respectively. The feedstream/salt solution is indicated as 'diluate' solution and the electrode rinse solution is indicated as ERS. Cation- (CEM) and anion exchange membranes (AEM) are installed together with bipolar membranes (BPM) in alternating series in an electrodialysis stack as depicted in Figure 2.4 [4].

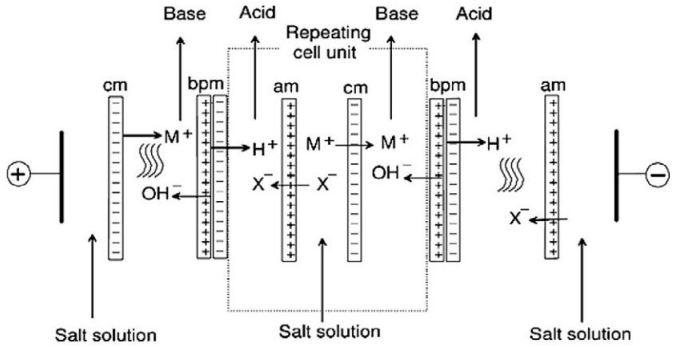

Figure 2.4: Schematic drawing illustrating the principle of electrodialytic production of acids and bases form the corresponding salts with bipolar membranes [2]. The outer membranes (end membranes) can be Anion Exchange End Membranes (AEEM) or Cation Exchange End Membranes (CEEM).

The cation and anion exchange membranes in the BPMED stack are the same as the ones use for ED (Figure 2.2). The bipolar membranes, which are composite membranes, are composed of three parts: an anion exchange layer, a cation exchange layer, and a hydrophilic interface at their junction, which allows the dissociation of water molecules in the hydrophobic layer under the presence of a direct current [4, 22, 53].

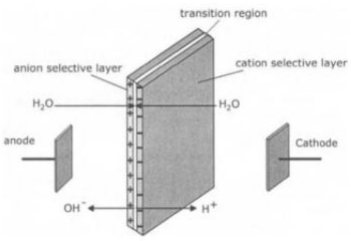

Figure 2.5: Schematic drawing illustrating the structure of a bipolar membrane, retrieved from Strathmann et al. [2].

Important BPMED membrane characteristics are adequate water dissociation capability, low electrical resistance, high permselectivity and a long lifetime under operating conditions (must be stable in highly concentrated alkaline and acid conditions)[4]. The feed water for BPMED must have a low viscosity to circulate easily in an electrodialysis cell and possess a relatively high mineral content, to allow a good electrical conductivity in order to decrease the global resistance of the cell [53]. Currently, major drawbacks of the BPMED technology include the high cost of equipment and the susceptibility to blocking [23, 53]. Factors currently limiting efficiency and increasing the energy consumption in the case of ammonium recovery are H^+ and OH^- leakage, dissolved NH_3 diffusion and ionic species diffusion [36].

Membrane properties
The most desirable properties for bipolar ion exchange membranes are:

- high selectivity for the counterions, complete exclusion of co-ions
- low electrical resistance
- excellent stability (in solution with extremely low and high pH values)
- high water dissociation capability
- high water permeability of the monopolar layers

First three are crucial for all ion exchange membranes ensuring the highest yield in combination with the lowest energy use. Bipolar membranes optimized for the production of a certain type of acid can be used, for example specifically for the production of sulfuric acid or organic acids. In these bipolar membranes, the structure is adapted in such a way that it has beneficial characteristics for this specific type of acid production. The structure and characteristics of anion exchange membranes are the same as the structure and characteristics of anion exchange end membranes and similarly the cation exchange membranes has the same structure and characteristics as the cation exchange end membranes [4].

2.3.2 Electrochemical and thermodynamic processes in BPMED

During the operation of the BPMED, various electrochemical and thermodynamic processes happen which explain the transportation of certain ions and other phenomena happening. Ion exchange membrane separation processes are determined by electrochemical, thermodynamic and kinetic parameters, of which the most important ones for the scope of this research are being described in the following paragraphs:

2.3.3 Transport of electrical charges and its energy use

The transport of electric charges (electric current) can be achieved by transport of electrons through solid materials or liquids. The electrical current (I) between the electron sources is proportional to the electric potential driving force (U), which is the driving force, described by Ohm's law:

$$U = RI \tag{6}$$

U is the electrical potential between two electron sources (Volt), I is the electrical current between the electron sources (Ampere) and R is the electrical resistance (Ohm).

For constant current, a certain I is constantly applied to the electrodialysis cell. The resistance is dependent on the specific resistance of the material, the distance between the electron sources and the cross section area through which the electrical current flows. The resulting electrical potential is the dependent variable in the case of (BPM)ED. For every element and stream in the ED there is a certain ohmic resistance, the sum of these partial ohmic resistances will result in the total resistance of the ED.

The energy consumption in electrodialysis with bipolar membranes is an additive of two terms:

- energy required for dissociation of water in the bipolar membranes
- electrical energy required to transfer salt ions from the diluate and protons and hydroxide ions from the transition region of the bipolar membranes into the acid and base solutions.

In practice, this total energy required in the process is given by the current passing though he stack multiplied with the voltage drop between the electrodes over a certain period of time [4]:

$$E = I\delta U t \tag{7}$$

E is the energy consumed in the production of acids and bases in electrodialysis with bipolar membranes in Joules. I is the current passing through the stack in Ampere. δU is the voltage applied across the stack between the electrodes in Volt and t is the time of operation in seconds, minutes or hours. In practice, the current density i is preferred in literature, relating the applied current I to the active surface of the used electrodes A [52]:

$$i\ (A \cdot m^{-2}) = \frac{I}{A} \tag{8}$$

Energy consumption and resistance
Electrical resistance of the ion exchange membranes is one of the factors determining the energy consumption of the electrodialysis process. However in most practical cases, the membrane resistance is considerably lower than the resistance of the diluate solutions, since the ion concentration in the membrane is relatively high. The electrical resistance of the membranes was assumed to be constant during all experiments.

2.3.4 Concentration polarization and Limiting current density

The rate of ionic transport across membranes depends on the electrical current density (i) applied to the cell [57]. Concentration polarization can occur in (BPM)ED as a result of the different rates of ion transport between the bulk solution and the membrane [4]. Concentration polarization occurs when the concentration of a specific component increases or decreases at the boundary layer close to the membrane surface due to the selective transport through the membrane. A concentration gradient between the membrane surface and the well mixed bulk increases diffusive ion transport towards the membrane interfaces in the diluate. The development of concentration polarization in ED and BPMED is related to the current applied and to the electrical conductivity (concentration of ions in the stream)[2, 4].

Below the limiting current density, the electric current is carried by salt ions migrating from the transition region between the anion and the cation exchange layer of the bipolar membrane. In steady state, these ions are replaced by salt ions transported from the bulk solutions into the transition region by diffusion and migration due to the fact that the ion exchange layers are not strictly permselective. When the ion concentration at the membrane surface approaches 0, the limiting current density (LCD) is reached and the salt transport from the transition region can no longer be compensated by the transport into the region and a drastic increase in the membrane resistance and enhanced water dissociation/splitting is observed [58]. After reaching the LCD, increasing the applied voltage does not result in an increased current [4, 59].

The performance of BPM increases with current density and considerably decreases with concentration of acid and base [26]. A concentration gradient is established in the solution in between the well mixed bulk and the membrane. The concentration of ions in the diluate boundary layer decreases towards the membranes surface and on the other side of the membrane, the concentration of ions in the concentrate boundary layer increases towards the membrane [52]. The flux (the action or process of flowing or flowing out) of the counterions is higher in the membrane than in the surrounding boundary layers [4].

Concentration polarization in electrodialysis results in a decrease in salt concentration at the membrane surface at in the diluate containing cell and the salt concentration at the membrane surface in the concentrate containing cell increased [60].

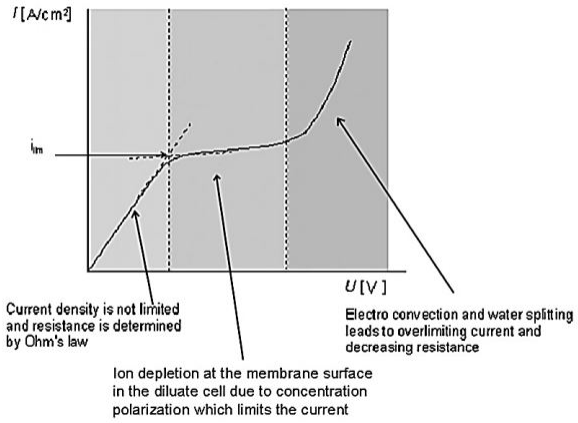

Figure 2.6: Current-potential curve in ED operated at constant flow velocities and constant diluate concentrations. On the x-axis the potential ϕ or U (V) is displayed and on the y-axes the applied current density I ($A \cdot cm^2$) is shown. Before reaching limiting current density, an increase in potential increases the current density. When ion depletion is reached, concentration polarization occurs which limits the current. After reaching the LCD a further increase of the voltage does not results in a rise of the current density. Retrieved from Strathmann et al. [2]

Concentration polarization can be reduced by adapting several parameters [4]:

- increasing linear flow velocity
- spacer geometry
- operating at lower current density

2.3.5 Thermodynamics in electrodialysis

A system always strives to an equilibrium, in which the Gibbs free energy on both sides is equal. For a system containing electrically charged components such as salts, acids or bases, there is an equilibrium when the electrochemical potential of all components which can be exchanged between the two phases is identical [2].

Transport of mass, heat, electrical charge and individual components between two systems separated by a semipermeable membrane only occurs when the two systems are not in equilibrium, which means that the two systems are in different thermodynamic states. For such a non-equilibrium condition, the driving force for any transport is based on differences or gradients in matter, heat or electrical potential across the membrane [4].

Even though an imbalance in pressure or electrical potential or activities of different components is present in a system, this system can be in equilibrium as long as the Gibbs free energy in both systems is the same. The electrochemical equilibrium between two phases is named the Donnan equilibrium which is obtained when an electrical potential difference between two phases is compensated by activity and pressure differences of the ions in those two phases [51]. The electrochemical potential of an ion is composed of the chemical potential (μ) the electrical potential (ϕ) and the valence of the ion (z). The basic concept of electrodialysis is built on the concept of electrochemical potential, which is the driving

force for mass transport. With neglecting the influence of pressure difference across the membrane the electrochemical potential can be described. The activity coefficient, ion concentration and activity are introduced leading to the electrochemical potential (η) [4]:

$$\frac{\eta_i}{dx} = RT\frac{(\gamma_i c_i)}{dx} + z_i F\frac{d\phi}{dx} \tag{9}$$

Where η_i is the electrochemical potential (J/mol), dx is the difference in distance (m), R the universal gas constant (-), T the temperature (K), γ_i the activity coefficient for species (-), C_i concentration of species (mol/L), F the Faraday constant ($C \cdot mol^{-1}$), z the valence of species z_i and ϕ the electrical potential (V).

Boundary layer
In case an ion exchange membrane is placed into an electrolyte solution, the fixed charges at the surface of the membrane create an electric field which will attract ions with opposite charge from solution. In this electric field (boundary layer) on the membrane surface, the concentration of oppositely charged ions is higher than in the bulk solution. The flow in the boundary layer is assumed to be stagnant, resulting in a concentration profile of ions surrounding it. Since the flux of ions is higher in the membrane phase than in the boundary layers, the concentration of ions in the boundary layer of the diluate decrease towards the membranes. The concentration of ions in the boundary layer of the acid and base increases towards the membrane. This is the already explained phenomenon concentration polarization [4, 61].

Transport of mass
Mass transport phenomena in electrolyte solutions can be described by the extended Nernst-Planck equation which shows the anion and cation fluxes of a completely dissociated salt. The extended Nernst-Planck flux equation can be used assuming an ideal solution (the activity of a component is identical to its concentration) and this equation is considering three modes of mass transport in ion exchange membranes: diffusion, migration and convection [52]. Assuming zero netto water transport through the membrane, convection can be neglected:

$$J_i = -D_i\frac{dC_i}{dx} - D_i\frac{z_i C_i F}{RT}\frac{d\phi}{dx} \tag{10}$$

Where J_i is the flux of ion i ($mol \cdot m^{-2} \cdot min$), D_i is the diffusion coefficient ($m^2 \cdot s^{-1}$), C_i concentration of species (mol/L), dx is the difference in distance (m), F the Faraday constant ($C \cdot mol^{-1}$), R the universal gas constant (-), T the temperature (K), z the valence of species z_i and ϕ the electrical potential (V).

Diffusion is a movement of molecular components due to a local gradient in the chemical potential. Migration is a movement of ions due to an electrical potential gradient. Convection is the movement of mass due to a mechanical force. It should be noted that the Nernst-Planck equation neglects any kinetic coupling between individual fluxes and that the activity coefficient is considered to be 1. However, this relation is easy to use due of the limited number of parameters while still describing the transport of ions in ion exchange membranes realistically [2, 4].

2.3.6 Overview of desired and undesired transport in BPMED treating ammonium sulfate diluate

An overview of these processes in BPMED is provided in Figure 2.7. Both electrochemical and thermodynamic processes are discussed in more detail in the following paragraphs.

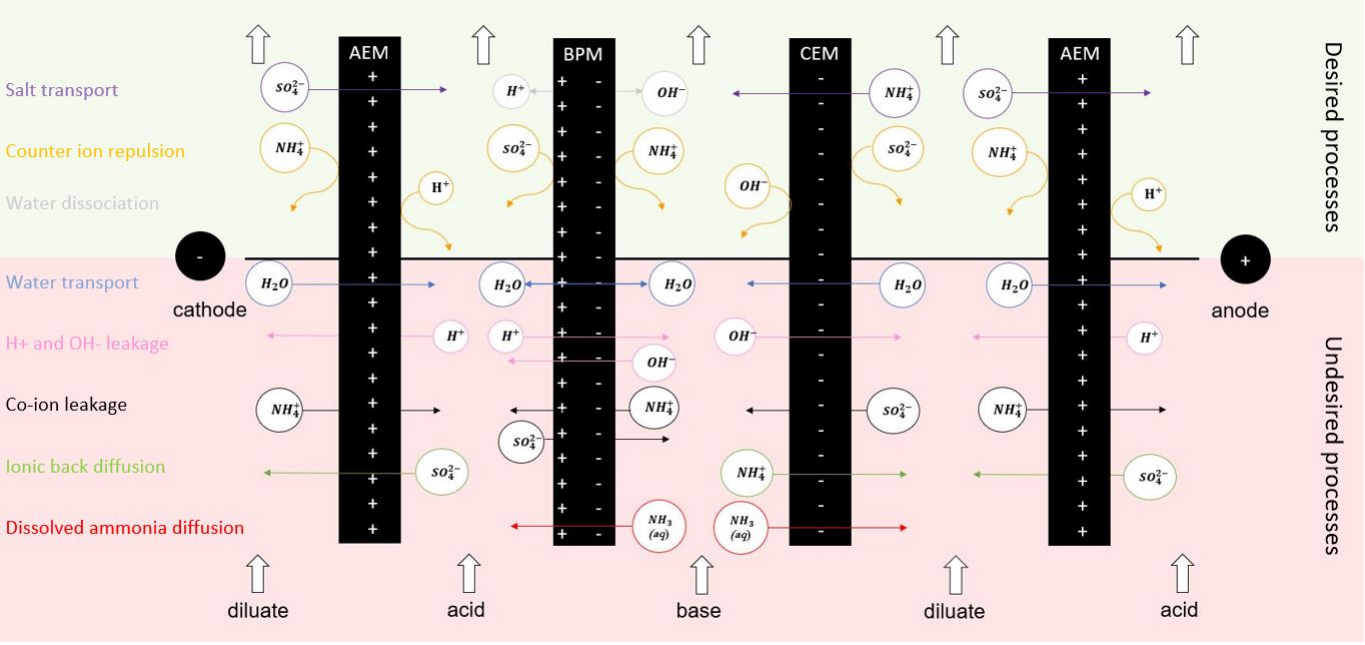

Figure 2.7: An overview of the processes potentially taking place in during bipolar membrane electrodialysis with ammonium sulfate as feed solution. In the light green plane, the desired processes are depicted, while the light red plane shows the undesired processes. Potential processes and transportation of ions from the ERS solution are not taken into account. Part of the ammonia (NH_3), when in the gas form, can leave the total system.

2.3.7 Ion electro-migration: Salt transport and counter ion repulsion

Ion exchange membranes are highly selective for counterions. Counterions are ions that carry a charge opposite to the fixed ions of the membrane.

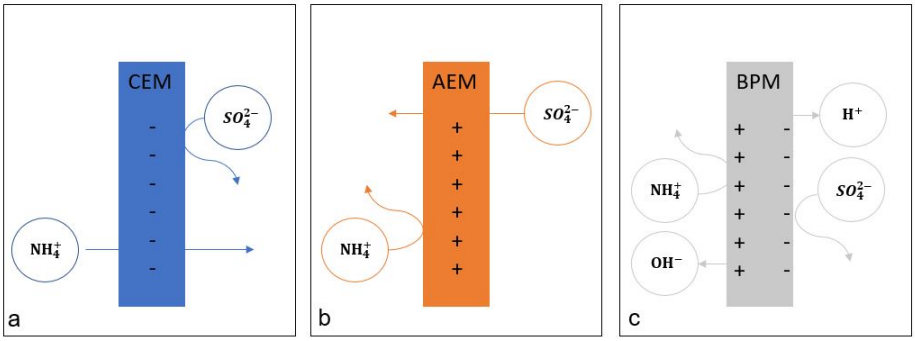

Figure 2.8: Visual representation of the (theoretical) selectivity of the a) Cation Exchange Membrane, b) Anion Exchange Membrane, c) Bipolar Membrane

The concentration of co- and counterions in ion exchange membranes is determined by the Donnan exclusion, with indicates that co-ions are more or less completely excluded from the membranes and their permeability is corresponding low. The permeability of counterions in a membrane is determined by the ion-exchange selectivity and the mobility selectivity. As a general rule, the counterions with the higher valance have a higher ion exchange selectivity than ions with lower valance and ions with lower valence and the smaller radius have a higher mobility in ion exchange membranes [4].

2.3.8 Water-transport and -dissociation

Pure water in solution dissolves in hydrogen ions and hydroxide ions with the following equilibrium:

$$2H_2O \longleftrightarrow H_3O^+ + OH^- \tag{11}$$

In case salt ions are still present in the diluate, the applied current i will result in migration of those salt ions towards the acid and base solution. During that process, the applied i is smaller than the LCD. In case no salt ions are left-over in the spacer regions between the two membranes, but the electrical potential gradient is still applied, the transport of the electrical charges through the membranes is accomplished exclusively by protons and hydroxyl ions which are available even in in pure water in a concentration of 10^{-7} due to the dissociation equilibrium of water. During this process, the applied current i is bigger than the LCD. At the anion exchange side, an alkaline solution is formed and at the cation exchange side, an acid solution is formed. This water splitting process however is high in energy use and therefore undesirable [22, 58].

Osmosis
Water transport between solutions separated by a (ion exchange) membrane due to osmotic pressure differences between solutions occurs when two aqueous salt solutions of different concentrations are separated by a membrane permeable for a solvent, but significantly less permeable for the solute. Then the transport of water from the more dilute solution into the more concentrated solution is observed [4, 61]. In case of (Bipolar Membrane) Electrodialysis, the ion exchange membranes are designed to prevent osmosis, but only allow ions to transport through the membrane. However, in various studies it was found that water is transported across the membrane and therefore limits the functionality of (BP)MED to produce a concentrated (acid and base) stream [40, 59, 62].

Ion hydration number and electro-osmosis
Another type of undesired transport in (BP)MED is electro-osmosis, which is defined as the flow of electrolyte that is in contact with a charged surface, due to the electrical potential gradient applied [3, 61]. Electro-osmosis refers to the water transported in the hydration shell of the ions migrating through the membrane due to an electrical potential gradient [4]. The hydration/salvation shell is the sphere of water molecules around each dissolved ion (Figure 2.9) [62, 63]. Electro-osmosis is of relevance in ion exchange membrane processes and in particular in electrodialysis, since it affects the efficiency of the process by the transport of water from the diluate to the concentrate solution. The amount of water accompanying the ions migration is linked to the hydration number of the ions transferring through the membranes during the ED process [3]. This is explained by the first hydration shell, in which the water molecules interact directly and strongly with the ion. It is due to electro-osmosis, i.e. the water carried by the migrating species and is thus related to their hydration. The hydration number for monovalent ion was found to be lower than that of divalent one, for cation and anion respectively [64].

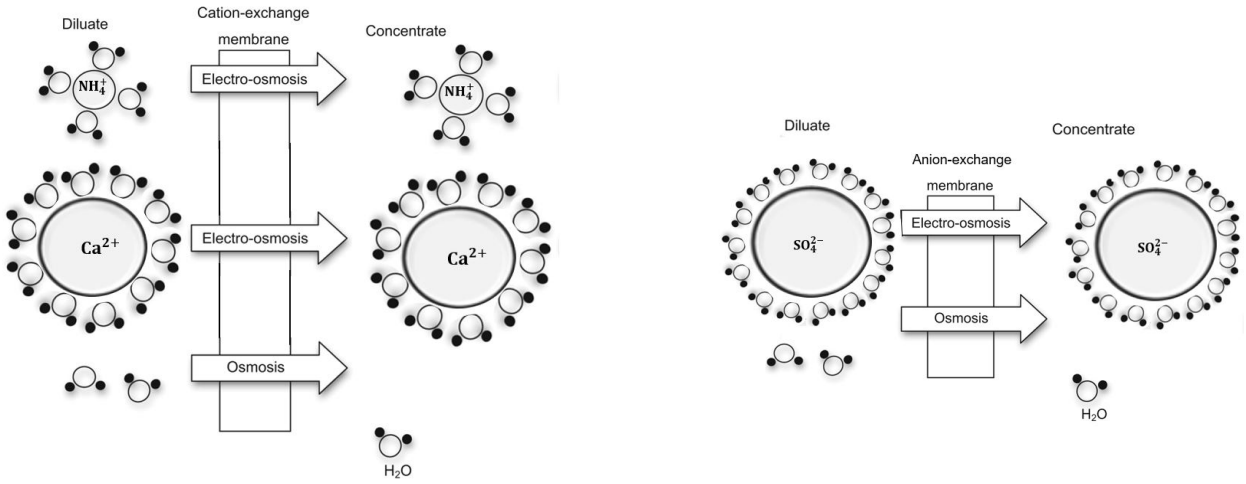

(a) Electro-osmosis and osmosis through a cation exchange membrane. The ammonium cation has up to 4 water molecules in its hydration shell passing through the cation exchange membrane and the calcium cation can bring up to 10 water molecules passing the membrane.

(b) Electro-osmosis and osmosis through an anion exchange membrane. The sulfate anion can bring up to 15 water molecules passing through the cation exchange membrane.

Figure 2.9: A visual representation of the concept of osmosis and electro-osmosis, adapted from Rottiers et al. [3]. The molecules are not shown proportionally.

The ion hydration number is independent from solution composition and current. Ammonium has 4 water ions tetrahedrally coordinated in the first hydration shell [65]. The first hydration shell of calcium consists of either 9 or 10 water molecules [66]. Up to 15 water molecules are found to be present in the first hydration shell of the sulfate anion [64].

2.3.9 Proton and hydroxide leakage

Generally, the permeation of protons is significantly higher (4 to 5 times) than that of other cations in cation-exchange membranes, making (undesired) transport of protons towards the base likely to happen. This is mostly due to different transport mechanisms of protons in an aqueous environment compared to other ions. Also the mobility of H^+ and OH^- ions in aqueous solution is very different than other ions. In general, small ions like H^+ and OH^- have a higher mobility (u) in water of 25°C than bigger ions like NH_4^+ (7.63 10^{-8} m^{2-1} V^{-1}), Ca^{2+} (6.17 10^{-8} m^{2-1} V^{-1}) and SO_4^{2-} (8.29 10^{-8} m^{2-1} V^{-1}). The mobility of H^+ ions is 36.23 10^{-8} m^{2-1} V^{-1} and the mobility of OH^- ions is 20.64 10^{-8} m^{2-1} V^{-1} [4, 67]. Smaller ions have a lower mobility than larger ions due to the smaller hydration shell and higher charges of divalent ions [4, 67]. For the specific case of protons in water, protons form clusters of hydronium ions, resulting in an easy transfer from one hydronium to the next hydronium via the tunneling mechanism. This mechanism results in an extraordinary high mobility of protons in water [4]. For certain applications such as the recovery of acids from a mixture, it would be desirable to have a cation exchange membrane with a very high proton selectivity [4].

The undesired transport of H^+ and OH^- from acid and base respectively towards the diluate can reduce the current efficiency of anions and cations maintaining charge balance. Furthermore, H^+ and OH^- ions compete with NH_4^+ and SO_4^{2-} for transportation over the membrane. Concentration, membrane permselectivity and temperature influence the transport of H^+ and OH^- [4].

2.3.10 Co-ion leakage

The ion exchange membranes are not only permeable to counter-ions, which are the desired acid and base ions created by BPMED treatment. Besides the permeability to counter-ions, the acid anions and the base cation can be transported transported across the bipolar membrane [4]. As shown in Figure 2.2, the co-ion can undesirably penetrate through the similar charged membrane. For bipolar membranes, the co-ion penetrates through the respective layer of the bipolar membrane as co-ion and is then transported across the bipolar junction into the other compartment. Such co-ion leakage results in salt impurities of the produced acid and base, limiting the use of this bipolar membranes for some applications. The undesired leakage of co-ions through the ion exchange membranes is related to their imperfect permselectivity. The transport number for co-ions through commercial ion exchange membranes is normally only very limited [68, 69].

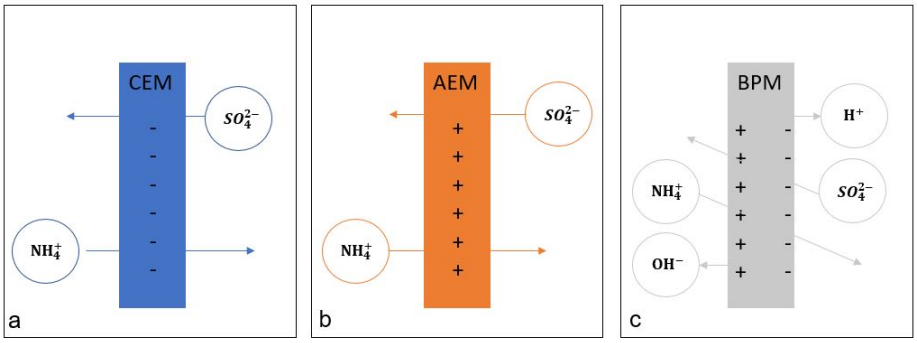

Figure 2.10: Visual representation of the co-ion leakage of a) Sulfate through the Cation Exchange Membrane, b) ammonium through the Anion Exchange Membrane, c) both sulfate and ammonium through the Bipolar Membrane. The latter one is observed mostly [4].

2.3.11 Ion (Back) diffusion

As described in the extended Nernst-equation, diffusion is an important factor influencing the fluxes of anions and cations. Diffusion is a movement of molecular components due to a local gradient in the chemical potential [58]. When large concentration gradients across the membrane are obtained, low molecular weight charged and non-charged components can diffuse through the membrane from the high concentration solution to the low concentration solution. This diffusion of charged components influences the current efficiency and can lead to contamination of sulfuric acid and/or ammonium hydroxide. Diffusion can happen between all streams, but is dependent on the concentration gradient, temperature, solvent properties mass of ions and time [4]. Back diffusion is the undesirable transfer of ions from concentrate to diluate. In this case, the back-diffused ions from acid or base towards diluate need to be retransported over the membrane, which requires extra energy. Therefore, back diffusion decreases the energy efficiency of the process. Since the process of desalination takes longer at a low current, (back)diffusion processes will be higher. Therefore the operation at higher i leads to an increase in current efficiency [2, 52].

2.3.12 Gas diffusion

Depending on the pH of a solution, ammonium can be present in the liquid form (NH_4^+) or in its gas form ammonia NH_3, given with the following equilibrium with a pKa of 9.24 [70]:

$$NH_4^+(eq) \longleftrightarrow NH_3(eq) + H^+(eq) \tag{12}$$

Gas diffusion in liquid media is described by Fick's law, assuming perfect mixing in each compartment of the stack [12, 58, 60, 69]:

$$J_x = -D \cdot C_x \tag{13}$$

In which J_x = diffusion flux, D is the diffusion coefficient and C_x is the concentration gradient between the two chambers. The diffusivity coefficient is dependent on a number of factors, but the most important are the following: type of gas and porous medium interface. reservoir pressure. reservoir temperature [71].

2.4 Performance Indicators

To assess the influence of temperature, concentration and pH on the treatment of ammonium sulfate-rich waters and to provide academic proof for the most optimal functioning of the BPMED for these type of waters, certain indicators were evaluated. The requirement for a BPM to be useful in practical applications are a low electrical resistance at high current density, a high water dissociation rate, a low co-ion transport number, a high ion-selectivity and a good chemical and thermal stability in strong acids and bases [68].

2.4.1 NH_4^+ current efficiency

For measuring the removal of NH_4^+, the NH_4^+ current efficiency ($\eta_{NH_4^+}$ - unitless) was determined, which is defined as the amount of charge equivalent transported as NH_4^+ over the supplied electric charge (Equation 14).

$$\eta_{NH_4^+} = \frac{z \cdot F \cdot n_{NH_4^+,d}}{N \cdot \sum_{t=0}^{t} (I_{\Delta t} \cdot \Delta t)} \cdot 100\% \tag{14}$$

Where z is the ion valence (1 for NH_4^+); F is the Faraday constant (= 96.485 $Cmol^{-1}$); $n_{NH_4^+}$ is the amount of NH_4^+ transported (depleted) from the diluate (mol); N is the number of cell triplets in the BPMED membrane stack (unitless, in our case N = 10); $I_{\Delta t}$ is the average electric current during each time interval ($A = C \cdot s^{-1}$) and Δt is the time interval (s).

This is the mathematical representation of a ratio of the number of ions removed from (in this case NH_4^+) the feed solution during a certain time period and the total amount of charge passing the membrane during this time period. The concept of current efficiency is an important parameter for describing the effectiveness of the BPMED membranes for a certain process, in this case ammonium removal, and is often used in literature [22, 45, 59, 72] . Theoretically, the charge transported as NH_4^+ should be equal to the electrical current supplied. However, there are several processes that can influence the current efficiency, for example diffusion, leakage processes and co-ion transport might influence the NH_4^+ current efficiency [36, 68, 69]. These are found to be the main processes limiting the current efficiency for the transport of ammonium and thereby resulting in an increased energy consumption [36].

2.4.2 Electrochemical energy consumption

To investigate the competitiveness of the BPMED technology as an ammonium sulfate stream treatment technology, the energy use should be taken into consideration. Based on the NH_4^+ transport from the diluate by BPMED, the electrical energy needed for transport of NH_4^+ over the membrane can be determined, known and described as the Electrochemical energy consumption (E_e - J $\cdot g{-}\mathrm{N}^{-1}$) [67]:

$$E_e = \frac{\sum_{t=0}^{t} (U_{\Delta t} \cdot I_{\Delta t} \cdot \Delta t)}{m_{NH_4^+,d}} \tag{15}$$

In which $U_{\Delta t}$ is the average electric potential during each time interval (V); $m_{NH_4^+}$ is the amount of transported NH_4^+ from diluate (g-N); $I_{\Delta t}$ is the average electric current during each time interval ($A = C \cdot s^{-1}$) and Δt is the time interval (s).

For all calculations concerning energy, only the energy for BPMED functioning was assessed. Other energy consuming aspects like power to drive the pump and energy needed to heat the solutions were not taken into account.

2.4.3 NH_4^+ and SO_4^{2-} removal efficiency

The removal efficiency of NH_4^+ and SO_4^{2-} can both be calculated based on their initial and final concentrations in the diluate and the diluate initial and final volume, as described by Guo et al. [67]:

$$NH_4^+ \text{ removal efficiency} = \frac{C_{NH_4^+,D}(t) \cdot V_D(t) - C_{NH_4^+,D,0} \cdot V_{B,0}}{C_{NH_4^+,D,0} \cdot V_{B,0}} \cdot 100\% \tag{16}$$

$C_{NH_4^+,D,0}$ (g/L) and $C_{NH_4^+,D}(t)$ (g/L) are the concentration of NH_4^+ in the diluate solution at time 0 and t (s), respectively and $V_{D,0}$ (L) and $V_D(t)$ (L) are the volumes of the diluate solution at time 0 and t (s), respectively.

Similarly, the SO_4^{2-} removal efficiency can be calculated by:

$$SO_4^{2-} \text{ removal efficiency} = \frac{C_{SO_4^{2-},D}(t) \cdot V_D(t) - C_{SO_4^{2-},D,0} \cdot V_{B,0}}{C_{SO_4^{2-},D,0} \cdot V_{B,0}} \cdot 100\% \tag{17}$$

$C_{SO_4^{2-},D,0}$ (g/L) and $C_{SO_4^{2-},D}(t)$ (g/L) are the concentration of SO_4^{2-} in the diluate solution at time 0 and t (s), respectively and $V_{D,0}$ (L) and $V_D(t)$ (L) are the volumes of the diluate solution at time 0 and t (s), respectively.

2.4.4 Purity of acid and base

For assessing the purity of the generated acid and base solution, the following equations were used as described by Szczygiełda et al. The purity is described as the concentration of the acid or base over the total concentration of ions present in solution [73]:

$$P_{acid} = \frac{[SO_4^{2-}] + [H^+]}{[SO_4^{2-}] + [NH_4^+] + [H^+] + [OH^-]} \tag{18}$$

$$P_{base} = \frac{[NH_4^+] + [OH^-]}{[SO_4^{2-}] + [NH_4^+] + [H^+] + [OH^-]} \tag{19}$$

The pH and pOH show respectively the acidity and the alkalinity of a solution. The $[H^+]$ and $[OH^-]$ concentrations in solution can found by titration, can be measured by a pH meter or can be calculated by the following equations:

$$pH + pOH = 14 \tag{20}$$

$$pH = -log[H^+] \tag{21}$$

$$pOH = -log[OH^-] \tag{22}$$

The $[NH_4^+]$ and $[SO_4^{2-}]$ concentrations were determined with spectrophotometric methods.

2.4.5 pH and Electrical conductivity

The development of pH and electrical conductivity during experiments was continuously monitored and evaluated, providing evidence for explanation of ion transport and functionality of BPMED.

3 Research Design and Methods

In this chapter the used and improved set-up for performing experimental work is described. At first, the set-up was optimized for the creation of optimal baseline conditions. Subsequently, with the optimized set-up, the experiments characterizing the influence of pH, concentration and temperature were performed. In this section, the materials used for creating the set-up and for collecting the data are described in detail. Furthermore, the experimental procedure is explained extensively.

3.1 Materials

3.1.1 Schematization of the set-up

The standardized set up consists of a BPMED in an electrodialysis unit. 0.5 and 1 liter borosilicate bottles were used for storing the acid, base, ERS and diluate stream, respectively. Those bottles were connected by piping tubes via the pump to the electrodialysis unit. From the electrodialysis unit, tubes recirculated the liquid back to the initial bottles, creating a circular system. The power supply connected to the BPMED maintained the constant current needed for the transport of ions over the membrane. Analytical data were tracked during the experiments by pH and EC sensors and by collecting samples. A visual representation of the set-up is provided in Figure 3.1.

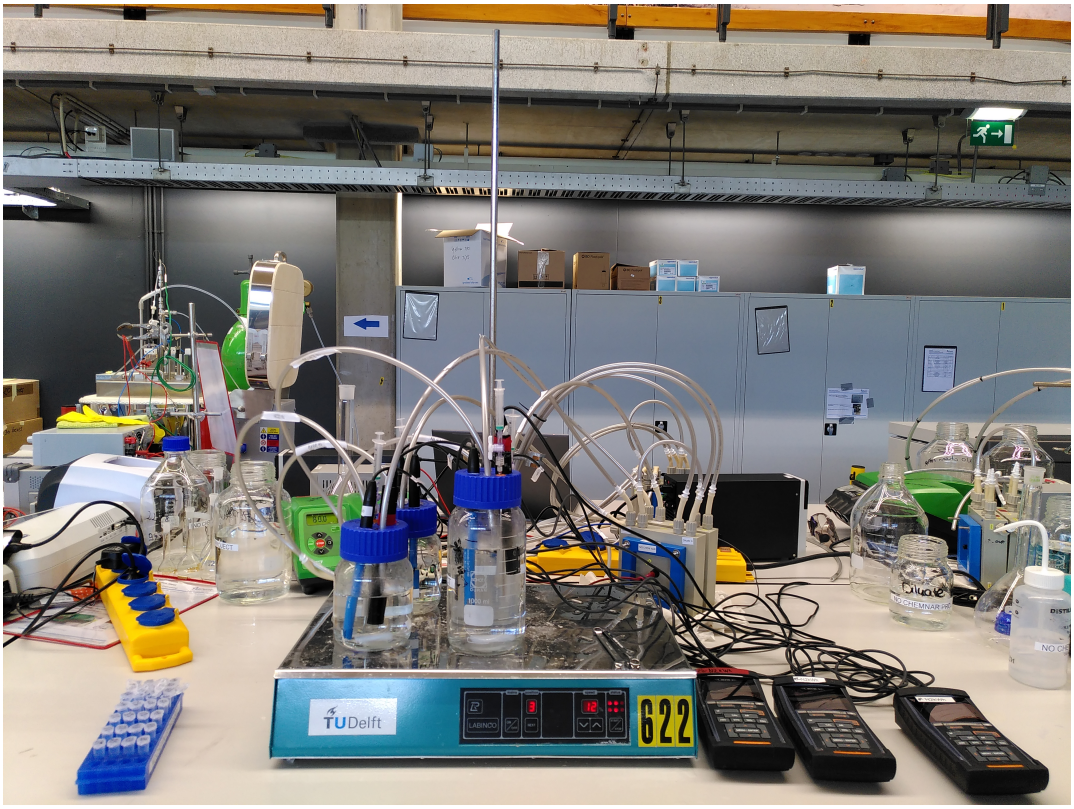

Figure 3.1: Visualisation of the set-up during the experiments researching the influence of pH and concentration.

3.1.2 Bipolar Membrane Electrodialysis

BPMED was the core technology used during this study. The BPMED consisted of an ED 64 004 cell electrodialysis unit of PCCell, which was used during all experiments. Pt/Ir- (platinum/iridium) coated Titanium was used as the anode and the cathode was made of V4A Steel. The electrode housing material consisted of Polypropylene. Each membrane stack consisted of:

- 9 Anion Exchange Membranes
- 10 Cation Exchange Membranes
- 2 Anion Exchange End Membranes
- 10 Bipolar membranes
- 30 Flow-spacers
- 2 Electrode spacers

After set-up development, bipolar membranes selective for organic acids were used (PC 100D). The membranes and spacers were organized in ten cell triplets with spacers in between the membranes, ensuring the equal spreading of water over the membranes. At both ends of the stack an Anion Exchange End membrane and their spacers created the boarder with the electrodes and thereby the electrode rinse solution. The configuration of each triplet consisted of an AEM, a CEM and a BPM, separated by spacers. A representation of the membrane stack is depicted in figure Figure 3.2. Mechanical stability of the membranes was assumed.

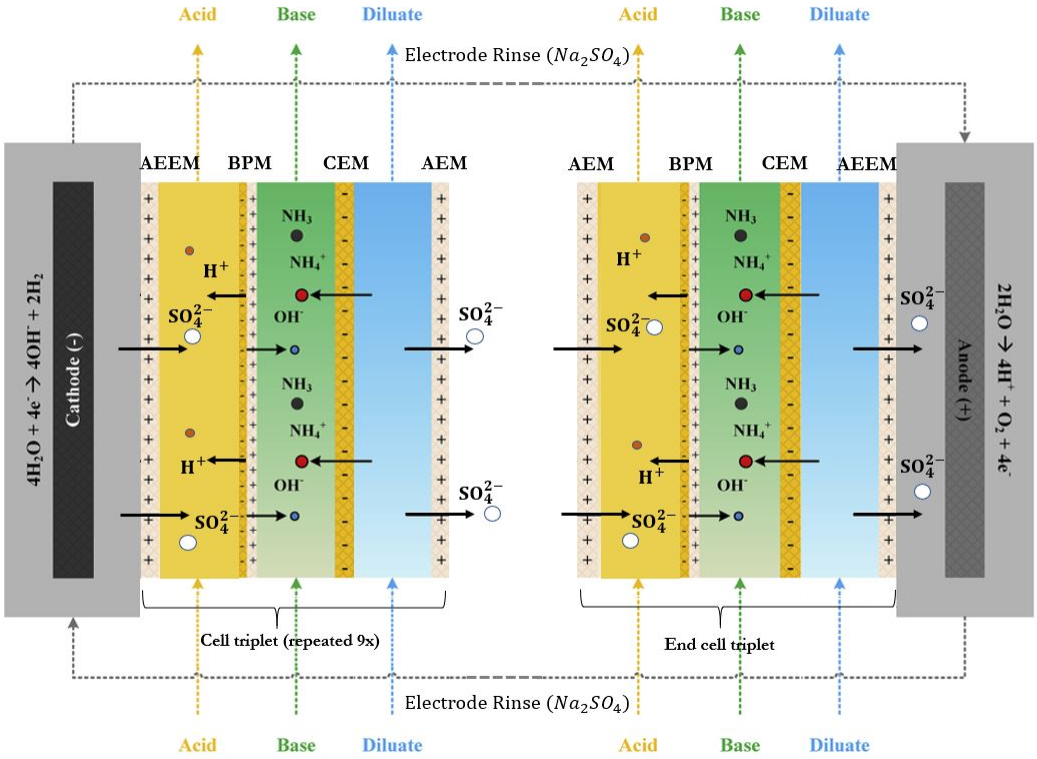

Figure 3.2: Schematic overview of the BPMED configuration and the associated ion fluxes

Cation-, anion- and bipolar membranes were sized 0.11 meter by 0.11 meter. The effective membrane area of all membranes was 0.08 * 0.08 meter.

3.1.3 Power supply

For the functioning of the BPMED, a current and voltage had to be applied to the electrodialysis unit. The TENMA 72-1330 is a power supply with a current range of 0.0 - 15.0 A and an electrical potential range of 0.0 - 60.0 V. All experiments were performed at 1.2 A, constant current with varying voltage.

3.1.4 Hydraulics

The 1 liter diluate and 0.5 L acid, base and electrode rinse solutions, stored in bottles were continuously mixed by magnetic stirrers on a mixing plate with equal settings for all experiments. The solutions were recirculated through the BPMED membrane stack by a calibrated peristaltic Watson-Marlow 520S pump with separate Watson-Marlow 313 pump heads for each solution.

In all experiments, the cross flow velocity (CFV) in all streams was set to 2 $cm \cdot s^{-1}$, based on the optimal velocity for a similar ED set up presented by Deckers [11]. It was assumed that for our BPMED set up, the same cross flow velocity could be used. The cross flow velocity can be calculated with this formula:

$$CFV = \frac{Flow\ rate\ Q}{Cross - sectional\ area\ A} \tag{23}$$

with Q in cm^3/s and A in cm^2.

The area of each spacer in the BPMED stack used during all experiments was 0.236 cm^2 (0.05 (thickness) · (length) ·0.59 (pore velocity), resulting in a desired flow rate of 16.9 L/h for each stream. The calibration curve of the pump is provided in Appendix A, which shows that a flow rate of 16.9 L/h is equivalent to 80.3 rpm. All experiments were operated with a flow rate of 80 rpm.

3.1.5 Temperature incubator

For the experiments performed at a certain temperature, the stability and consistency of the surrounding temperature was crucial. To ensure this temperature stability to a certain extent, the experiments researching the influence of temperature were performed in a temperature stable incubator, with a range of 15 - 60 °C. The incubator was set at the desired temperature overnight.

3.1.6 Chemicals

During the experiments, several chemicals were used:

- $(NH_4)_2SO_4$ salt
- Na_2SO_4 salt
- H_2SO_4 solution 2.5 M
- NH_4OH solution 25%

The used salts were of analytical grade (Sigma Aldrich Reagent Plus, 99%). The used solutions were supplied by Acros Organics.

3.1.7 Performance indicators

To analyze the experiments, several parameters were followed during the experiments:

- **Electrical Conductivity (EC), pH and temperature**
  Continuous measurements of pH, EC and temperature during experiments were carried out through calibrated sensors placed in bottles for acid solution, base solution, diluate solution and ERS. WTW TetraCON 925 was used to measure EC while WTW IDS SenTix 940 was used to measure the pH. These sensors correct the pH for temperature via the Nernst Equation. The data was shown and stored at WTW digital precision meters Multi 3630 IDS, automatically saving the temperature in °C as well. Data was stored once per second and exported in a xlsx. file, for processing of data.

- **Ammonium (NH_4^+) and Sulfate(SO_4^{2-}) concentrations in solution initially and at the end of the experiment**
  At time t=0, t=5, t=10, t=30, t=60, t=90, t=120, t=150 and t=180 minutes, a sample of 2 mL was collected from the acid, base, diluate and ERS solutions. For all experiments, the concentrations NH_4^+ and SO_4^2- at t=0 and t=180 (for the temperature experiments t=0 and t=150) were measured using MACHEREYNAGEL NANOCOLOR Ammonium 50, Ammonium 200, Ammonium 2000 and Sulfate 200 test kits after dilution. Dilutions were performed by a Thermo Scientific 10–100 µL Finnpipette F2 pipette, a Thermo Scientific 100–1000 µL Finnpipette F1 pipette and a Thermo Scientific 500–5000 µL Finnpipette F2 pipette. The ammonium and sulfate concentrations per liter were measured by a spectrophotometer NANOCOLOR VIS II, based on UV-Vis spectroscopy and the cloudiness created by reaction with barium, respectively.

- **Mass of the solutions**
  The initial and final mass of the bottles was measured with the calibrated Kern PCB 6000-1 digital precision balance with 1 decimal precision. These masses could be converted to volumes by the density of pure water. Consequently, the volume transfer during the experiment could be analysed and the mass balance could be checked for. A correction was performed for the mass of salt initially present in solution.

- **Voltage and Current provided by powersupply**
  The current and voltage applied by TENMA 72-1330 power supply functioning at constant current with varying voltage was tracked and stored in an xlsx file for further analysis and calculations of resistance.

- **Temperature sensors**
  During the experiments, the temperature within the liquids was measured by the EC and pH sensors. The surrounding temperature was monitored by temperature sensors of the Greisinger G 1700er Serie.

3.2 Experimental Methods

In this section a more detailed elaboration is provided on the experimental procedure. The preparation of all experiments was identical.

- Preparation of the start solutions: 0.01 M $(NH_4)_2SO_4$ solution (0.66 g per 0.5 liter demineralized water) for the acid and base initial solution. 1 M Na_2SO_4 solution (71 g per 0.5 liter demineralized water) for the ERS solution. The diluate solutions were, dependent on the desired concentration

ammonium sulfate, in the range of 50-250 g/L $(NH_4)_2SO_4$. For the continuation of this report, the streams are called Acid, Base, Diluate and ERS. The ERS was reused for the duplicate experiment since the ERS solution was assumed to be not of influence on the experiment and in this way salt use was limited.

- The solutions were adjusted as explained in section 3.3. The ERS solution was always acidified by the addition of 8 ml H_2SO4 1 M solution, since this resulted in a desired pH of 2. The diluate solution was acidified or alkalized by H_2SO4 1 M solution or NH_4OH 25% solution respectively to create the desired pH (section 3.2.1).
- The prepared solutions were weighted and always put in the same position to keep the hydraulics constant.
- The piping tubes were cleaned with demineralized water before the start of every experiment to make sure that the experiment was not influenced by the prior experiment.

The experiments were performed in duplicate sequencing batch experiments (SBE's), since this is found to be an appropriate way of measuring [36]. In a batch-mode configuration, a given volume of salt solution is driven in close cycle through the membrane stack until the desired product concentration is obtained [23]. With this batch mode, the process can be easily adjusted to individual demands with respect to product concentration and flow. The Acid, Base, Diluate and ERS stream were continuously circulated through the system, without differences in hydraulic resistance. The pH and concentration experiments were operated using water with on average 22°C in room temperature environment for 180 minutes, of which the BPMED was turned on for 178.5 minutes. At t=0, t=5, t=10, t=20, t=30, t=60, t=90, t=120, t=150 an t=180 minutes, a sample of 2 milliliters was taken of the Acid, Base, Diluate and ERS solution. The pH and EC of all solutions was checked before starting the experiment to track unusualities and the values of EC, pH and temperature were continuously monitored and saved during the experiments. Two experiments per day were performed.

3.2.1 Investigating the effect of pH

The experiments were performed with diluate solutions of 50 g/L $(NH_4)_2SO_4$ solution with a pH in the range pH 2, 3, 4, 5, 6, 7, 8, 9 and 10, all other parameters were kept consistent. By dissolving 50 g/L $(NH_4)_2SO_4$ in 1 liter demineralized water, the solution had a pH of 5.3. By the adjustments made as described in Table B.2, the solutions with the desired pH were created. The volume needed to be added was determined by a pH probe. Because for the diluate solutions of pH 2, 3, 4 and 5 an addition of H_2SO4 was required, these pH diluates are for the scope of this project considered as the 'acidic spectrum' or 'low pH range'. The pH 6, 7, 8, 9 and 10 solution required the addition of NH_4OH and are therefore considered as the 'alkaline spectrum' or 'high pH range' in this report.

3.2.2 Investigating the effect of concentration

The experiments on the effect of concentration were performed consistently with the pH experiments and temperature experiments, with selectively varying the initial diluate $(NH_4)_2SO_4$ concentration. Experiments were performed in duplicate for 50 g/L $(NH_4)_2SO_4$, 100 g/L $(NH_4)_2SO_4$, 150 g/L $(NH_4)_2SO_4$, 200 g/L $(NH_4)_2SO_4$ and 250 g/L $(NH_4)_2SO_4$. The duration of the experiment was 180 minutes. The pH for these experiments was fixed at the optimum pH level found in the previous experiments. In Table B.2 in Appendix B, the adjustments of the diluate solutions containing $(NH_4)_2SO_4$ is depicted.

3.2.3 Temperature experiments

The temperature experiments were performed by placing the whole set-up in an incubator, as depicted in Figure 3.3. All equipment was checked for its functionality at these temperatures.

As a result of the pH experiments, the pH of the diluate solution used for all temperature experiments was adjusted with 160 uL 1M H_2SO4 solution and it furthermore contained 50 g/L $(NH_4)_2SO_4$. The temperature experiments were performed in duplicates at a temperature of 20°C, 25°C, 30°C, 35°C and 40°C. The incubator was activated at the desired temperature the evening before the experiment, with the initial Acid, Base, Diluate and ERS solutions placed in there. At that moment, the mass of the bottles including solutions was measured and a sample was taken (t=-1), to keep track on both ammonia volatilization and water evaporation during the night. The mass weighted and the samples taken at t=0 (just before the start of the experiment) were used for further calculation. For the duplicate experiments, the same procedure was used, but with making the solutions during the morning and using them in the afternoon. During the experiment, the temperature inside the incubator was monitored with a temperature sensor.

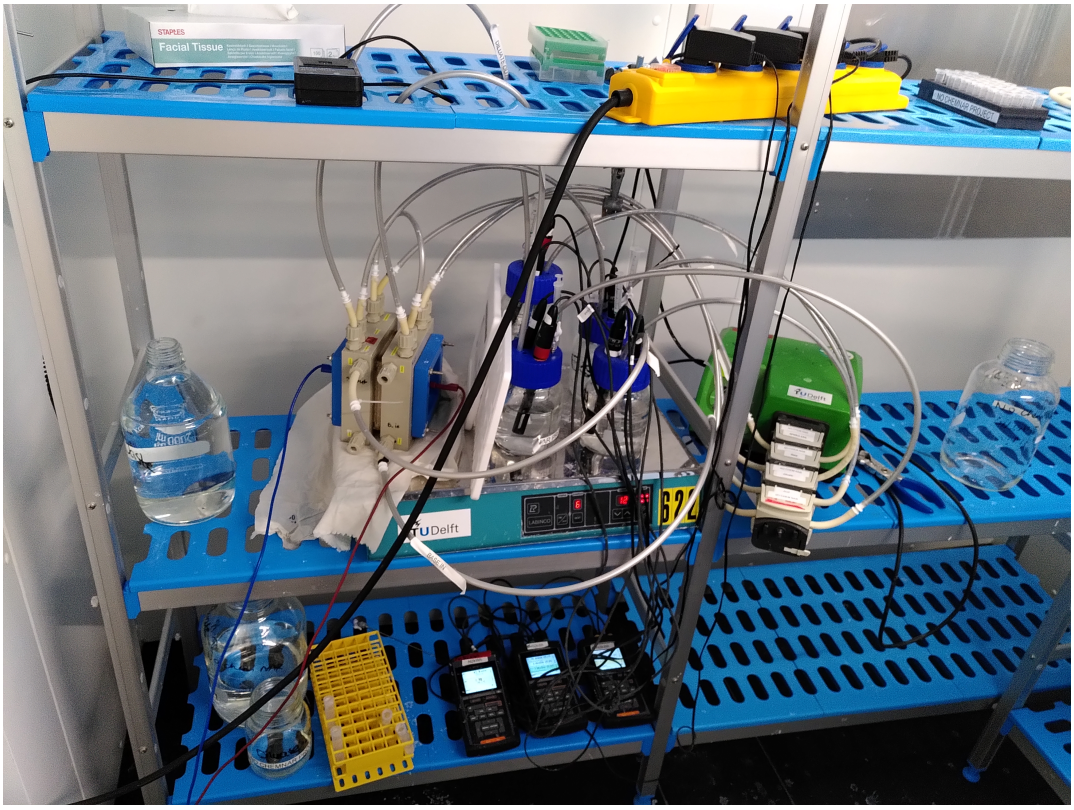

Figure 3.3: Visualisation of the set-up during the experiments researching the influence of temperature.

3.2.4 Concentration analysis

The sulfate and ammonium concentrations were measured in batches, all with the same dilutions to keep the analysis as consistent as possible. The samples were always analysed in duplicates and the average of the sample was used. It was also checked whether ammonium would diffuse out of the tubes, but that was invalidated. The ERS final sulfate and ammonium concentrations of the first experiment were used as initial concentrations for ERS for the second experiment.

3.3 Set-up development

Before starting the actual experiments researching the influence of pH, concentration and temperature on ammonium sulfate removal with BPMED, the set-up was developed and experiments were optimized to create the most optimal conditions. In this section, the reasoning behind the choices made is being discussed. It should be noted that those were singlicate experiments without corrections performed on the sulfate concentrations measurements. The removal percentage was based on theoretical start concentrations, which were randomly checked by concentration analysis. However, these experiments provide a clear guideline towards the most optimal set-up.

3.3.1 LCD determination

Initially, it was decided that the diluate concentration used for the experiments was set to 50 g/L . The Limiting Current Density was determined for a diluate stream of 5 g/L, aiming for 90% removal efficiency. The Limiting Current Density could not be determined for 50 g/L $(NH_4)_2SO_4$, since the power supply could not provide the needed current. The LCD was determined with an ED cell, by recirculating the diluate and concentrate stream. Starting at 0 A current and 0 V voltage, with increasing the current manually with steps of 0.01 A. By reaching the maximum voltage of 30 V, the experiment was stopped. The minimum resistance during the experiment stands for the value of the LCD. The LCD for 5 g/L $(NH_4)_2SO_4$ was found to be 194 $A \cdot cm^{-2}$, equal to a constant current of 1.24 A for one experiment, and for 196 $A \cdot cm^{-2}$, equal to a constant current of 1.26 A for this membrane (Appendix D). In earlier work, the current was set to a certain percentage of the LCD, based on an optimization between energy consumption and membrane surface [59]. However, because the LCD in our case was determined for 90% removal efficiency with still components present in the diluate preventing the increase of energy consumption, the current applied to the cell (I) was set constant at 1.2 A for all experiments. It was assumed that this LCD calculated for the ED cell could be applied to the BPMED cell as well.

3.3.2 Concentration determination

Determination of ammonium (NH_4^+) and sulfate (SO_4^{2-}) concentrations can be done by various methods like Ion Chromatography (IC) and tube tests based photometric measurements. A comparison was made for known concentrations $(NH_4)_2SO_4$ in miliQ water. It was found that the concentration of ammonium could be determined precisely, both with IC and tube tests (Appendix B, Table B.3). The sulfate concentration measurements showed difficulties with precision, especially for higher concentrations. The deviation was found to be higher for IC measurements and therefore the decision was made to use the tube tests for concentration determination of both ammonium and sulfate.

3.3.3 Acid and Base start concentrations

To provide an initial electrical conductivity ensuring the capacity to conduct current, the acid and base initial streams required the addition of a small amount of ions. Several options were researched:

- 0.01 M $(NH_4)_2SO_4$ in both acid and base
- 0.01 M H_2SO4 in the acid and 0.01 M NH_4OH in the base
- 0.01 M $(NH_4)_2SO_4$ in the acid and 0.01 M NH_4OH in the base

The first option, with $(NH_4)_2SO_4$ in both acid and base, would result in a small pollution of SO_4^{2-} in the base and NH_4^+ in the acid. In the second option, with H_2SO4 initially in the acid and NH_4OH

initially in the base, there would be no pollution based on the initial concentrations, but on the other hand, there might be a difference in the driving force for ions to move during the experiment. The last option researched was based on the fact that the produced sulfuric acid can be reused in the stripper/scrubber system, while the produced ammonium hydroxide might be of interest for selling purposes. In that particular case, a high purity of the ammonium hydroxide base is more important than a high purity of sulfuric acid.

As can be seen in Appendix B, Table C.1, the first option with 0.01 M $(NH_4)_2SO_4$ in both acid and base is found to have the smallest ammonium pollution of the acid with a high ammonium yield towards the base. Therefore, the decision was made to start with an initial start concentration of 0.01 M $(NH_4)_2SO_4$ in both acid and base.

3.3.4 Choice of volume

During all experiments, the $(NH_4)_2SO_4$ salt was dissolved in 1000 mL water for the diluate solution. The acid, base and ERS salts were dissolved in 500 mL water. This ratio of 1:2 was mostly to acquire a more concentrated acid and base stream.

3.3.5 Timespan of experiment

Initial test experiments were performed for a duration of 120 minutes resulting in an ammonium removal efficiency of 60%. Later experiments were investigated for a longer duration. By evaluating the ammonium removal during the time span of the experiment, the ammonium concentration at different time instants was measured, as depicted in Appendix B, Table B.4. To gain an ammonium removal efficiency of 90% for an initial 50 g/L $(NH_4)_2SO_4$ diluate solution, a time span of 180 minutes was found to be convenient for the pH and concentration experiments.

During the temperature experiments it was found that constant current could not be assured at all temperature for the full time span of 180 minutes. However, the presence of constant current is crucial for ensuring the amount of power going through the membrane. Consequently, it was decided to stop the temperature experiments after 150 minutes and compare the results accordingly.

3.3.6 Electrode Rinse Solution

The Electrode Rinse Solution is necessary in the set-up to ensure the capacity to transfer current originating at the electrodes throughout the entire stack. Usually a high salt concentration is used resulting in a high Electrical Conductivity which would decrease membrane resistance and therefore decrease energy consumption [74]. 1 M $NaNO_3$ salt solution was used as ERS solution in prior BPMED experiments [36]. Since the anion for the experiments in this research is SO_4^{2-}, the decision was made to use a 1 M Na_2SO_4 solution as Electrode Rinse Solution, which equals 71 gram Na_2SO_4 per 0.5 liter demineralized water.

During the first trial experiments, it was found that the pH of the ERS was not consistent over the experiments, which could have an impact on the experiment, even though the only functionality it should have is transporting current from electrodes to the stack. In some cases the ERS tended to acidify which implies H^+ leakage towards the ERS, whereas in other cases no H^+ leakage seemed to occur. In the case of acidifucation, the final ERS had a pH between 2 and 2.25. The pH of the ERS seemed to have an effect on the eventual ammonium an sulfate concentrations. The theoretical explanation behind these phenomena are out of scope for this research. It should be noted that in this case, no buffering component is present in any of the solutions, which can result in a big pH change by only little H^+ leakage. It might be that still quite some H^+ is present in the tubes and stack, which

eventually penetrates towards the ERS in the next experiment. As a consequence to the inconsistency in ERS solution, the decision was made to use an acidified ERS consisting of 1 M Na_2SO_4 solution of pH 2.

3.3.7 Type of membrane

Initially, a PC 100 membrane with Cation Exchange End Membranes (CEEM) was used in the BPMED stack, which is especially made for the production of sulfuric acid. The PC 100 membrane was compared to the PC 100D cell, with bipolar membranes made for the production of organic acids. The two membranes were compared both with CEEM. Both the PC 100 and PC 100D were tested with an ERS consisting of 1 M Na_2SO_4 pH 5.7 solution and with an acidified ERS of 1 M Na_2SO_4 pH 2.25 solution. Some observations were:

- The PC 100 membranes resulted in a more acidic base and a less basic acid than the PC 100D membrane.
- A higher concentration of sulfate ended up in the acid solution acid by using the PC 100 membrane, as well as smaller losses of ammonium to ERS were found, compared to the PC 100D membrane.
- The current provided by the power supply was not constant from the start of the experiment for the PC 100D membrane stack. Apparently, the initial resistance on the PC100D compared to the PC 100 membrane was found to be higher.

By comparing the concentrations of NH_4^+ and SO_4^{2-} in the acid, base, diluate and ERS solution after running the experiment for 120 minutes, it became clear that for both an ERS at pH 5.7 and ERS at pH 2.25 the PC 100D cell seemed to perform better for the sake of this research. Less pollution of ammonium towards the acid was observed for the PC 100D cell. Consequently, more of the removed NH_4^+ ended up in the final base solution. Interestingly, the pollution of the base with SO_4^{2-} was found to be minimal. The removal efficiency of both sulfate and ammonium seemed comparable for both type of membranes. Based on these observations, the decision was made to continue with a PC 100D bipolar membrane stack. In Appendix B, a more detailed explanation is provided.

3.3.8 Type of End membranes

For the PC 100 and PC 100D stack with CEEM, it was found that a substantial amount of NH_4^+ was lost to the ERS solution (circa 9%). This is undesirable, since this loss pollutes the ERS and it diminishes the potential ammonium yield in the base. End membranes are the barrier between the stack and the ERS solution, and can therefore selectively allow anions or cations to pass. As can be seen in Figure 3.1, the use of Anion Exchange End Membranes (AEEM) can let SO_4^{2-} ions selectively pass from the ERS over the membrane towards the acid solution at the cathode and vice versa. On the other hand, SO_4^{2-} from the diluate solution can be transferred to the ERS and vice versa at the anode. By using an AEEM, NH_4^+ (theoretically) will not get lost towards the ERS, but SO_4^{2-} can, which was confirmed (Appendix B, C.0.2). The choice was made for minimization of ammonium losses and therefore the PC 100D stack with AEEM membranes was used in further experiments.

3.3.9 Mass correction for salt dissolution

The experiments were performed with salts dissolved in the acid, base, diluate and ERS volumes. Since the concentrations of the diluate and ERS were significant (50-250 g/L and 142 g/L, respectively), a correction for the mass of these salts had to be performed. By research it was found that dissolving 50 g/L $(NH_4)_2SO_4$ in 1 liter demineralized water, resulted in an increase in mass of 50 g. Similarly, the addition of 100 g/L, 150 g/L, 200 g/L and 250 g/L $(NH_4)_2SO_4$ resulted in the increase of mass of 100g, 150, 200 g and 250 g. The addition of 71 g Na_2SO_4 to 0.5 liter demineralized water resulted in an increase of 71 g of mass. The initial mass of diluate and ERS were therefore corrected by amount of grams salt added. The initial volumes of acid and base were not corrected, since the dissolution of 0.66 g $(NH_4)_2SO_4$ to 0.5 liter had negligible impact. Because it was not known where the salts would end up, some assumptions based on concentrations and theoretical knowledge were made. Firstly, for the pH experiments a removal ammonium and sulfate efficiency between 80 and 90% was found, so a correction of 5 g subtracting from the final diluate mass was performed. Since the acid contains a high concentration of both NH_4^+ and SO_4^{2-}, and since SO_4^{2-} is a heavier ion than NH_4^+, the correction was made by 35 grams subtraction from the acid and 10 g subtraction from the base. It was assumed that the Na_2SO_4 present in the ERS only circulated in the ERS, so 71 gram was subtracted from the final ERS mass.

Moreover, for the concentration measurements, a similar correction was performed. The concentrations of acid and base were corrected with a subtraction of 35 g and 10 g respectively. The final diluate mass was corrected with the left-over part of the initial mass $(NH_4)_2SO_4$. The 71 g Na_2SO_4 was subtracted from the final ERS mass.

For the temperature measurements, the same correction was performed on the masses as was done for the pH experiments, since these experiments had an initial concentration of 50 g/L $(NH_4)_2SO_4$ as well.

3.3.10 Sulfate measurement correction

The prior steps in the set-up development were mostly based on the ammonium concentrations found in solution. As deliberated already, the sulfate measurements were not found to be as accurate as the ammonium concentration measurements. The sulfate concentrations in solution were found to be estimated higher by the MACHEREYNAGEL NANOCOLOR tube tests than the actual value. Therefore, the total mass balance was found to be higher than 100%. which made the measurements less reliable. One of the reasons for the sulfate inaccuracy could be found in inaccuracies in performing the dilution. Since the volumes were of high expected sulfate concentrations, high dilution factors had to be performed for being able to use the sulfate 200 MACHEREYNAGEL NANOCOLOR tube tests. By performing a larger dilution, the relative error can become higher and therefore create a bigger deviation from the real value. Therefore this dilution factor was researched by performing the dilution in various volumes, resulting in the conclusion that no dilution errors were made. Secondly, there seemed to be a trend in the worsening accuracy of the sulfate kits by an increasing concentration value within the range of the sulfate 200 kits. For higher values, a bigger mistake was found to be present (Figure 3.4). Consequently, a correction on the sulfate concentrations measured by the MACHEREYNAGEL NANOCOLOR sulfate 200 tube tests had to be performed to create reliable results.

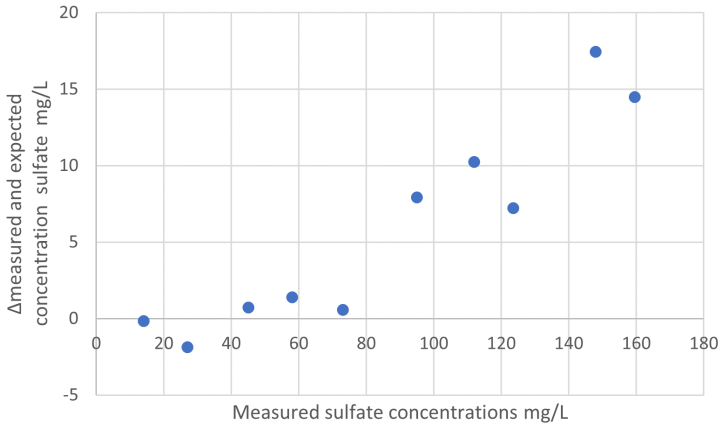

Figure 3.4: Calibration curve showing the deviation between the expected and measured SO_4^{2-} concentration in solution.

For values with a concentration between 20 and 40 mg/L SO_4^{2-} no correction was performed. Between 40 and 80 mg/L SO_4^{2-}, the concentration was lowered with 1 mg/L SO_4^{2-}. By a concentration higher than 80 mg/L SO_4^{2-}, no correction was performed. No measurements of above 90 mg/L were performed.

After correction, the sulfate measurements were still not found to be fully accurate. Therefore, the total of 200 % SO_4^{2-} (Acid + Base + Diluate + ERS) was spread over those streams based on their percentagewise contribution to the sum of concentrations.

4 Results

In this results section, an overview on the obtained results is given. In section 5, a more detailed elaboration on the results and the scientific interpretation of the results is presented.

4.1 General observations

Some important phenomena were observed during all experiments:

- During the experiments carried out, the pH of the acid, diluate and ERS streams initially decreased. Furthermore, the pH and EC had an equal decline over time as depicted in Appendix H, Figure H.0.1 for pH 4 diluate (which is similar to other experiments). The pH of the acidified ERS volume was about 1.8 at t=180. For the diluate, a decrease in pH was observed for most of the experiments, except the experiments with high diluate pH and high temperature. Similarly, the acid stream showed a decrease in pH resulting in a pH of approximately 1. The base stream eventually showed an increase in pH during all experiments resulting in a pH of approximately 10.5 The electrical conductivity during the experiments showed a similar pattern for all experiments too (Appendix H, Figure H.0.1b). The EC in the ERS slightly increased over time. The EC of the diluate decreased over time, eventually approaching 0 S/cm. The EC of both acid and base increased.

- Volume losses with an average of 4% based on the initial and final weight were found in the both pH and concentration experiments. For the temperature experiments, these losses were observed to be 10% on average. These losses were caused by either evaporation, spilling or left over volume in the membrane and tubes.

- (Undesired) Ammonium leakage and sulfate leakage towards the acid and base respectively were found to be present during all experiments. Leakages of more than 40% of the initial ammonium concentration in the diluate towards the acid stream were observed where only 1% of the initial sulfate concentration leaked into the base stream.

- The physical membrane elements and the cell appeared to have been affected by the exposure of extreme conditions during the experimental work. As visible in Figure 4.1, parts of the cell rods were corroded, mostly towards the anode side of the cell. The corrosion was also visible in the corners of the membranes. Additionally, scaling of the membranes was observed.

- The final sulfate concentration in the base was lower than the initial sulfate concentration in the base. This showed movement of sulfate from the base towards the acid stream.

- For all experiments (unless stated differently) the ERS solution of duplicate 1 was re-used as ERS solution for duplicate 2. Observations showed that the pH and EC of the ERS lowered during most of the experiments and consequently the initial ERS pH and EC of the second duplicate always started with a lower initial pH. Furthermore it was found that in all experiments, sulfate was transported away from the ERS, resulting in lower sulfate concentrations at t=180 min.

- As a test, the NH_4^+ concentration in the acid, base, diluate and ERS stream was tested immediately after volume extraction from the streams and after 1, 2 and 3 days. No difference in NH_4^+ concentration was found between those measurements, indicating that NH_4^+ did not leave the solution in the form of ammonia after time.

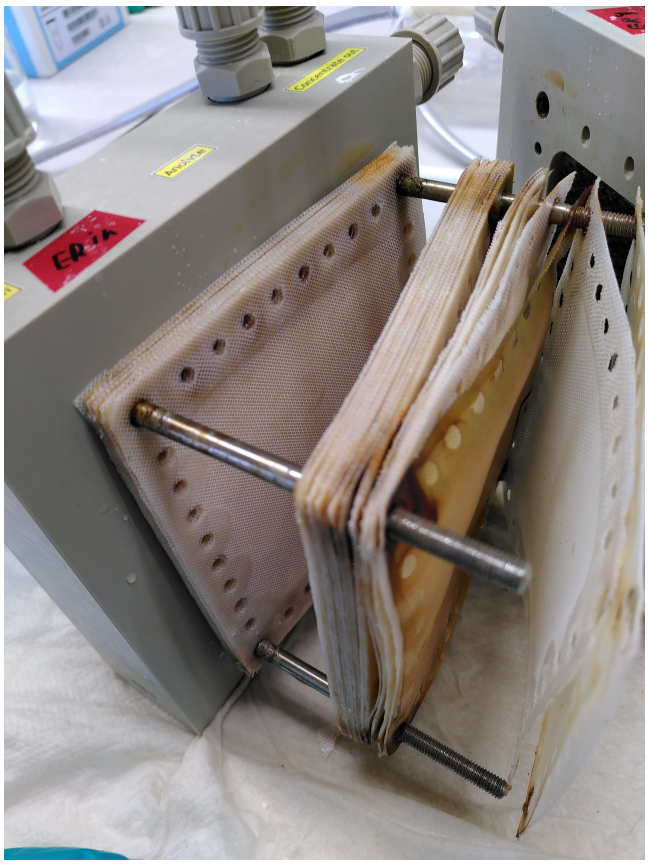

Figure 4.1: Physical damage of the BPMED membrane stack and cell after running all experiments performed during the time span of this thesis. Corrosion is visible on the rods of the cell and in the corners of the membrane stack. Scaling was observed as well, but is not clearly visible in this figure.

4.2 Influence of pH

In this section the influence of the initial pH of the diluate on the treatment by BPMED is assessed by presenting and analyzing the results.

The experiments with diluate having initial pH 2, 3, 4 and 5 were all performed with the same initial amount of NH_4^+ (13652 mg) present in the diluate, but with a difference in initial SO_4^{2-} mass, due to the addition of sulfuric acid for pH correction. For the experiments with an initial diluate pH of 6, 7, 8, 9, and 10, different amounts of initial NH_4^+ were present in solution but the same amount of SO_4^{2-} (36348 mg) was present. Therefore, the diluate pH 2, 3, 4 and 5 experiments were comparable and similarly, the initial diluate pH 6, 7, 8, 9, an 10 experiments were comparable. Consequently, both pH ranges were evaluated separately.

4.2.1 Electrochemical energy consumption

The electrochemical energy consumption based on the NH_4^+ transported from the diluate for different initial diluate pH is depicted in Figure 4.2. It was found that the electrochemical energy consumption decreased with increasing pH. Comparing the experiments with initial diluate pH between 2 and 5, the experiment with an initial pH of 2 was observed to have the highest electrochemical energy consumption of 22.68 $\pm$0.75MJ*kg$^{-1}_{NH_4^+}$. A diluate solution with initial pH of 5 had a smaller electrochemical energy consumption of 19.57 $\pm$0.5MJ*kg$^{-1}_{NH_4^+}$. The experiments with an intermediary initial diluate pH were following this decreasing electrochemical energy consumption trend. In the alkaline range (diluate with pH 6, 7, 8, 9 and 10), the electrochemical energy consumption showed a decreasing trend as well.

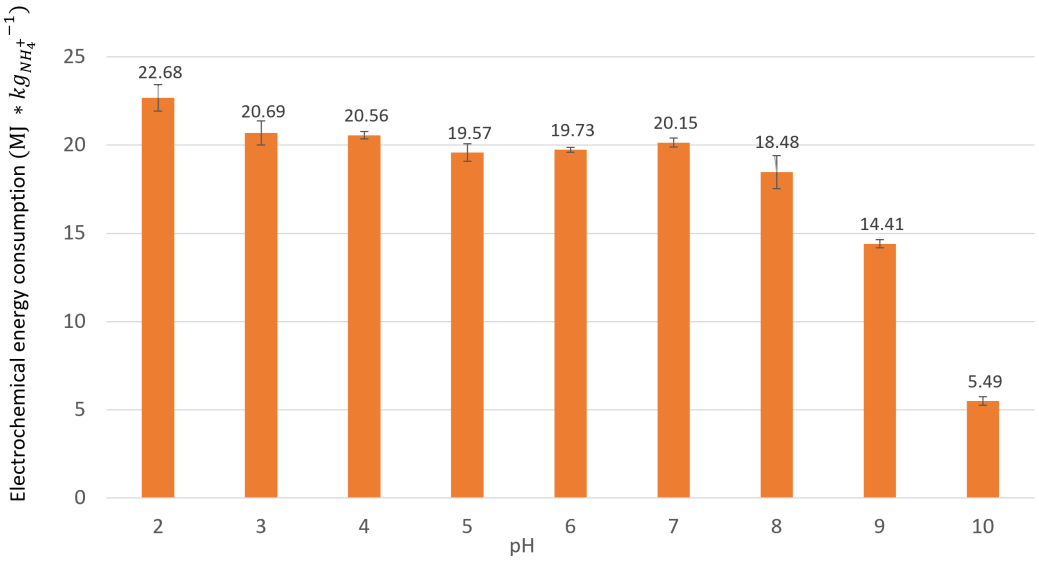

Figure 4.2: Electrochemical energy consumption for 50 g/L $(NH_4)_2SO_4$ diluate with varying pH in $MJ \cdot kg_N H_4^+$ at room temperature. The bars represent the average of two experiments; the error bars depict variations between experiments.

4.2.2 NH_4^+ current efficiency

The NH_4^+ current efficiency increased with pH, as depicted in Figure 4.3. In other words: the current needed for the transportation of the same amount of NH_4^+ decreased with increasing pH. The NH_4^+ current efficiency for pH 3, 4, and 5 was found to be similar, however the difference with pH 2 is clear. The NH_4^+ current efficiency of 48% for the pH 2 experiment was clearly lower compared to the NH_4^+ current efficiencies of 52% and 54% for the pH 3 and pH 4 & 5 experiment, respectively. For pH 6 to 10, the NH_4^+ current efficiency was observed to be even higher. It should be noted that the addition of more NH_4^+ to the initial diluate solution resulted in a higher amount of NH_4^+ ions that could potentially be transported with increasing initial diluate pH.

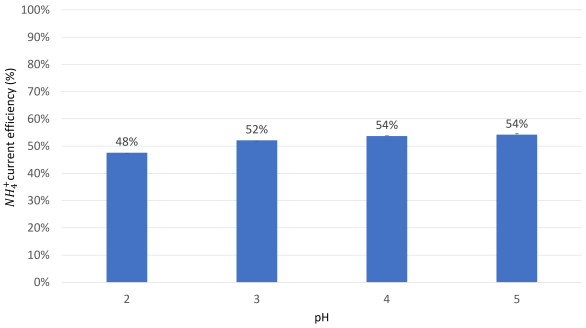

(a) NH_4^+ current efficiency for 50 g/L $(NH_4)_2SO_4$ diluate solutions with pH 2 - 5 at room temperature. The diluate solutions contained the same amount of ammonium. The bars represent the average of two experiments; the error bars depict variations between experiments.

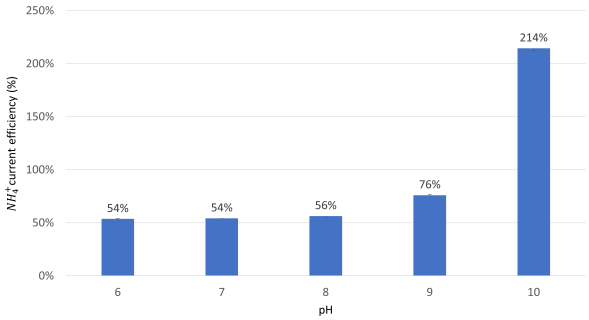

(b) NH_4^+ current efficiency for 50 g/L $(NH_4)_2SO_4$ diluate solutions with pH 6 - 10 at room temperature. The diluate solutions contained the same amount of sulfate. The bars represent the average of two experiments; the error bars depict variations between experiments.

Figure 4.3: Influence of pH on NH_4^+ current efficiency

4.2.3 Concentrations and Purity

The final NH_4^+ concentrations reached in the base and the final SO_4^{2-} concentrations reached in the acid are presented in Table 4.1. The concentration of NH_4^+ was increasing in the base with increasing initial diluate pH. No clear trend could be observed for the SO_4^{2-} concentration in the acid. The purity of the acid was slightly decreasing with increasing pH. The purity of the base was found to be constant with increasing pH. The notable initial diluate pH 10 solution showed a clearly lower acid purity and slightly higher base purity. The purity values are presented in Table 4.2.

Table 4.1: Final (a) SO_4^{2-} concentrations (mg/L) and (b) NH_4^+ concentrations (mg/L) in the acid and base stream respectively for varying initial diluate pH.

pH	Final SO_4^{2-} concentration in acid (mg/L)		
2	61581	±	2537
3	66603	±	1265
4	63016	±	2967
5	66603	±	2719
6	64088	±	2735
7	64645	±	2855
8	63796	±	2930
9	68342	±	2229
10	67313	±	410

(a) SO_4^{2-} concentrations (mg/L) at t=180 in the acid stream at varying initial diluate pH.

pH	Final NH_4^+ concentration in base (mg/L)		
2	10730	±	70
3	11565	±	235
4	11640	±	130
5	12165	±	155
6	12075	±	65
7	12125	±	85
8	11600	±	200
9	13500	±	500
10	22500	±	500

(b) NH_4^+ concentrations (mg/L) at t=180 in the base stream at varying initial diluate pH.

Table 4.2: Final purities of the acid and base stream at t=180 with initial diluate streams containing 50 g/L $(NH_4)_2SO_4$ at room temperature with varying pH

pH	Purity acid			Purity base		
2	86.5%	±	0.7%	94.1%	±	0.2%
3	85.7%	±	0.2%	95.3%	±	0.2%
4	85.7%	±	0.4%	96.1%	±	0.0%
5	85.5%	±	0.6%	95.9%	±	0.5%
6	84.2%	±	0.2%	94.9%	±	0.5%
7	85.3%	±	0.5%	96.6%	±	0.4%
8	84.2%	±	1.6%	92.4%	±	0.1%
9	83.7%	±	0.3%	94.3%	±	2.3%
10	76.8%	±	0.2%	97.0%	±	0.6%

4.2.4 Removal Efficiency

The removal efficiency of both NH_4^+ and SO_4^{2-} with increasing pH is shown in Figure 4.3. In the diluate pH range pH 2-5, the NH_4^+ and SO_4^{2-} removal efficiency elevated. In the diluate range pH 6-10, the NH_4^+ removal efficiency was found to be decreasing, while the SO_4^{2-} removal efficiency raised with increasing pH.

Table 4.3: Percentagewise removal of NH_4^+ and SO_4^{2-} from the initial diluate 50 g/L $(NH_4)_2SO_4$ solution with a certain pH.

pH	NH_4^+ removal from diluate			SO_4^{2-} removal from diluate		
2	83.6%	±	0.5%	84.4%	±	2.0%
3	92.0%	±	0.1%	93.5%	±	0.2%
4	94.4%	±	0.2%	94.5%	±	0.3%
5	95.1%	±	0.7%	91.9%	±	1.1%
6	94.2%	±	0.6%	90.5%	±	1.7%
7	94.8%	±	0.4%	91.3%	±	0.4%
8	94.9%	±	2.2%	92.7%	±	2.9%
9	97.3%	±	0.9%	94.7%	±	0.6%
10	79.5%	±	1.0%	98.9%	±	0.0%

4.2.5 Potential development over time

Zooming in on the acidic spectrum, differences were detected in the potential development over time between the initial diluate pH 2 and initial diluate pH 5 experiments (Figure 4.4). Towards the end of the experiment a slight increase in potential was found for the pH 5 experiment, which was not present for both pH 2 experiments. A similar increase of potential towards the end of the experiment was observed for initial diluates with pH 3 and 4.

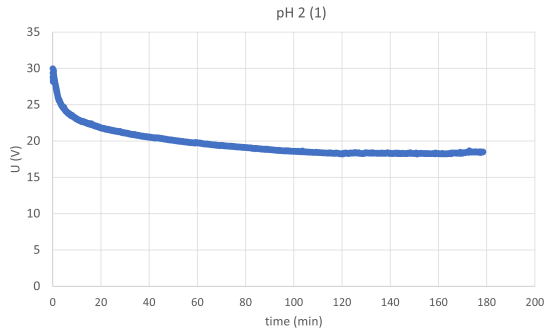

(a) Potential/Voltage development over time for 50 g/L $(NH_4)_2SO_4$ diluate solution of pH 2 duplicate 1.

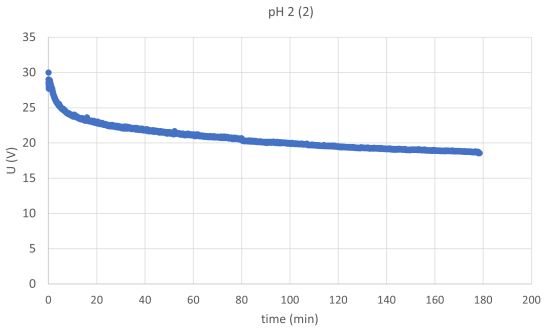

(b) Potential/Voltage development over time for 50 g/L $(NH_4)_2SO_4$ diluate solution of pH 2 duplicate 2.

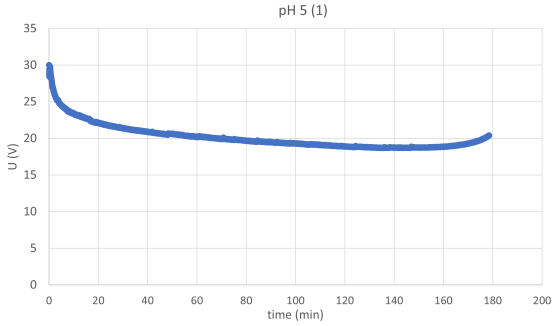

(c) Potential/Voltage development over time for 50 g/L $(NH_4)_2SO_4$ diluate solution of pH 5 duplicate 1.

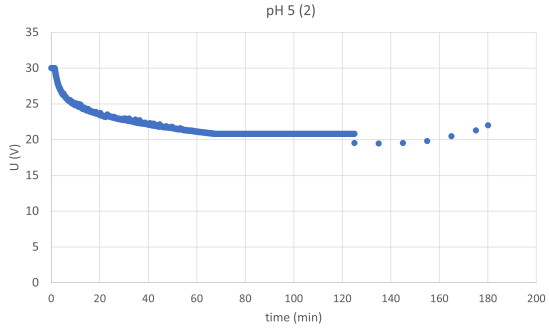

(d) Potential/Voltage development over time for 50 g/L $(NH_4)_2SO_4$ diluate solution of pH 5 duplicate 2. Since and error happened with transmission of power supply data after 80 minutes, the potentials were written down manually every 10 minutes (see dots)

Figure 4.4: Evolution of potential for the initial diluate pH 2 and initial diluate pH 5 duplicate experiments.

Zooming in on the alkaline spectrum, differences were found in the potential development over time between the initial diluate pH 6, 9 and 10 experiments (Figure 4.5). In the course of potential over time for the pH 6 experiments, towards the end of the experiment a slight increase in potential was observed, which was similar as for the prior discussed initial diluate pH 6 experiment. The pH 9 initial diluate showed an steeper increase of potential earlier during the experiment. For the pH 10 experiments, the potential increase was shown even earlier during the time span of the experiment, eventually reaching the plateau of 30 Volt, resulting in varying current.

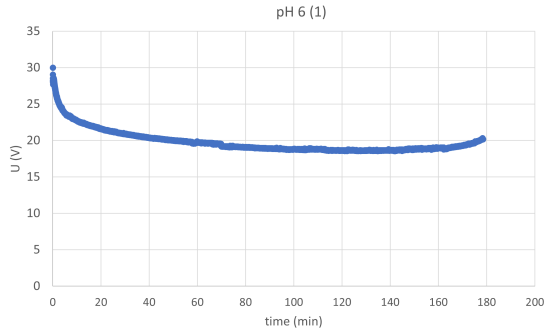

(a) Potential/Voltage development over time for 50 g/L $(NH_4)_2SO_4$ diluate solution of pH 6 duplicate 1.

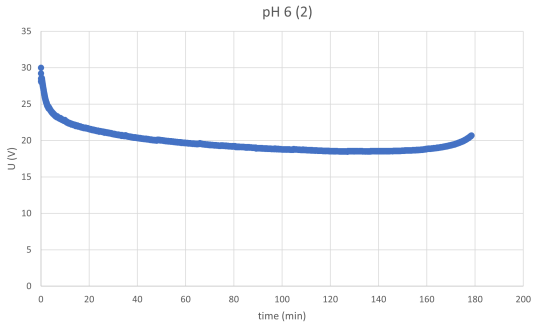

(b) Potential/Voltage development over time for 50 g/L $(NH_4)_2SO_4$ diluate solution of pH 6 duplicate 2.

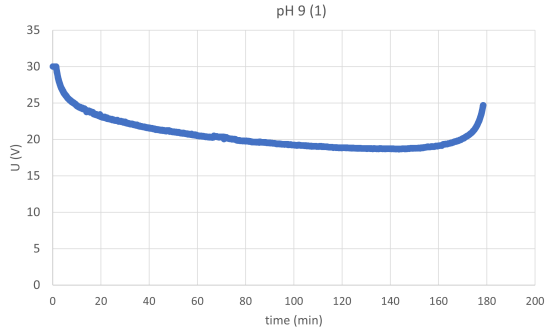

(c) Potential/Voltage development over time for 50 g/L $(NH_4)_2SO_4$ diluate solution of pH 9 duplicate 1.

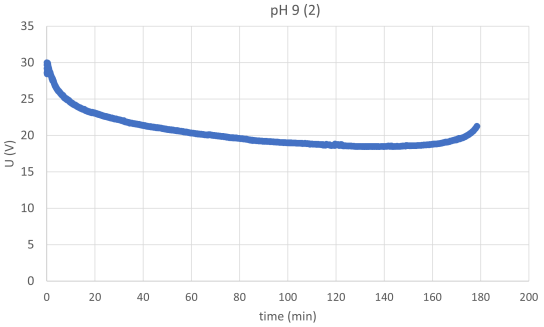

(d) Potential/Voltage development over time for 50 g/L $(NH_4)_2SO_4$ diluate solution of pH 9 duplicate 2.

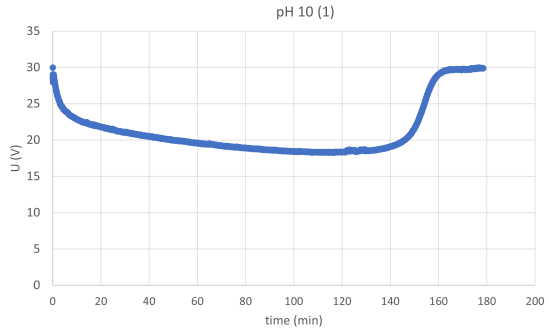

(e) Potential/Voltage development over time for 50 g/L $(NH_4)_2SO_4$ diluate solution of pH 10 duplicate 1.

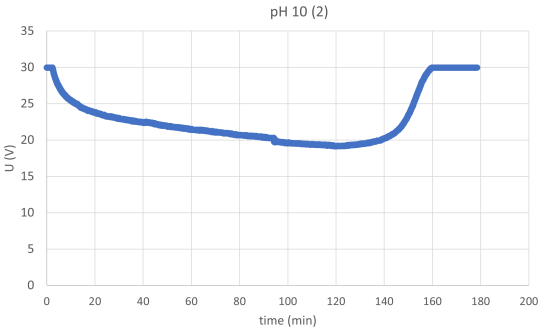

(f) Potential/Voltage development over time for 50 g/L $(NH_4)_2SO_4$ diluate solution of pH 10 duplicate 2.

Figure 4.5: Evolution of potential for the initial diluate pH 6, 9 and 10 duplicate experiments.

4.2.6 Redistribution of NH_4^+ and SO_4^{2-}

The ions present in the initial diluate solutions containing 50 g/L $(NH_4)_2SO_4$ (NH_4^+ and SO_4^{2-} ions) and additional H_2SO4 and NH_4OH were spread over the base, acid, diluate and ERS solutions during the 180 minutes of BPMED treatment. Only a small percentage of the initially present NH_4^+ (0,0% - 0,3%) ended up up in the ERS solution (loss). With increasing pH of the diluate in the acidic spectrum (pH 2-5), an increasing amount of NH_4^+ was transported towards the acid solution, which is undesired (pH 2: 36.8% ± 1.2; pH 5: 45.0% ± 0.7 %). However, more NH_4^+ is transported towards the base solution as well, which is desired (pH 2: 39.4% ± 0.1; pH 5: 43.3% ± 0.5 %). The percentage of NH_4^+ concentration left-over in the diluate after 180 minutes was found to be highest for the diluate with

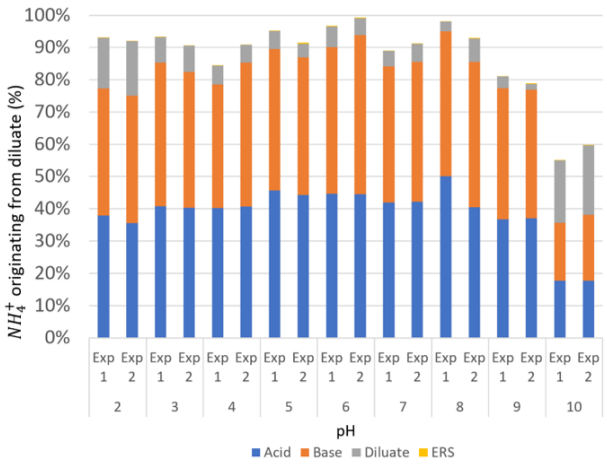

Figure 4.6: Redistribution of NH_4^+ originating from diluate solution after 180 minutes BPMED treatment of 50 g/L $(NH_4)_2SO_4$ diluate solutions for varying pH for the duplicate experiments (Exp1 and Exp2).

initial pH 2 (16.4 % ± 0.5 %) in the acidic spectrum. In the alkaline spectrum the initial pH 10 diluate solution showed to have the highest percentage of NH_4^+ concentration left-over in the diluate (20.5 % ± 1.0 %). In the acidic part, diluate with pH 5 had the lowest final NH_4^+ percentage left-over (4.9 % ± 0.7 %). The sum of NH_4^+ percentages in the acid, base, diluate and ERS stream did not reach 100 % due to losses because of volatilization or volume losses or inaccuracies in measurements. Also in the alkaline spectrum (pH 6-10), the absolute finale concentrations of NH_4^+ in both acid (Table 4.1) and base were found to increase with pH (acid pH 6: 11985 ± 335 mg/L NH_4^+; acid pH 10: 20300 ± 100 mg/L NH_4^+), which was in line with the increasing purity of the base. An overview of the percentage redistribution of NH_4^+ is provided in Figure 4.6.

The SO_4^{2-} redistribution originating from the initial diluate solution is shown in Figure 4.7. The total percentage exceeded the 100 % because of SO_4^{2-} transportation from the ERS stream towards the acid, base and or diluate stream or because of measurement errors. It was found that with higher pH, a smaller amount of SO_4^{2-} was left over in the diluate after 180 minutes. With increasing pH in the acidic spectrum (pH 2-5), an higher amount of SO_4^{2-} was transported towards the acid solution, which is desired (pH 2: 82% ± 2,5; pH 5: 99.9 % ± 0.7 %), see also Table 4.1. The percentage of SO_4^{2-} transported towards the base solution did not show a clear variation with pH (pH 2: 0,9% ± 0.0; pH 5: 0.7% ± 0.0 %). However, in the alkaline spectrum (pH 6-10), the absolute concentration of SO_4^{2-} transported to the acid stream (Table 4.1) was observed to slightly increase. The SO_4^{2-} concentration in the base was found to stay (more or less) equal with increasing pH (base pH 6: 644 ± 71 mg/L SO_4^{2-}; base pH 10: 695 ± 131 mg/L). The diluate solution was found to have less SO_4^{2-} ions present after 180 minutes BPEMD treatment with higher pH in the alkaline spectrum (pH 6: 9.5 ± 1.7 %; pH 10: 1.1 ± 0.0 %). In absolute numbers it was detected that for initial diluate pH 6 there was 3948 ± 674 mg/L SO_4^{2-} still present in diluate solution after 180 minutes, for the initial diluate pH 10 solution this was found to be 435 ± 11 mg/L SO_4^{2-}.

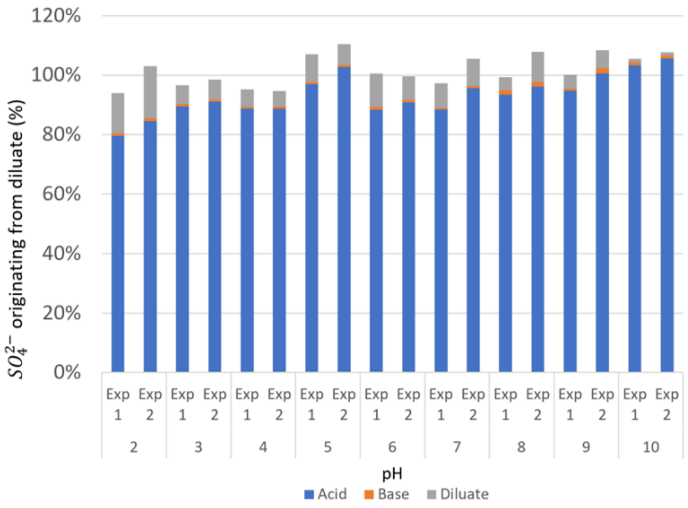

Figure 4.7: Redistribution of SO_4^{2-} originating from diluate solution after 180 minutes BPMED treatment of 50 g/L $(NH_4)_2SO_4$ diluate solutions for varying pH for the duplicate experiments (Exp1 and Exp2). The sulfate values were corrected as described in section 2.4.5. The ERS values were not visualized.

4.2.7 Final pH and EC values

In Appendix H, the final pH and EC values of the acid-, base-, diluate- and ERS stream are provided. A slightly increasing trend in the diluate final pH was found with rising initial diluate pH in the acidic spectrum (pH 2: 2.33 ± 0.03; pH 5: 2.51 ± 0.01). The electrical conductivity of the acid- base- and ERS solutions showed the same pattern for the varying initial diluate pH. However, the final EC of the diluate for the pH 2 experiments were higher than the final diluate EC of initial diluate solutions with pH 3, 4 and 5 (pH2: 1.58 ± 0.04 $*10^4$ $\mu S \cdot cm^{-1}$; pH 5: 5.92 ± 0.43 $*10^3$ $\mu S \cdot cm^{-1}$).

In the alkaline spectrum the acid, base and diluate streams were showing an elevation in final pH with higher initial diluate pH. The final diluate pH for the initial diluate pH 9 showed a rapid increase of pH towards the end of the experiment, see Figure H.2 in Appendix H. The diluate of the initial diluate pH 10 solution did not acidify, but showed an increase of pH towards the end of the experiments, which came together with a declining EC as depicted in Appendix H, Figure H.3. The final EC values of the acid streams lowered with increasing initial diluate pH in the alkaline spectrum, for pH 6: 1.23 ± 0.02 $*10^5$ $\mu S \cdot cm^{-1}$; pH 10: 9.46 ± 0.01 $*10^5$ $\mu S \cdot cm^{-1}$. The final EC values of the base streams were slightly higher with increasing initial diluate pH in the alkaline spectrum, for pH 6: 6.51 ± 0.38 $*10^3$ $\mu S \cdot cm^{-1}$; pH 10: 6.90 ± 0.25 $*10^3$ $\mu S \cdot cm^{-1}$. The final EC of the diluate solutions was detected to be rapidly reducing with increasing pH in the alkaline spectrum, up to almost no conductivity left after 180 minutes (pH 6: 6.55 ± 0.70 $*10^3$ $\mu S \cdot cm^{-1}$; pH 10: 928 ± 5 $\mu S \cdot cm^{-1}$).

4.2.8 Volume distribution

It was observed that with increasing pH and with the same total volume losses, more volume eventually ended up in the base stream. Less volume was left over in the diluate solution after 180 minutes for high diluate pH.

4.3 Influence of ammonium sulfate concentration

In this section the influence of the initial $(NH_4)_2SO_4$ concentration in the diluate on the treatment by BPEMD is assessed.

4.3.1 Electrochemical energy consumption

As shown in Figure 4.8, the electrochemical energy consumption lowered with an increasing initial $(NH_4)_2SO_4$ concentration in the diluate solution. The electrochemical energy consumption for 50 g/L $(NH_4)_2SO_4$ was found to be 20.56 ± 0.21 $MJ * kg^{-1}_{NH_4^+}$, while the electrochemical energy consumption for 250 g/L $(NH_4)_2SO_4$ was observed to be 12.78 ± 0.64 $MJ * kg^{-1}_{NH_4^+}$. The values for initial diluate concentrations of 100 g/L, 150 g/L 200 g/L and 250 g/L $(NH_4)_2SO_4$ showed a similar decreasing trend in electrochemical energy consumption.

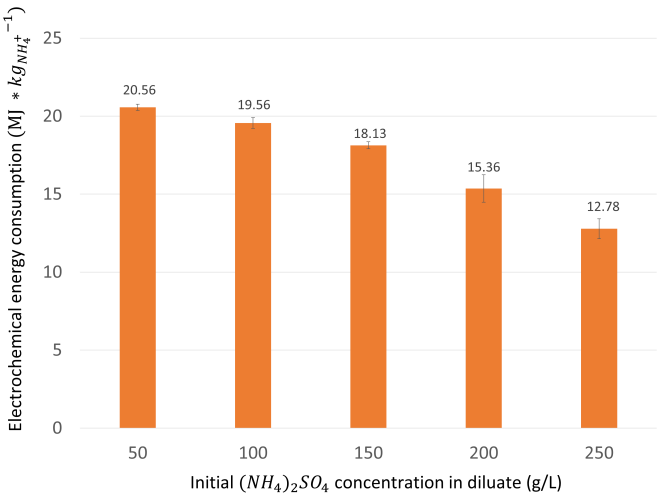

Figure 4.8: Electrochemical energy consumption for varying initial diluate $(NH_4)_2SO_4$ concentrations with pH 4 at room temperature in $MJ \cdot kg_{NH_4^+}$. The bars represent the average of two experiments; the error bars depict variations between experiments.

4.3.2 NH_4^+ current efficiency

The NH_4^+ current efficiency was found to be increasing with an increasing initial $(NH_4)_2SO_4$ concentration. The NH_4^+ current efficiency for an 50 g/L $(NH_4)_2SO_4$ initial diluate concentration was found to be 54 ± 0 %. The NH_4^+ current efficiency for an 250 g/L $(NH_4)_2SO_4$ initial diluate concentration was found to be 74 ± 6 %. For the same amount of current applied, more NH_4^+ was transported from the initial diluate solution.

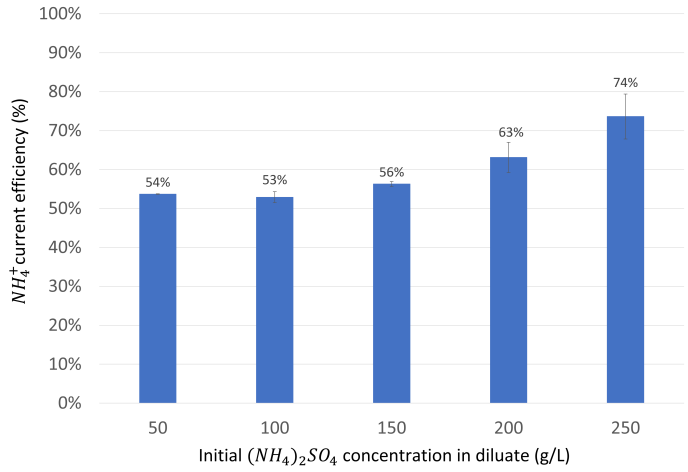

Figure 4.9: NH_4^+ current efficiency for varying initial diluate $(NH_4)_2SO_4$ concentrations with pH 4 at room temperature. The bars represent the average of two experiments; the error bars depict variations between experiments.

4.3.3 Concentrations and Purity

Both the purity of the acid as well as the purity of the base were found to decrease with an increasing initial diluate $(NH_4)_2SO_4$ concentration as shown in Table 4.4.

Table 4.4: Final purities of the acid and base stream at t=180 with initial diluate streams of pH 4 at room temperature with varying $(NH_4)_2SO_4$ concentrations.

$(NH_4)_2SO_4$ concentration (g/L)	Purity acid			Purity base		
50	85.7%	±	0.4%	96.1%	±	0.0%
100	84.1%	±	0.8%	93.5%	±	0.6%
150	82.0%	±	0.9%	93.0%	±	0.4%
200	82.2%	±	1.3%	88.7%	±	1.5%
250	83.0%	±	1.2%	89.6%	±	1.3%

Although the purities of both acid and base decreased with higher $(NH_4)_2SO_4$ concentration in the diluate, the SO_4^{2-} concentration in the acid and the NH_4^+ concentration in the base were higher with an increasing initial diluate concentration of $(NH_4)_2SO_4$, as shown in Table 4.5. In the final acid solution of the 50 g/L $(NH_4)_2SO_4$ experiment the NH_4^+ was 10505 ± 185 mg/L and the final acid concentration of the 250 g/L experiment contained 13985 ± 375 mg/L NH_4^+. In the final base solution of the 50 g/L $(NH_4)_2SO_4$ experiment the SO_4^{2-} concentration was found to be 4778.0 ± 7.3 mg/L and the final base concentration of the 250 g/L experiment contained 1742.8 ± 262.12 mg/L SO_4^{2-}.

Table 4.5: Final SO_4^{2-} concentrations (mg/L) and NH_4^+ concentrations (mg/L) in the acid and base stream respectively for varying initial diluate concentrations.

$(NH_4)_2SO_4$ concentration (g/L)	Final SO_4^{2-} concentration in acid (mg/L)		
50	63016	±	2967
100	65336	±	2663
150	60081	±	5302
200	63937	±	4828
250	68011	±	4167

(a) SO_4^{2-} concentrations (mg/L) at t=180 in the acid stream at varying initial $(NH_4)_2SO_4$ concentrations in diluate.

$(NH_4)_2SO_4$ concentration (g/L)	Final NH_4^+ concentration in base (mg/L)		
50	11640	±	130
100	13005	±	205
150	13845	±	45
200	15010	±	500
250	14920	±	160

(b) NH_4^+ concentrations (mg/L) at t=180 in the acid stream at varying initial $(NH_4)_2SO_4$ concentrations in diluate.

4.3.4 Removal Efficiency

In Figure 4.10 the removal of NH_4^+ (4.10a) and the removal of SO_4^{2-} (4.10b) are presented. With increasing initial $(NH_4)_2SO_4$ concentration of the diluate, an increasing absolute mass of NH_4^+ was removed from the diluate solution after 180 minutes of operation. With increasing initial $(NH_4)_2SO_4$ diluate concentration, a decreasing absolute mass of SO_4^{2-} was removed from the diluate solution after 180 minutes of operation.

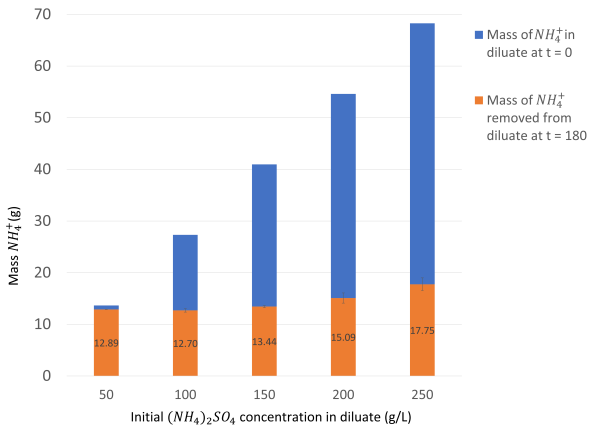

(a) Visualisation of the difference between the initial and final NH_4^+ mass for diluate solutions with varying initial $(NH_4)_2SO_4$ diluate concentrations at pH 4 and room temperature. The bars represent the average of two experiments; the error bars depict variations between experiments

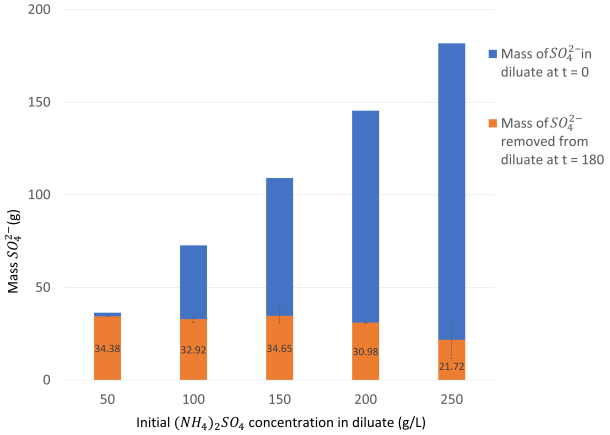

(b) Visualisation of the difference between the initial and final SO_4^{2-} mass for diluate solutions with varying initial $(NH_4)_2SO_4$ diluate concentrations at pH 4 and room temperature. The bars represent the average of two experiments; the error bars depict variations between experiments

Figure 4.10: Absolute mas of NH_4^+ and SO_4^{2-} removed from diluate for varying initial $(NH_4)_2SO_4$ concentrations.

In Table 4.6, the percentagewise removal of NH_4^+ and SO_4^{2-} from the initial diluate solutions is given. Both NH_4^+ and SO_4^{2-} removal decreased with increasing initial diluate $(NH_4)_2SO_4$ concentration.

Table 4.6: Percentagewise removal of NH_4^+ and SO_4^{2-} from the initial diluate $(NH_4)_2SO_4$ pH 4 solution of a certain concentration.

$(NH_4)_2SO_4$ concentration (g/L)	NH_4^+ removal from diluate			SO_4^{2-} removal from diluate		
50	94.4%	±	0.2%	94.5%	±	0.3%
100	46.5%	±	1.2%	45.3%	±	2.7%
150	32.8%	±	0.5%	31.8%	±	3.6%
200	25.3%	±	0.5%	21.3%	±	0.4%
250	26.0%	±	1.8%	11.9%	±	5.6%

4.3.5 Final pH and EC values

Appendix H shows an overview of the final pH and EC values of the acid, base, diluate and ERS streams. The diluate pH was observed to have a higher final pH with increasing initial $(NH_4)_2SO_4$ concentration (50 g/L: 2.50 ± 0.4; 250 g/L: 3.0 ± 0.1). The minimal pH was also found to be higher for a higher initial diluate concentration. The final pH in the acid showed an increasing trend as well. For the 50 g/L an final acid pH of 0.85 ± 0.2 was detected and for the 250 g/L initial diluate an final pH of the acid of 1.05 ± 0.1 was registered. The final pH in the base was not found to be changing with increasing initial $(NH_4)_2SO_4$ concentration.

The electrical conductivity of the acid lowered with higher initial diluate concentration (50 g/L: 1.20 ± 0.02 $*10^5$ $\mu S \cdot cm^{-1}$; 250 g/L: 1.11 ± 0.01 $*10^5$ $\mu S \cdot cm^{-1}$). The final EC of the base was found to be increasing with increasing initial diluate concentration (50 g/L: 5.96 ± 0.14 $*10^3$ $\mu S \cdot cm^{-1}$; 250 g/L: 9.11 ± 0.63 $*10^3$ $\mu S \cdot cm^{-1}$). The final EC of the base increased with increasing initial diluate concentration (50 g/L: 6.63 ± 0.0 $*10^3$ $\mu S \cdot cm^{-1}$; 250 g/L: 1.65 ± 0.01 $*10^5$ $\mu S \cdot cm^{-1}$). The ERS EC did not change with higher initial diluate concentration.

4.4 Influence of temperature

In this section the influence of the initial diluate temperature on the treatment by BPEMD is assessed. The experiments on the influence of temperature were performed for a duration of 150 minutes since LCD was reached before 180 minutes of operation for the 30°C, 35°C and 40°C experiments.

4.4.1 Membrane functionality

As already stated in section 4.1, the physical damage on the membrane was observed in the form of scaling and corrosion. However, besides the visible changes of the membrane stack, the functionality of the BPMED was affected as well. After exposure of the BPMED stack to 40°C, the functionality showed to be different than before the exposure of the membrane to this high temperature. A decrease in the absolute NH_4^+ removal from the diluate was observed and the total energy consumption increased. In this section, the results after exposure of the membrane to 40°C are depicted with grey bars. Those results were not used for the average purity and concentration values.

4.4.2 Electrochemical energy consumption

The electrochemical energy consumption lowered with higher initial temperature of the diluate solution. The initial diluate solution with 50 g/L $(NH_4)_2SO_4$, pH 4 and a temperature of 20°C had an electrochemical energy consumption of 20.3 ± 0.49 $MJ * kg^{-1}_{NH_4^+}$. The initial diluate solution with 50 g/L $(NH_4)_2SO_4$, pH 4 and a temperature of 40°C was found to have an electrochemical energy consumption of 15.9 ± 0.33 $MJ * kg^{-1}_{NH_4^+}$. The intermediate temperatures were showing an intermediate electrochemical energy consumption following the decreasing trend. Interestingly, the electrochemical energy consumption values for 30°C, 35°C and 40°C were found to be close. The electrochemical energy consumption for experiments performed after exposure of the membrane to 40°C were higher than the electrochemical energy consumption of experiments performed before and during exposure to 40°C.

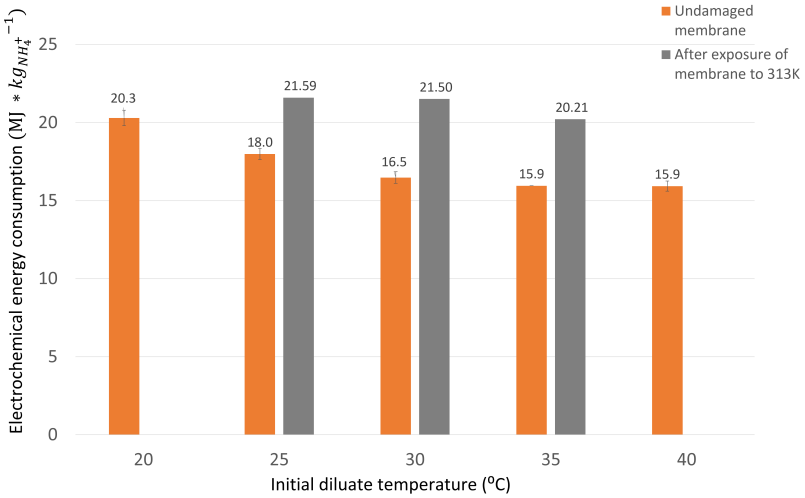

Figure 4.11: Electrochemical energy consumption for 50 g/L $(NH_4)_2SO_4$ diluate solutions with pH 4 at varying initial temperatures in $MJ \cdot kg_N H_4^+$. The orange bars represent the average of two experiments; the error bars depict variations between experiments. The grey bars represent one experiment each.

4.4.3 NH_4^+ current efficiency

The NH_4^+ current efficiency was observed to have an increasing trend with initial diluate $(NH_4)_2SO_4$ temperature. The NH_4^+ current efficiency increased from 57% ± 1% for 20°C to 61 % ± 0 % for 40°C. The NH_4^+ current efficiencies for experiments performed after exposure of the membrane to 40°C were found to be lower than the NH_4^+ current efficiency of experiments performed before and during exposure to 40°C.

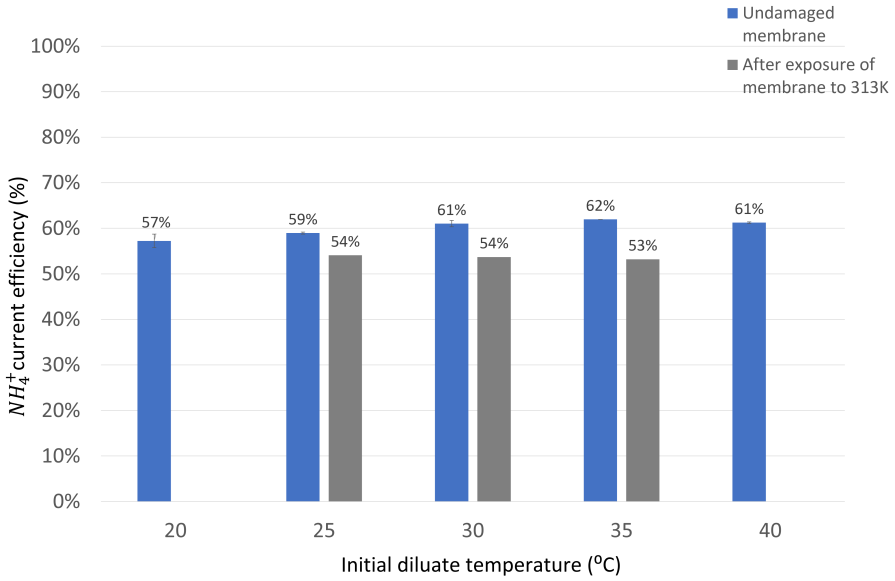

Figure 4.12: NH_4^+ current efficiency for 50 g/L $(NH_4)_2SO_4$ diluate solutions with pH 4 at varying initial temperatures. The blue bars represent the average of two experiments; the error bars depict variations between experiments. The grey bars represent one experiment each.

4.4.4 Concentrations and Purity

The purity of both acid and base were found to be decreasing with increasing initial diluate temperature, as is shown in Table 4.7.

Table 4.7: Final purities of the acid and base stream at t=150 with initial diluate streams of 50 g/L $(NH_4)_2SO_4$ and pH 4 at varying temperatures. For the purity values of 20°C, 25°C, 30°C and 40°C, the average of the data of two experiments (using the undamaged membrane) was given. The purity of the 35°C experiment was the value of one experiment only.

Temperature (°C)	Purity acid			Purity base		
20	85.4%	±	0.2%	97.1%	±	0.0%
25	83.0%	±	1.0%	96.4%	±	0.1%
30	83.5%	±	0.3%	91.0%	±	5.2%
35	81.0%	±	0.0%	93.0%	±	0.0%
40	79.3%	±	0.7%	91.0%	±	0.8%

The final SO_4^{2-} concentration in the acid was (undesirably) lowered with increasing temperature. The final NH_4^+ concentration was (undesirably) lowered with increasing temperature, see Table 4.8 a and b.

Table 4.8: (a) final SO_4^{2-} concentrations (mg/L) and (b) final NH_4^+ concentrations (mg/L) in the acid and base stream respectively for varying initial diluate temperatures. For the SO_4^{2-} and NH_4^+ concentrations of the diluate solution of 20°C, 25°C, 30°C and 40°C, the average of the data of two experiments (using the undamaged membrane) was given. The concentrations of the 35°C experiment was the value of one experiment only.

Temperature (°C)	Final SO_4^{2-} concentration in acid (mg/L)		
20	58400	±	800
25	55400	±	4200
30	60200	±	1400
35	55200	±	0
40	50400	±	1600

(a) SO_4^{2-} concentrations (mg/L) at t=150 in the acid stream at varying initial diluate temperatures.

Temperature (°C)	Final NH_4^+ concentration in base (mg/L)		
20	11515	±	145
25	11300	±	30
30	11310	±	230
35	10300	±	0
40	9715	±	315

(b) NH_4^+ concentrations (mg/L) at t=150 in the acid stream at varying initial diluate temperatures.

The NH_4^+ and SO_4^{2-} concentrations in the diluate at t=150 min appeared to be decreasing as well with higher temperature. For 20°C a NH_4^+ concentration of 2907.5 ± 7.5 mg/L was found after 150 minutes and for 40°C a NH_4^+ concentration of 1664 ± 25 mg/L was shown after 150 minutes. The SO_4^{2-} concentration after 150 minutes was detected to be 5800 ± 50 mg/L for 20°C and 2525 ± 375 mg/L for 40°C. The desalination was therefore found to be increasing with higher temperature.

However, the increased NH_4^+ and SO_4^{2-} removal from the diluate with increasing temperature showed to find its destination at the undesired acid and base stream, respectively. With increasing temperature, the (undesired) NH_4^+ concentration in the acid increased (20°C: 9952.5 ± 7.5 mg/L; 40°C: 13168 ± 127.7 mg/L). Similarly for SO_4^{2-}, the (undesired) SO_4^{2-} concentration in the base increased with temperature (20°C: 345 ± 5 mg/L; 40°C: 960 ± 120 mg/L), which is confirmed by the decreasing purities depicted in Table 4.7.

4.4.5 Removal Efficiency

In Table 4.9 and overview is given from the removal efficiency of NH_4^+ and SO_4^{2-} with increasing temperature. The removal efficiency of both NH_4^+ and SO_4^{2-} was found to be higher with increasing diluate and surrounding temperature.

Table 4.9: Percentagewise removal of NH_4^+ and SO_4^{2-} from the initial diluate 50 g/L $(NH_4)_2SO_4$ pH 4 solution of different temperature.

Temperature (°C)	NH_4^+ removal from diluate			SO_4^{2-} removal from diluate		
20	82.0%	±	0.5%	86.6%	±	0.3%
25	86.6%	±	0.0%	90.1%	±	0.6%
30	89.3%	±	1.0%	92.2%	±	0.0%
35	90.6%	±	0.0%	92.9%	±	0.0%
40	89.5%	±	0.2%	94.0%	±	0.9%

4.4.6 Final pH and EC values

In Appendix H, the final pH and EC values of the acid, base, diluate and ERS streams for different temperatures are given after 150 minutes of BPMED treatment. All the diluate solutions were at pH 4 and had a concentration of 50 g/L $(NH_4)_2SO_4$. From observations it was known that the final pH of the acid was increasing with increasing temperature (20°C: 0.93 ± 0.01; 40°C: 1.21 ± 0.01). The final pH of the base elevated with higher temperature (20°C: 10.42 ± 0.04; 40°C: 9.86 ± 0.05). The diluate pH was found to be increasing with increasing temperature (20°C: 2.3 ± 0.02; 40°C: 8.3 ± 0,1), which

is described in detail in the next section. The final pH of the ERS increased with temperature as well (20°C: 1.72 ± 0.08; 40°C: 2.04 ± 0.03).

The final EC of the acid decreased with increasing initial diluate and surrounding temperature (20°C: 1.13 ± 0.01 $*10^5$ $\mu S \cdot cm^{-1}$; 40°C: 8.62 ± 0.17 $*10^4$ $\mu S \cdot cm^{-1}$). The final EC of the base was slightly lower at higher temperature (20°C: 5.08 ± 0.14 $*10^3$ $\mu S \cdot cm^{-1}$; 40°C: 6.32 ± 0.5 $*10^3$ $\mu S \cdot cm^{-1}$). The diluate EC was decreasing with initial diluate temperature (20°C: 1.81 ± 0.05 $*10^4$ $\mu S \cdot cm^{-1}$; 40°C: 7.93 ± 0.2 $*10^3$ $\mu S \cdot cm^{-1}$). The EC of the ERS was slightly decreasing with temperature.

4.4.7 pH path in acid, base, diluate and ERS stream during temperature experiments

In Figure 4.13 the development of pH over time is depicted in the acid, base, diluate and ERS solution for initial diluate solutions with a temperature of 20°C, 25°C, 30°C, 35°C and 40°C. With an increasing initial temperature of the diluate, the diluate pH was found to rapidly increase towards the end of the experiment. A higher temperature resulted in the pH of the diluate to be increasing earlier during the experiment.

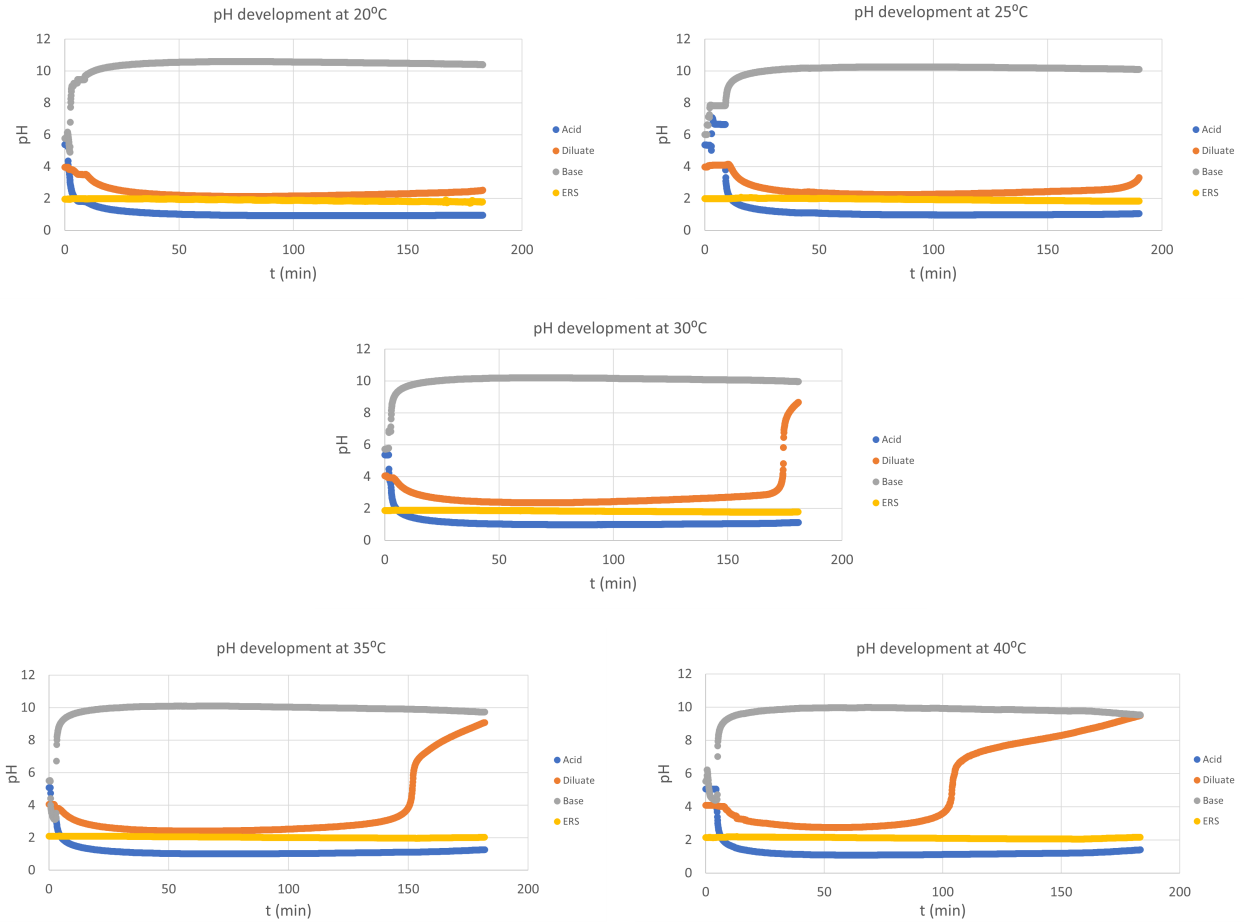

Figure 4.13: Evolution of pH of the acid, base, diluate and ERS solution during experiments with an initial diluate solution of 50 g/L $(NH_4)_2SO_4$ pH 4 at 20°C, 25°C, 30°C, 35°C and 40°C.

4.5 Concentration evolution over time

The evolution of NH_4^+ and SO_4^{2-} concentrations in the acid, base and diluate stream over time is depicted in Figures 4.14 and 4.15, at 20°C, room temperature (between 17°C and 20°C), 30°C and 40°C. It should be noted that the concentrations of NH_4^+ and SO_4^{2-} for the 20°C and Room temperature were analyzed at t=0, t=10, t=30, t=60, t=90, t=120, t=150 and t=180 minutes and the concentrations of NH_4^+ and SO_4^{2-} for the 30°C and 40°C experiments were analyzed at t=0, t=10, t=30, t=60, t=90, t=120 and t=150 minutes. The duration of the latter experiments was shortened due to reaching limiting current density before 180 minutes. During all experiments, the temperature increase of the diluate was measured. Part (± 2°C) of the temperature increase of the diluate solution during the experiments was found to be due to stirring and pumping, as confirmed by the 'zero current' and 'background temperature' experiment (Appendix E , Appendix F).
The NH_4^+ removal from the diluate followed a similar pattern for different initial diluate temperatures. The NH_4^+ concentration in the diluate showed a close to linear decrease over time. The concentration of NH_4^+ in the base increased quickly during the beginning of the experiment resulting in a roughly exponential increase towards the end of the experiment. Over time, the concentration of NH_4^+ in the acid appeared to be increasing as well, with a faster increase towards the end of the experiment. For the initial diluate of 40°C, it was observed that the concentration of NH_4^+ in the acid exceeded the concentration of NH_4^+ in the base towards the end of the experiment. With higher initial diluate temperature, the decrease of NH_4^+ concentration in the diluate was found to accelerate. With increasing temperature, the final concentration of NH_4^+ in the base decreased, while the concentration of NH_4^+ in the acid increased.

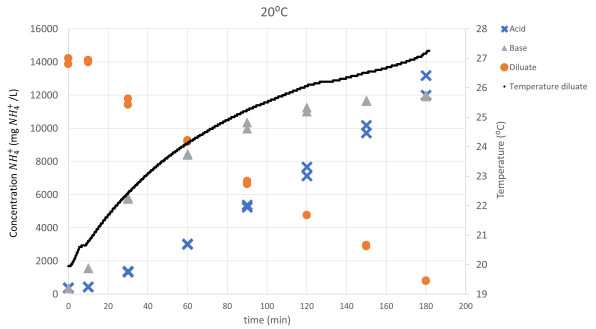

(a) Evolution of NH_4^+ concentration (mg/L) over time in the acid-, base-, and diluatestream for 50 g/L $(NH_4)_2SO_4$ initial diluate solution with pH 4 at 20°C.

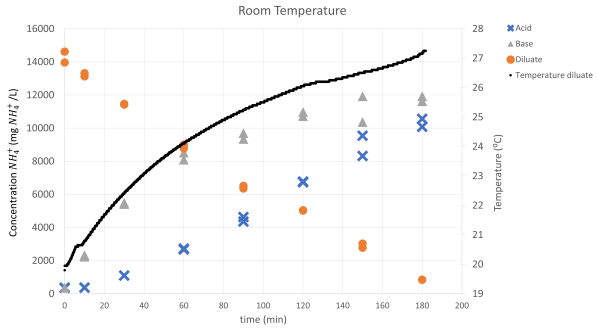

(b) Evolution of NH_4^+ concentration (mg/L) over time in the acid-, base-, and diluatestream for 50 g/L $(NH_4)_2SO_4$ initial diluate solution with pH 4 at Room Temperature.

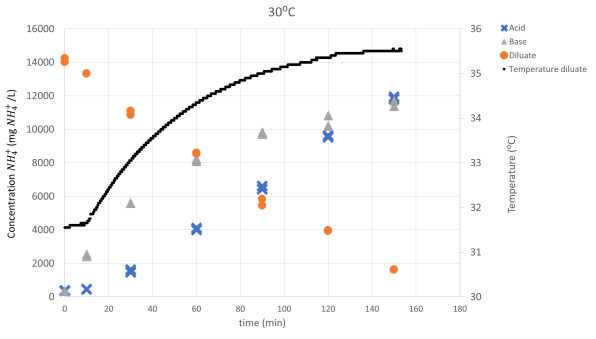

(c) Evolution of NH_4^+ concentration (mg/L) over time in the acid-, base-, and diluatestream for 50 g/L $(NH_4)_2SO_4$ initial diluate solution with pH 4 at 30°C.

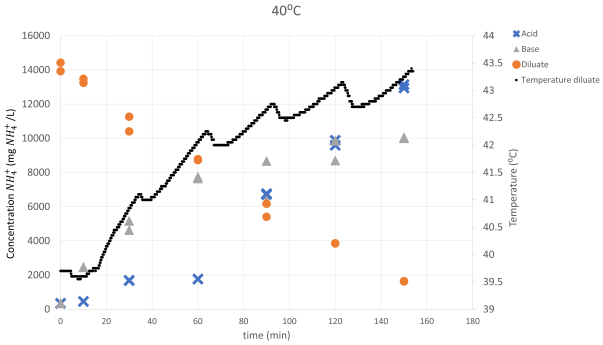

(d) Evolution of NH_4^+ concentration (mg/L) over time in the acid-, base-, and diluatestream for 50 g/L $(NH_4)_2SO_4$ initial diluate solution with pH 4 at 40°C.

Figure 4.14: Evolution of NH_4^+ concentration (mg/L) over time for various diluate initial temperatures.

The SO_4^{2-} concentrations in acid, base and diluate solution followed a similar pattern for initial diluate solutions of 20°C, room temperature, 30°C and 40°C. The final SO_4^{2-} pollution towards the base was low for all temperatures. The concentration of SO_4^{2-} in the diluate lowered over time, with an initial fast decrease, followed by a less steep decrease. With higher initial diluate temperature, the SO_4^{2-} concentration in the diluate was found to decrease faster. The rise of SO_4^{2-} concentration in the acid followed a close to linear pattern. With increasing initial diluate temperature, the final SO_4^{2-} concentration in the acid appeared to be lower.

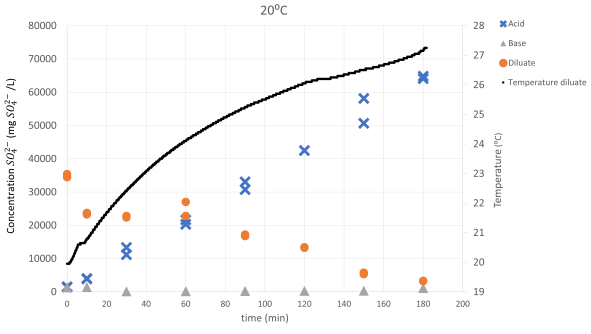

(a) Evolution of SO_4^{2-} concentration (mg/L) over time in the acid-, base-, and diluatestream for 50 g/L $(NH_4)_2SO_4$ initial diluate solution with pH 4 at 20°C.

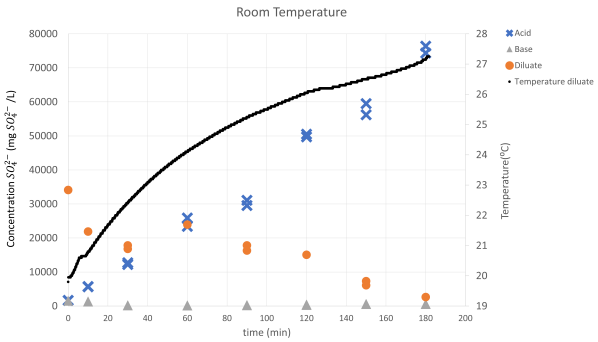

(b) Evolution of SO_4^{2-} concentration (mg/L) over time in the acid-, base-, and diluatestream for 50 g/L $(NH_4)_2SO_4$ initial diluate solution with pH 4 at Room Temperature.

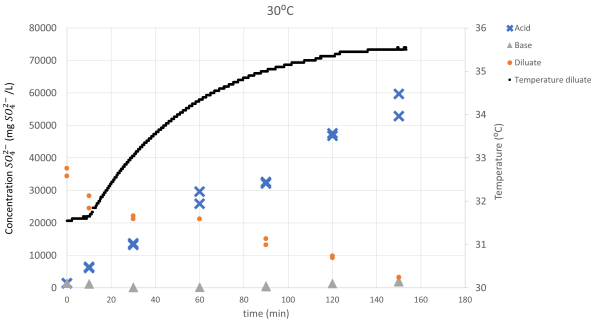

(c) Evolution of SO_4^{2-} concentration (mg/L) over time in the acid-, base-, and diluatestream for 50 g/L $(NH_4)_2SO_4$ initial diluate solution with pH 4 at 30°C.

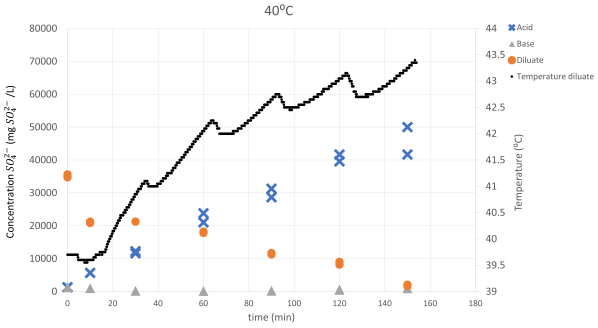

(d) Evolution of SO_4^{2-} concentration (mg/L) over time in the acid-, base-, and diluatestream for 50 g/L $(NH_4)_2SO_4$ initial diluate solution with pH 4 at 40°C

Figure 4.15: Evolution of SO_4^{2-} concentration (mg/L) over time for various diluate initial temperatures.

5 Discussion and Outlook

5.1 Discussion General Observations

The absolute NH_4^+ and SO_4^{2-} removal were expected to be equal for all experiments, since constant current was applied for the same duration. However, the pH, concentration and temperature of the diluate were found to affect the removal of NH_4^+ and SO_4^{2-}, resulting in variations in removal efficiency by BPMED treatment and the thereby produced acid and base. In this chapter, the underlying principles explaining the phenomena observed in chapter 4 are interpreted and compared with literature.

5.1.1 Proton and hydroxide leakage

The fast decrease of pH (acidification) in the diluate and acid stream during the first 10 minutes of the experiments was caused by proton leakages as confirmed by various literature [54, 63, 68, 69]. Since H^+ is a small ion with a small electric charge, it has a very high mobility and can easily find its way towards other streams because of the concentration gradient [4]. In water, protons form clusters of hydronium ions, and those protons can be transferred from one hydronium to the next hydronium via the tunneling mechanism. This mechanism results in an extraordinary high mobility of protons in water [4]. Proton leakage is seen as one of the limitations of BPMED use for salt conversion, since it limits the current efficiency for the transport of ammonium and is thereby resulting in an increased energy consumption [36, 68]. H^+ leakage due to high H^+ concentrations in the diluate and acid for the pH 2 - 5 diluate streams was found, since proton leakage through the anion-exchange membrane is proportional to the acid concentration [39]. The base stream was most likely to face acidification as well by movement of H^+ from the diluate through the CEM, but this was masked by the rapid increase of negatively charged ions.

Hydroxide ions have, similarly to H^+, a very different mobility in aqueous solution than other ions like NH_4^+ and SO_4^{2-}. The mobility of OH^- ions is ca 6 times higher than that of NH_4^+ and SO_4^{2-} because of the tunneling mechanism as described for H^+ ions [4]. OH^- ions can pass the bipolar membrane and thereby lower the pH in the diluate stream. OH^- leakage is described as another limitation of BPMED [36, 69]. However, alkalizing of solutions was hardly observed during this study.

5.1.2 Dissolved ammonia diffusion and ammonia volatilization

Ammonia diffuses through the membranes independently of current in the form of dissolved ammonia diffusion, so when ammonia is in gaseous form surrounded by water [36, 39]. It was found that dissolved ammonia diffuses from the base towards the acid (for these experiments circa 40 % of the initial NH_4^+ diluate ended up in the acid), which was confirmed by various literature [36, 39, 68, 69]. Ammonia diffusion is seen as one of the limitations of BPMED treatment of ammonium rich water due to the lower purity of produced acid and base and the decrease in NH_4^+ current efficiency, similarly found in other literature [36, 39, 68, 69, 72]. Another reason for ammonium losses from the base is ammonia volatilization. Since ammonium ions are in equilibrium with the volatile ammonia with an dissociation constant of 9.3, ammonia volatilization increases with higher pH of the stream [70]. This volatilized ammonia can, dependent on the type of membrane, also pass the membrane [75]. However, volatized ammonia was assumed not to be able to pass the membranes used in this research due to the small pore size. However volatile ammonia could leave the entire system in gasform.

5.1.3 Background temperature and ion diffusion without current

The temperature increase of the diluate, acid, base and ERS solutions was similar for all experiments. The increase in temperature was found to be mostly due to mixing, only slightly due to pumping, as visible in Appendix F. Without applying current to the BPMED stack, the NH_4^+ concentration in the acid slightly increased, while the concentration NH_4^+ in the base slightly decreased after 180 minutes. Small amounts of NH_4^+ were transported towards the ERS without applying current. The diluate showed a small decrease in NH_4^+ concentration after 180 minutes. These variations of NH_4^+ concentration after 180 minutes were due to the diffusion of NH_4^+ with concentration gradient as confirmed by van Linden et al. [36]. NH_4^+ originating from the diluate was spread over the low NH_4^+ concentration acid, base and ERS streams. Another explanation for the difference in NH_4^+ concentrations at t=0 minutes and t=180 minutes was the solution present in the tubes from the prior experiment. For SO_4^{2-}, little to no transportation from the diluate was observed. The SO_4^{2-} concentration in the ERS was decreasing, while the SO_4^{2-} concentration in the acid an base slightly increased during the 180 minutes recirculation. The small transport of SO_4^{2-} was driven by ionic diffusion and presence of ions from the prior experiment. An overview of the ion transport without applied current is provided in Appendix E.

5.2 Discussion on influence of pH

The diluate solutions with 50 g/L $(NH_4)_2SO_4$ at room temperature were all adjusted with different volumes of H_2SO4 and NH_4OH for obtaining the requested pH. Since the diluate solutions in the range pH 2-5 required H_2SO4 addition and the diluate solutions in the range pH 6-10 required NH_4OH, those two pH ranges were accordingly compared.

5.2.1 Low pH range (pH 2-5)

At low diluate pH, the competition between NH_4^+ and H^+ ions was found to result in worse performance of BPMED treatment of ammonium sulfate streams with pH 2 than pH 5.

As depicted in Figure 4.2, the electrochemical energy consumption was decreasing with increasing pH in the pH 2-5 range. Since the initial NH_4^+ amount present in these diluate solutions was equal, the decreasing electrochemical energy consumption indicated the influence of initial diluate pH on the energy consumption per transported NH_4^+ ion. The electrochemical energy consumption is influenced by the total energy consumption and the amount of transported NH_4^+ (see section 2). Since the current, duration and the electrochemical energy consumption of the experiments were (approximately) the same, the only changing factor resulting in the higher electrochemical energy consumption was the amount of transported NH_4^+. The higher electrochemical consumption at pH 2 than at pH 5 was found to be the result of competition between ions for their transport over the membrane, which was explained by literature to be a likely phenomenon in electrodialysis [73, 76, 77]. In a diluate pH 2 solution, more competition between H^+ ions and NH_4^+ ions occurred than in a diluate pH 5, resulting in a lower absolute and percentagewise NH_4^+ removal for pH 2 (Table 4.3). The final concentrations of NH_4^+ in the diluate of pH 2 were found to be higher than the final NH_4^+ concentrations in the diluate at pH 5 (Table 4.2), proofing the competition.

Likewise, the competition between NH_4^+ and H^+ could explain the increasing trend in NH_4^+ current efficiency with pH (Figure 4.3a). Cherif et al. confirms the decreasing current efficiency due to competition of ions [69]. The only changing factor influencing the NH_4^+ current efficiency was the amount of NH_4^+ transported from the diluate. At a lower initial diluate pH, the NH_4^+ current efficiency loss was caused by transportation of $H+$ ions instead of the desired transportation of NH_4^+. Therefore,

with the same amount of current, less NH_4^+ ions were transported since part of the current is being used for the transportation of H^+ ions, resulting in a decreasing NH_4^+ current efficiency with increasing pH.

The competition between H^+ and NH_4^+ ions was confirmed by the evolution of potential over time. As visible in Figure 4.4, the potential increased slightly towards the end of the experiments with diluate of pH 2, while the potential of the experiments with diluate of pH 5 did not. This increase in potential can be explained by a higher resistance, approaching the LCD [4]. A higher resistance in BPMED can be the result of a relatively low mineral content in the diluate solution, allowing a smaller electrical conductivity [53]. Since a bipolar membrane is responsible for a resistance in the order of 10 $\Omega\ cm^2$ and the anion- and cation exchange membranes have a resistance of 1 to 2 $\Omega\ cm^2$ each, the resistance of the BPM affects the total resistance for desalination of the diluate the most [4]. Therefore, a diluate solution with less ions present (lower salt concentration) will result in an increase in electrical resistance. In the pH 5 diluate solution, after 180 minutes less ions were present than for the pH 2 diluate solution, resulting in less electrical conductivity and therefore a higher resistance and higher measured potential.

Since it was found that the total energy consumption for the experiments at pH 2 and pH 5 was nearly unaffected, several parameters can be excluded from being of influence during BPMED treatment at low pH:

- The conductivity did not affect the energy consumption. The higher EC for low pH did not result in a lower energy consumption due to a lower resistance.
- The voltage was found to be (almost) unaffected by the pH of the diluate, thereby implying that the resistance over the membrane stack was equal for all experiments [4, 78].

The sulfate removal efficiency was higher for the pH 5 diluate than for the pH 2 diluate (Table 4.3). Since sulfate has a pKa of 1.9 [79], more SO_4^{2-} ions were present in the bisulfate ion HSO_4^- form in the pH 2 diluate than in the pH 5 diluate. HSO_4^- has a lower charge and is reported to have a smaller hydration shell (up to six ions for a stable molecule) than the SO_4^{2-} ion [80]. Both charge and hydration shell influence the mobility of HSO_4^-, but which factor is dominant for this particular case was not found in literature. However, the increased sulfate removal for diluate pH 5 suggests that the double charge of SO_4^{2-} was the reason for higher removal with pH 5 than with pH 2 containing part of the sulfate in its single charged HSO_4^- form.

The higher ammonium and sulfate removal efficiencies were confirmed by the NH_4^+ and SO_4^{2-} concentrations in the diluate for pH 2 and pH 5 after 180 minutes. For pH 2 both the NH_4^+ and SO_4^{2-} concentrations were found to be higher after 180 minutes than for the initially pH 5 diluate stream (Table 4.3). The final pH of the diluate was found to be higher for the pH 5 than for the pH 2 diluate, due to the initially higher H^+ concentration in the diluate of pH 2 (Appendix H.0.1). Even though part of the H^+ ions was transported over the membrane by the applied current, more H^+ ions were left-over in the pH 2 diluate solution after 180 minutes than in the pH 5 diluate solution.

The final NH_4^+ concentration in the base was found to be increasing with pH 2 to pH 5 (Table 4.1b). Since less NH_4^+ could be removed from the diluate pH 2 solution due to competition with H^+, less of the NH_4^+ from the diluate ended up in the base. Furthermore, for the pH 5 solution, the NH_4^+ concentration in the acid was found to be higher than for pH 2. This undesired phenomenon could happen due to higher NH_4^+ concentration in the base and the resulting dissolved ammonia diffusion towards the acid solution because of concentration gradient [4]. However, the purity of both acid and base increased

comparing pH 2 and pH 5. The increasing NH_4^+ concentration in the acid was compensated by a percentagewise higher increase of SO_4^{2-} concentration in the acid. The slightly lower pH and slightly higher EC for the diluate pH 2 final base solution could be explained by the higher H^+ concentration present in the acid for the pH 2 experiment than for the pH 5 experiment, due to the competition between H^+ and NH_4^+. The NH_4^+ most likely leaves the base by dissolved NH_3 diffusion due to the high pH (pKA = 9.3), which increases the H^+ concentration in the base and therefore lowers the pH. This is confirmed by the slightly higher EC in the base of pH 2 than in the base of the pH 5 experiment.

The final SO_4^{2-} concentration in the acid was higher for diluate pH 5 than for diluate pH 2 solution (Table 4.1a) due to the higher removal efficiency. The final pH of the acid for pH 2 diluate stream was lower, due to more H^+ leakage towards the membrane stack with higher H^+ concentrations in diluate solution with initial pH of 2. This explained the higher EC of the acid for the initial diluate pH 2 solution as well.

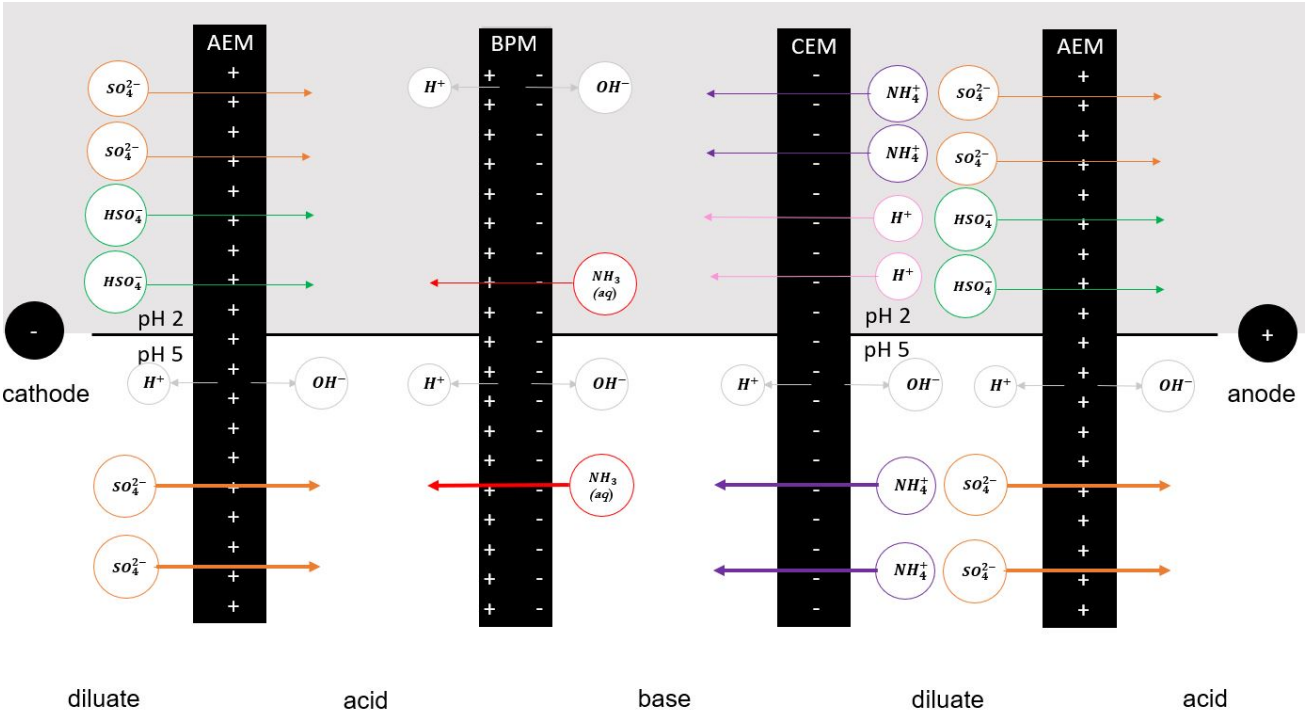

Figure 5.1: The most important phenomena potentially happening for diluate pH 2 and pH 5 solutions. This figure only represents the effect of (low) pH, so other potential phenomena irrelevant for the effect of pH are not depicted. The transport of NH_4^+ (purple) from diluate to base passing the CEM is higher at pH 5 than at pH 2 due to the competition between NH_4^+ and H^+ ions (in grey). The same amount of NH_4^+ ions is initially present in the diluate of pH 2 and pH 5, but the amount of H^+ ions is higher in the pH 2 diluate. SO_4^{2-} removal (orange) is higher for pH 5, due to more ions present in the SO_4^{2-} than in the bisulfate (HSO_4^- - green) form of diluate pH 5 compared to diluate pH 2. More sulfate is present (in SO_4^{2-} or HSO_4^- form) at pH 2, due to pH adjustifications with H_2SO_4, resulting in a pH 2 diluate. Slightly more enhanced water splitting was observed for diluate pH 5 (grey), but it is unclear whether that happened at the CEM and/or AEM. More dissolved ammonia diffusion from base towards the acid was observed for pH 5 (red), due to the higher NH_4^+ concentration in the base for pH 5. A thicker arrow indicates a higher transport number of the ion compared to a thinner arrow. The thickness of the arrows is relative to the other diluate pH, but not relative to other ions. The size of the ions is not at scale.

5.2.2 High pH range (pH 6-10)

The functionality of BPMED for the treatment of diluate with high pH was found to be influenced mostly by dissolved ammonia diffusion, forcing OH^- leakage and enhanced water splitting.

In the high pH spectrum, the electrochemical energy consumption was found to be decreasing with initial diluate pH (Figure 4.2). This was not due to the energy consumption per experiment, since the energy consumed for the treatment of initial diluate pH 10 was found to be higher than for initial diluate pH 6. In Figure 4.5, the evolution of potential for pH 6, 9 and 10 over time is presented, were the rapid increase in voltage was found to come earlier with increasing pH. This resulted in a higher total energy consumption per 180 minutes. It was observed that the LCD was reached within less than 180 minutes for the diluate pH 10 experiments. The explanation for this phenomenon could be the increasing resistance with increasing pH. Since the diluate solution towards the end of the pH 10 diluate experiment contained too little ions for charge transmission, enhanced water splitting started occurring at the CEM and/or AEM resulting in an increase in resistance and therefore in energy consumption, which was confirmed by Strathmann et al. [58]. Mani et al. states that the watersplitting process operates at significantly higher current densities than conventional electrodialysis and therefore generates a greater amount of heat [22].

Since the reason for decreasing electrochemical energy consumption with increasing pH could not be found in the energy consumption per experiment, the increased electrochemical energy consumption with increasing pH was due to difference in NH_4^+ transportation for different pH diluates. The absolute mass of NH_4^+ transported was found to be much higher for the pH 10 diluate than for the pH 6 diluate. First of all, there could be less competition between NH_4^+ and H^+ ions for transport over the membranes at pH 10 than at pH 6. Furthermore, in pH 10 diluate, a substantial part of the NH_4^+ is present in the form of NH_3, resulting in higher dissolved ammonia diffusion through the membrane stack and in part of the NH_3 being volatilized, leaving the entire system. Lastly, the concentration gradient between the initial diluate solution and the initial base is larger for pH 10 than for pH 6, which could result in dissolved ammonia diffusion/co-ion leakage due to imperfect selectivity of the membranes. Ammonia diffusion from the diluate during BPMED treatment was confirmed by various literature [36, 72].

The NH_4^+ current efficiency reaching over 200 % was confirming the major influence of ammonia diffusion (Figure 4.3b). A NH_4^+ current efficiency higher than 100% indicates that more NH_4^+ ions were transported than theoretically could be assured by the applied current. This phenomenon could be explained by the transport of NH_4^+ due to difference in concentration gradient, due to dissolved ammonia diffusion and due to losses of ammonia because of volatilization. With higher pH, more losses of NH_4^+ were observed, due to more volatilization of NH_4^+ with pH 10 and because of the higher concentration gradient of NH_4^+ at pH 10. The ammonium loss observed based on the mass balance was found to be 10% at maximum (90% recovery) for the pH experiments with a pH between 2 and 8. However, for the pH 9 diluate and the pH 10 diluate, losses of 20% and 43% were observed respectively, indicating that higher volatilzation of ammonia happened due to the high pH of the diluate.

Proton leakage towards the diluate happened during the first half hour of the experiment. Later on in the experiment, a slight increase in diluate pH was found for all experiments. However, for the pH 9 experiment, a rapid increase in diluate pH towards the end of the experiment was observed (Appendix H, Figure H.2) and for the pH 10 experiment no acidification of the diluate was observed at all (Appendix H, Figure H.3). Towards the end of the experiment with diluate pH 10, the pH of

both diluate and acid were slightly increasing while the base pH was slightly decreasing. The rapid increase in pH of the diluate towards the end of the experiment could be explained by 2 phenomena. First of all, the extremely low final electrical conductivity in the diluate could leading to the increased resistance (Appendix H, Figure H.3). The pH increase of the diluate and acid stream could be the result of enhanced water splitting, which also confirms the increasing resistance towards the end of the experiment [58]. OH^- ions were alkalizing the diluate and acid stream, while in the meantime the base stream was acidified with H^+ ions produced by water splitting. The enhanced water splitting occurred most likely both on the AEM and CEM. NH_4^+ and SO_4^{2-} have a similar mobility and therefore (according to the Einstein relation) a similar diffusion coefficient [4, 67, 81]. Based on the observed final concentrations, the SO_4^{2-} ion was found to be the limiting ion after 180 minutes BPMED treatment for diluate pH 9 and 10. This resulted in enhanced water splitting at the AEM, which is also observed in literature [82]. Enhanced watersplitting at the AEM would result in an increased H^+ concentration in the diluate and an increased OH^- concentration in the acid. The latter is visible in Figure H.2 and Figure H.3 in Appendix H. The increasing OH^- concentration in the diluate could be the result of enhanced water splitting at the CEM.
Another reason for the rapid increase in diluate pH for pH 9 and 10 could be the forced movement of OH^- from the base to the diluate. The higher dissolved ammonia diffusion and ammonia volatilization for pH 10, made NH_4^+ leave the base in the ammonia form. To ensure charge balance, OH^- ions were forced to leave the base as well. These OH^- ions were passing both the CEM and AEM membrane, resulting in an increased pH of the diluate and acid respectively.

The final SO_4^{2-} concentration in the diluate was decreasing with increasing pH, showing the improved removal efficiency of SO_4^{2-} under high pH (Table 4.3). With higher concentrations, membranes can get more permeable for ions and therefore SO_4^{2-} could be able to pass the membrane easier in the form of leakage. Research should be performed on more reasons for the improved SO_4^{2-} removal. Although the reasoning behind the increased sulfate removal with increasing diluate pH is not completely elucidated, several explanations for higher sulfate removal could be excluded:

- Competition between OH^- and SO_4^{2-} transportation over the membrane is NOT the reason for the higher SO_4^{2-} removal. If competition would be case, with higher pH (more OH^-) less SO_4^{2-} removal would be expected.
- The high increase in voltage towards the end of the experiment could provide an enlarged electrical pull for the SO_4^{2-} ions to leave the diluate. However, the high increase in voltage is most likely *the result* of the limiting SO_4^{2-} concentration.

The decreasing purity of the acid could be explained by dissolved ammonia diffusion and/or co-ion leakage of NH_4^+ towards the acid (Table 4.2). With higher pH, a bigger faction of the diluate NH_4^+ will be present in the ammonia form and therefore more dissolved ammonia diffusion can take place than with lower pH. Additionally, in the pH 10 diluate a higher NH_4^+ concentration was present in the diluate than in the pH 6 diluate, creating a bigger concentration gradient between the diluate and base (and acid), resulting in a higher driving force for ion transport.

The volume ending up in the base solution was found to be higher with increasing pH, which could be explained by electro-osmosis. Since more NH_4^+ ions were transport to the base, more surrounding water molecules were transported with them.

Taking all results together, but taking the practical application into consideration as well, the decision was made to continue with a diluate pH 4 for both the concentration experiments and the temperature experiments. The removal efficiency, electrochemical energy consumption and the obtained acid and base purity were (close to) optimal and at the same time, the practical implementation is achievable with only adjusting the pH 2-3 feed stream with little base dosage.

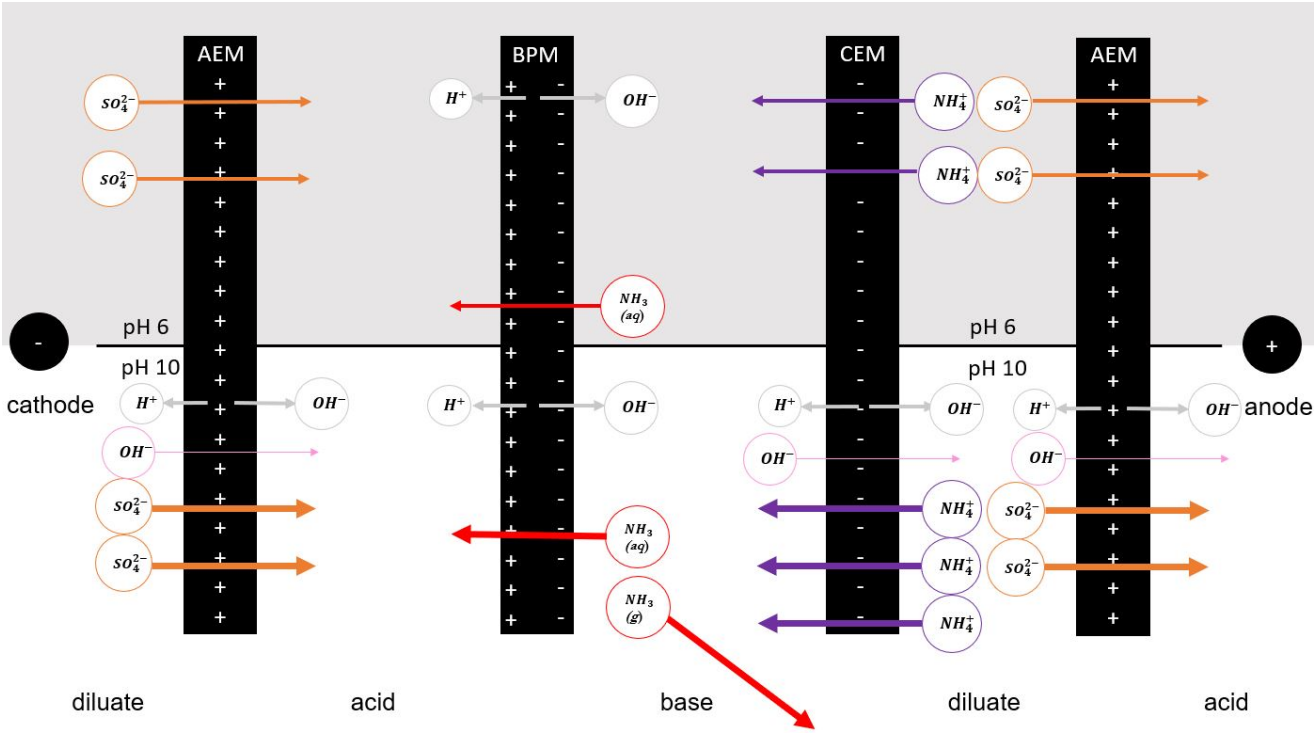

Figure 5.2: The most important potential phenomena for diluate pH 6 and pH 10 solutions. This figure only represents the effect of (high) pH, so other potential phenomena irrelevant for the effect of pH are not depicted. Enhanced watersplitting (grey) happened both at the CEM and AEM, even though the enhanced water splitting at the AEM is more likely due to the observed faster depletion of SO_4^{2-} ions than NH_4^+ ions. More NH_4^+ removal (purple) was observed for pH 10 due to: (1)less H^+ competition for the pH 10 than for the pH 6 experiment (2) the concentration gradient of NH_4^+ between the initial diluate and base is so big (since a lot more NH_4^+ was added to the pH 10 solution), that dissolved ammonia diffusion /co-ion leakage due to imperfect selectivity of the membranes is more likely to occur at pH 10 (3) Ammonium in diluate pH 10 for a bigger fraction in the NH_3 (g) (red) form than for the pH 5 diluate, so in general, ammonia diffusion is more expected. The higher SO_4^{2-} removal (orange) can not be fully explained, but might be partly due to higher leakages with high concentrations present. Since more NH_4^+ was leaving the base, OH^- is also forced to leave the base, passing the CEM to go to the diluate and thereafter passing the AEM towards the acid (pink). A thicker arrow indicates a higher transport number of the ion compared to a thinner arrow. The thickness of the arrows is relative to the other diluate pH, but not relative to other ions. The size of the ions is not at scale.

5.3 Discussion on influence of concentration

Dissolved ammonia diffusion, imperfections in membrane functionality and the sulfate activity coefficient were found to influence the functionality of BPMED with various initial diluate concentrations.

With increasing $(NH_4)_2SO_4$ concentration, the electrochemical energy consumption was found to be decreasing and the NH_4^+ current efficiency was found to be increasing (Figure 4.8 and Figure 4.9). The energy use per experiment decreased with increasing initial concentration. With a higher NH_4^+ concentration present in the initial diluate, the transport of NH_4^+ over the membrane with constant current required a lower voltage (Appendix G.1). This lower voltage could be explained by the smaller resistance over the membrane, due to smaller concentration polarization which is confirmed by literature [83]. The higher concentration gradient between diluate and acid/base solution with increasing initial concentration provided a larger driving force for motion of ions and is therefore resulting in a lower potential: with the same amount of current, the transportation of ions is found to cost less energy [4]. With higher initial concentration, a lower potential and therefore a lower energy consumption for the same amount of NH_4^+ transported is needed [4].

The amount of NH_4^+ and SO_4^{2-} ions transported from the diluate was expected to be independent of the initial $(NH_4)_2SO_4$ concentration. With constant current, the same amount of charge could be transported during the same time period and therefore the same amount of ions could be transported, independent from the concentration [4, 84]. However, as depicted in Figure 4.10, it was found that the absolute amount of NH_4^+ ions removed from the diluate increased with increasing diluate concentration. On the other hand, the absolute SO_4^{2-} removal from the diluate was found to be lowered with higher concentration. The higher than expected NH_4^+ removal and lower than expected SO_4^{2-} removal can be partly explained by imperfections in the membrane functionality and dissolved ammonia diffusion.

Exchange of NH_4^+ and H^+ between the diluate and acid solution as an explanation for the increased NH_4^+ removal with increasing concentration is unlikely. The increase of NH_4^+ concentration in the acid stream was indeed found with increasing initial diluate concentration, but the final diluate pH was found to increase. The exchange of NH_4^+ and H^+ might therefore play a role, but cannot explain the increased NH_4^+ removal with increasing diluate concentration. Consequently, the increased NH_4^+ removal from the diluate and the increased NH_4^+ concentration in the acid (and base) could be clarified by more ammonia diffusion with increasing initial diluate concentration, due to the higher concentration gradient [4]. However, in the research of Linden et al. it was found that the ammoniacal nitrogen equilibrium shifts for TAN concentrations of 1.5 and 10 g/L (NH_4HCO_3) from 9.4 to 9.6. Therefore, for a higher ammonium concentration, the pKA for the ammoniacal nitrogen equilibrium is most likely even higher. Higher concentrations have a lower fraction of the total TAN in the ammonia form [36]. This shows that despite the lower ammonia fraction with higher concentration, the absolute concentration gradient was high enough to facilitate the increasing ammonia diffusion trend with increasing concentration.

Furthermore, co-ion leakage of NH_4^+ due to imperfections in the membrane functionality were explaining the increased NH_4^+ removal by increasing concentrations. These co-ion leakages through bipolar membranes were observed in literature before [69]. The gradient driven NH_4^+ transport can be considered to be beneficial, since it increased the removal efficiency. On the contrary, the co-ion leakage resulted in a higher NH_4^+ concentration in the acid with increasing initial diluate concentration, what explained the decreased purity of the acid with increasing initial diluate concentration. The increased amount of NH_4^+ removed from the diluate resulted in an increase of NH_4^+ current efficiency with

increasing initial $(NH_4)_2SO_4$ concentration.

The absolute amount of SO_4^{2-} removal from the diluate was found to be slightly decreasing with increasing initial diluate concentration (Figure 4.10). In case this decreasing SO_4^{2-} removal can be confirmed with newly performed concentration measurements, the lower SO_4^{2-} removal might be associated with the formation of $(NH_4)SO_4^-$ ion pairs.

The active SO_4^{2-} concentration is not equal to the theoretical SO_4^{2-} concentration, due to the low activity coefficient of sulfate salts [67, 85, 86]. The activity describes the intermolecular interaction between solute and solvent or in other words: to what extend the effectiveness of each molecule is equal to its theoretical effectiveness [87]. SO_4^{2-} ions have the capacity to form ion pairs with NH_4^+, resulting in $(NH_4)SO_4^-$ ion pairs, whereby the activity of the SO_4^{2-} ion is affected [88]. After correction of ion pair formation, the molal activity coefficient of the stable ion pair $(NH_4)SO_4^-$ was found to be 0.545, which means that the effective concentration of SO_4^{2-} ions is 0.545 of the absolute concentration [88]. The $(NH_4)SO_4^-$ ion pair has a larger size than the SO_4^{2-} ion, resulting in a lower transport flux due to the smaller diffusion coefficient of larger ions [67, 89]. $(NH_4)SO_4^-$ has a singular charge and therefore feels a smaller electrical attraction by the applied current compared to the double charged SO_4^{2-} ion as shown in the extended Nernst-Planck equation (Equation 10). However, Reardon et al. state that the fraction of $(NH_4)SO_4^-$ ion pairs is independent of the salt concentration and therefore the effective concentration of SO_4^{2-} ions does not decrease with increasing initial diluate concentration [88]. $(NH_4)SO_4^-$ ion pair formation in electrodialysis and its impact on the sulfate removal have not been described before in literature. Apparently, the competition between $(NH_4)SO_4^-$ and SO_4^{2-} ions for transportation over the membrane results in less sulfate removal for higher concentrations. From the results in this research, it is expected that both the lower valence of the ion pair and the larger $(NH_4)SO_4^-$ ion size compared to the SO_4^{2-} ions can negatively influence the sulfate removal efficiency with higher concentration. Consequently, more $(NH_4)SO_4^-$ ions stay in the diluate solution for higher initial concentration. However, the exact reasoning behind higher SO_4^{2-} removal with higher concentrations remains uncertain.

The decreasing trend in final diluate pH with increasing initial diluate concentration is explained by the buffering capacity of SO_4^{2-}. With its pKa of 1.92, the added SO_4^{2-} is buffering with the equilibrium $SO_4^{2-} + H^+ \longleftrightarrow \mathrm{SO}_4^{2-}$, whereby the H^+ ions were buffered by the additional SO_4^{2-} [90]. Therefore, the slightly increasing SO_4^{2-} concentration in the acid could buffer the H^+ ions in the acid and consequently the pH of the acid could be slightly increasing with the initial diluate concentration. Similarly, the increase of NH_4^+ concentration in the base will be mostly in the ammonia form an thereby releasing H^+ in the base solution. With higher initial diluate concentration, more ammonia and therefore more H^+ ions will be present in solution, thereby decreasing the pH of the base.

In any case, it should be noted that with increasing initial $(NH_4)_2SO_4$ concentration, the left over amount $(NH_4)_2SO_4$ (NH_4^+ and SO_4^{2-} ions) was higher after 180 minutes of BPMED treatment. So for achieving the same NH_4^+ and SO_4^{2-} removal, a longer duration of treatment would be necessary, eventually resulting in higher energy consumption.

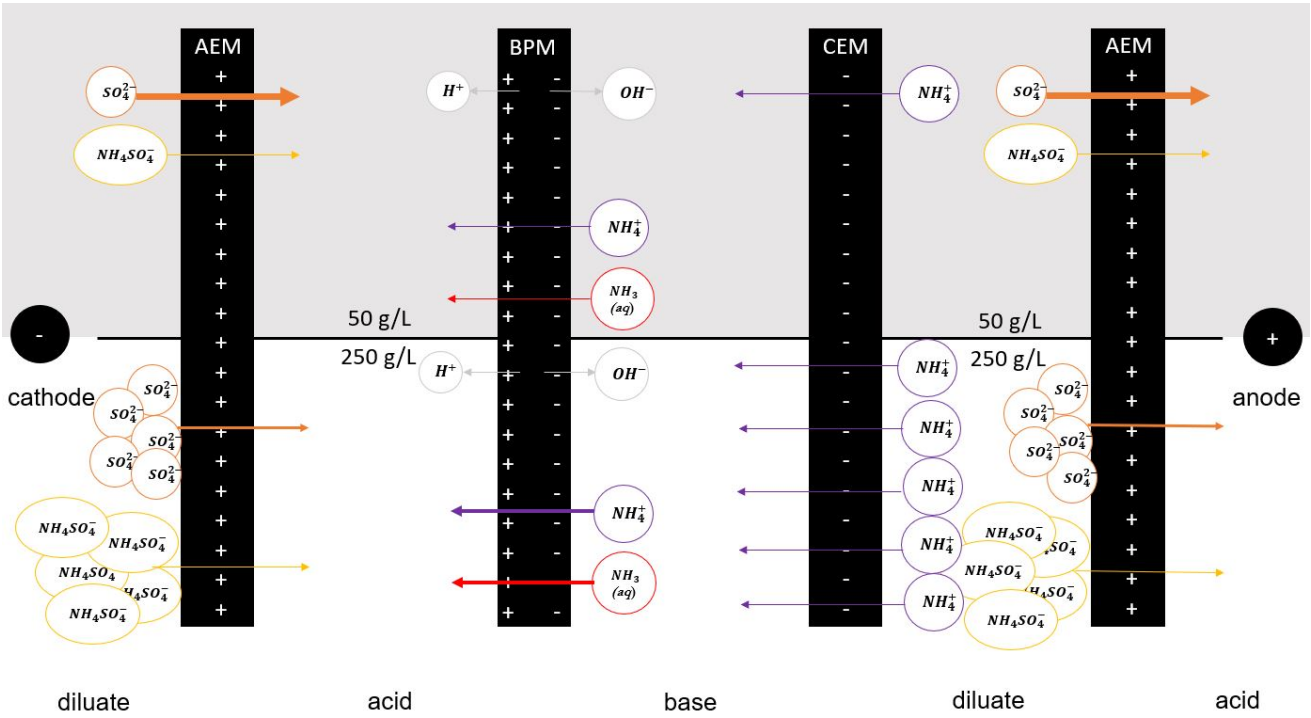

Figure 5.3: The most important potential phenomena for diluate pH 4 with a concentration of 50 and 250 g/L $(NH_4)_2SO_4$. This figure only represents the effect of concentration, so other potential phenomena irrelevant for the effect of concentration are not depicted. More ammonium removal from the diluate was observed (purple) with higher concentrations due to imperfections in the membrane, letting the larger concentration gradient for 250 g/L result in a higher ammonium removal. Since the final NH_4^+ concentration in the base increased with concentration, more co-ion leakage of NH_4^+ ions towards the acid happened as well as more dissolved ammonia diffusion (red), resulting in a lower purity. The removal of sulfate (orange) decreased with increasing concentration potentially due to more ions present in the $(NH_4)SO_4^-$ co-ion pair (yellow), experiencing less electrical force to leave the diluate solution. A thicker arrow indicates a higher transport number of the ion compared to a thinner arrow. The thickness of the arrows is relative to the other diluate concentration, but not relative to other ions. The size of the ions is not at scale.

5.4 Discussion on influence of temperature

Proton leakage, dissolved ammonia diffusion, co-ion leakage and the solute diffusion coefficient were found to be influencing BPMED treatment at different temperatures.

Literature describes that temperature impacts the performance of almost all membrane processes [91]. In this research the electrochemical energy consumption was found to be decreasing with higher initial diluate and surrounding temperature, while the NH_4^+ current efficiency was increasing (Figure 4.11 and Figure 4.12). The electrochemical energy consumption was decreasing with increasing temperature due to the fact less energy was consumed for the transportation of more NH_4^+ with increasing temperature. The lower power consumption with higher temperatures was confirmed by literature, stating that different temperature conditions can decrease the membrane voltages and thereby decrease the resistance [40, 61]. The lower power consumption (due to smaller resistance) with increasing temperature could be explained by the fact that temperature affects both the viscosity and the density of solutions [91]. The viscosity and density of water are decreasing with increasing temperature, which makes the fluid pass the membrane with less resistance and thereby lowering the energy consumption with temperature, as confirmed by literature [92, 93]. The membrane itself, depending on its properties, can also become more elastic and therefore perform smaller resistance [4].

The decrease in electrical energy consumed per experiment with temperature came together with the increase of NH_4^+ removal from the diluate, resulting in a lower electrochemical energy consumption and increasing NH_4^+ current efficiency for the constant current experiments, which was confirmed by literature [45]. The increasing NH_4^+ removal with temperature can be explained by the apparently decreasing competition between the H^+ and NH_4^+ ions in the diluate to be transported over the membrane with increasing temperature. Lorrain et al. describes the decrease of proton leakage with increasing temperature, due to the second dissociation constant of sulfuric acid and due to less organization of the hydration water molecules around the cation and therefore, to a reduction of the kinetics of proton entry into the membrane [63]. Due to less proton leakage toward the diluate, higher NH_4^+ removal efficiencies can be achieved.

Furthermore, temperature affects the diffusivity and mobility of solutes [91]. The higher removal of both NH_4^+ and SO_4^{2-} with a higher temperature can be explained by a higher ion mobility, which is described as a dominant effect on the decrease in the membrane's stack resistance as well [40]. So with increasing temperature, ions move faster and more easily through solution, which would enhance NH_4^+ and SO_4^{2-} transportation from the diluate. On top of that, with higher temperature, more of the NH_4^+ ions are present in the gaseous ammonia form and can therefore escape from equilibrium [94]. Ammonia could leave the system or diffuse within the boundaries of the system. This was confirmed by the decreasing final NH_4^+ and SO_4^{2-} concentration in the diluate with increasing temperature (Table 4.8). The decreasing trend in final EC in the diluate validated that.

The SO_4^{2-} removal from the diluate increased with temperature (Table 4.9). The transportation of ions is, similarly as for NH_4^+, easier due to the higher mobility of ions with increasing temperature and due to the lower density and viscosity of water at with higher temperature [91]. The equal current therefore results in lower resistance and therefore a lower voltage usage. In a diluate pH 4, only small amounts of OH^- were present. Therefore competition between OH^- and SO_4^{2-} was unlikely. However both H^+ and OH^- ions could theoretically pass the AEM [4]. H^+ diffusion from the acid towards the diluate would contribute to the current. Less H^+ diffusion with increasing temperature would suggest

smaller H^+ leakage from acid to diluate at higher temperature, therefore resulting in less competition between H^+ and NH_4^+ for transportation over the membrane. With smaller H^+ concentrations in the diluate at higher temperature, SO_4^{2-} has more possibility to leave the diluate (since less cations can 'keep' SO_4^{2-} in the diluate).

The lower competition between H^+ and NH_4^+ at higher temperatures could explain the higher SO_4^{2-} removal. With increasing temperature, the ammonium diffusion from the diluate towards the acid increases. This diffusion does not contribute to the current, but is along with the diffusion gradient. To maintain charge balance, SO_4^{2-} is forced to leave the diluate together with the ammonium ions. However, this forced SO_4^{2-} removal did not result in an evident increase in SO_4^{2-} concentration in the acid.

The decrease in NH_4^+ concentration in the base stream and the decrease of the SO_4^{2-} concentration in the acid stream with increasing temperature resulted in a lower purity of acid and base (Table 4.7, Table 4.8b). The NH_4^+ concentration in the acid and the SO_4^{2-} in the base both slightly increased with temperature. The increase of NH_4^+ concentration in the acid with temperature was most evident, apparently due to ammonia diffusion and/or co-ion leakage originating from the base. Since increasing temperature showed a lower final diluate EC (i.e. little ions present in the diluate after 150 minutes) the buffering capacity of the diluate became smaller with increasing temperature. In Figure 4.13, it is visible that with the increase in diluate pH, the acid pH increased slightly as well and the base pH slightly decreased from the moment the less steep increase in diluate pH happened. This suggests that because of NH_3 leaving the base with dissolved ammonia diffusion, co-ion leakage or by volatilization, OH^- was forced to leave the base solution as well, ending up in the acid and diluate stream. This was confirmed by the rapid increase of diluate pH (increase in OH^- concentration) which was observed earlier in time with higher temperature (Table H and Figure 4.13). Since NH_3 formation happens more with increasing temperature, this phenomenon was found earlier with increasing temperature. This was also confirmed by the total NH_4^+ % (addition of NH_4^+ in all streams) that was found to show a slight decrease with temperature. Another explanation of the phenomena shown in Figure 4.13 could be the transportation of NH_4^+ from the diluate towards the base stream and thereby buffering the OH^- ions present in the base solution, decreasing the base pH. However, this explanation seems unlikely since the ammonium concentration in the base was found to be lowered with increasing temperature. Furthermore, since less SO_4^{2-} ions were removed from the diluate at higher temperatures due to less proton leakage, the final SO_4^{2-} concentration in the acid is lower for higher concentration. Also co-ion leakage of SO_4^{2-} might have happened. With increasing NH_4^+ concentrations in the acid, this eventually results in lower acid purities (Table 4.7).

Between the 20°C, 25°C and 30°C experiments, a clear difference was found in electrochemical consumption, NH_4^+ current efficiency and ammonium removal. However, an increasing temperature did not further improve the electrochemical energy consumption and NH_4^+ current efficiency. On the other hand, a temperature higher than 30°C was found to negatively affect the NH_4^+ concentration in the base, the SO_4^{2-} concentration in the acid and both acid and base purity. Therefore the performance of BPMED at 30°C was considered optimal and is evidently recommended for further implementation.

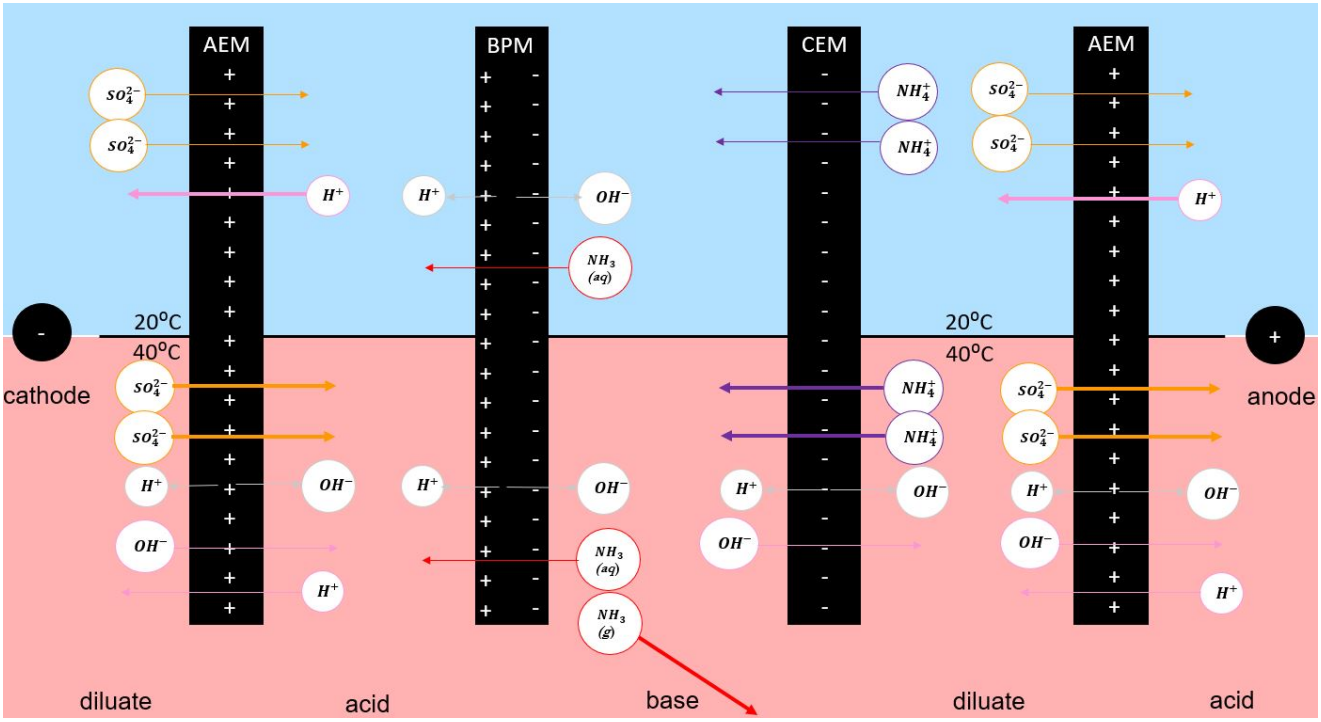

Figure 5.4: The most important potential phenomena for diluate pH 4 of 20°C and 40°C. This figure only represents the effect of temperature, so other potential phenomena irrelevant for the effect of temperature are not depicted. Enhanced watersplitting (grey) happened both at the CEM and AEM due to limited EC in the diluate of 40°C after 150 minutes. Both more NH_4^+ (purple) and SO_4^{2-} (sulfate) removal were observed at 40°C due to lower viscosity of water and higher diffusivity of ions. The higher sulfate removal at higher temperatures was also the result of less H^+ leakage (pink) at higher temperatures: since the H^+ concentration in the diluate is smaller, more NH_4^+ and (to maintain charge balance) more SO_4^{2-} could leave the diluate, resulting in a higher SO_4^{2-} removal. Another explanation for the forced higher SO_4^{2-} removal can come from the higher NH_4^+ removal due to dissolved ammonia diffusion (red), co-ion leakage and ammonia volatilization (red). Ammonia leaving the base earlier with higher temperature resulted in the forced transport of OH^- (pink) ions towards the diluate and thereafter towards the acid. Both purity of acid and base decreased with increasing temperature due to more dissolved ammonia diffusion. A thicker arrow indicates a higher transport number of the ion compared to a thinner arrow. The thickness of the arrows is relative to the other diluate temperature, but not relative to other ions. The size of the ions is not at scale.

5.5 Concentration evolution over time

In Figure 4.14 and Figure 4.15, the concentrations of NH_4^+ and SO_4^{2-} are shown over time. The increase in the NH_4^+ concentration in the acid over time could be clarified by the fact that dissolved ammonia diffusion takes places from the base towards the acid, as confirmed by van Linden et al. [59]. Since the concentration of ammonium in the base increases over time by formation of NH_4OH, the difference in gradient between the acid and base stream increases, which enlarges the driving force for ammonia to diffuse towards the acid stream [4]. Another factor of influence can be the increased temperature of the streams, which enlarges the volatilized ammonia fraction. It was found that with increasing temperature, the final NH_4^+ concentration in the acid after 150 minutes exceeded the NH_4^+ concentration in the base after 150 minutes. The acid could hold NH_4^+ better, due to the lower pH with the NH_4^+ equilibrium more on the NH_4^+ side. Ammonia back diffusion towards the diluate was not observed and was unlikely, since transportation against the electrochemical driving force is inefficient.

The difference between the room temperature experiment and the 20°C experiment is small, but visible. The slightly lower temperature in the room could partly explain this difference. Furthermore, the difference in set-up difference could play a role. The set-up for the 20°C experiment in the incubation room was slightly different, affecting the loss in volume and the flow efficiency of the streams. Additionally, the incubator created an environment, resulting in different relative humidity for the experiments on temperature influence. The relative humidity was found to play a role on the functionality of BPMED treatment [44].

5.6 Membrane damage

Even though the specifications of the PC 100D membrane allow it to function at 40°C, the outcomes of this thesis show differently. Experiments 25°C(3), 30°C(3) and 35°C(2) had higher concentrations NH_4^+ present in the diluate after 150 minutes than 25°C(1) 25°C(2), 30°C(1) 30°C(2) and 35°C(1), respectively. The sulfate removal was found to be unaffected. A higher energy consumption per experiment and a smaller absolute NH_4^+ removal efficiency were found after exposure to 40°C. Together this resulted in a higher electrochemical energy consumption and a lower NH_4^+ current efficiency for the experiments performed after exposure to 40°C. Apparently, the membrane functionality is affected by exposure to high temperatures, which is confirmed by literature [4, 44]. The lower NH_4^+ removal suggests a decrease in NH_4^+ selectivity of the membrane due to changes in membrane structure affecting the membrane ion transport properties and selectivity after exposure to 40°C, as stated by Strathmann et al. [4]. Literature supports on the fact that the operating temperature can affect the structure and the mechanical properties of the membranes because of basic polymer or re-crystallization and aging due to loss of water or plasticizing agents [4]. The changes in membrane properties were found to be time and temperature dependent as confirmed by Marrony et al. and Strathman et al. [4, 44].

5.7 Limitations of this study

5.7.1 Experimental limitations

Sulfate inaccuracies
Even though a correction was performed on the measured SO_4^{2-} concentration, the mass balance of SO_4^{2-} exceeded 100%, which is theoretically impossible. Practically, residues of the prior experiments might add up to the values of the current experiment, but then losses should be visible in the prior experiment, which was not the case. Consequently there was still an inaccuracy in the sulfate measurements after correction. The difficulty with these concentration measurements is that for the sulfate concentration measurements, high dilution factors were used (up to 2000 times). In a high dilution factor, a small error can have a big impact. However, dilutions were performed multiple times in different ways, but the same error kept being present. One explanation might be the presence of inaccuracies in the pipetted volume. However, all pipettes were calibrated before use and the pipettes were consistently used.

On top of that, known NH_4^+ concentrations were also tested with various dilutions factors and with the same pipettes, all providing the accurate NH_4^+ concentration. This contradicts the hypothesis in experimental inaccuracies. Similarly for sample taking: taking samples in an incorrect way (non mixed) could result in deviating concentrations. However, concentrations of NH_4^+ were found to be accurate with this way of sample taking. assuming a completely homogeneously spread of ions over solution, rejecting this explanation rejected

Alternatively, an explanation for the inaccuracy in SO_4^{2-} measurements could be the interference of NH_4^+ ions with SO_4^{2-} ions. Kelland et al. describe the effect of various cations on the formation of barium sulfate, which is the compound on which the measurement kits are based [95]. It has been shown that when additional sodium chloride is present, barium sulfate crystal growth is decreased significantly compared to when no additional salt is added. This is due to the increased solubility (and therefore, lower supersaturation) of barium sulfate created by the increased ionic strength. However, this would suggest a lower bariumsulfate crystal growth and therefore a lower concentration detected, which is not the case.

The influence of this inaccuracy in sulfate measurements can have an impact on the results. Since the initial determined sulfate correction curve (Figure 3.4) did not compensate the full error, an additional correction was performed for the SO_4^{2-} concentrations in the acid, base and diluate. For the pH experiments the summed up SO_4^{2-} concentrations were found to have a total error of circa 20 %. The error for the concentration experiments was found to be circa 15 % and for the temperature experiments no second correction was needed. The experiments on the influence of temperature were most likely not in need of a correction due to their bigger volume loss. Both pH and concentration experiments were found to have a maximum volume loss of 5%. However, the temperature experiments were facing volume losses up to 12%. The explanation for this larger loss in volume for the latter experiments can be found in the difference in set-up, which could apparently be improved. Evaporation of water could not be an explanation for the increased volume losses, since in that case higher NH_4^+ and SO_4^{2-} concentrations would be expected (due to concentration).

A second correction was therefore required for both pH and concentration experiments. The total percentage of 200 % SO_4^{2-} (Acid + Base + Diluate + ERS) was spread relatively over the 4 streams based on their fraction in the total percentage. Even though the overall conclusions stay valid, this correction might have some consequences:

- The SO_4^{2-} concentration in the acid stream might turn out to be higher (up to 10% correction),

since for the SO_4^{2-} concentration in the acid is high compared to the base and diluate solution and therefore has a larger absolute correction.

- The SO_4^{2-} concentration in the base stream might turn out to be higher (up to 10% correction).
- The SO_4^{2-} concentration in the diluate after 180 or 150 minutes can turn out to be higher (up to 10 %), insinuating a slightly lower SO_4^{2-} removal efficiency.
- The purity of the acid could increase and the purity of the base could decrease.
- The SO_4^{2-} electrochemical energy consumption and SO_4^{2-} current efficiency were not shown. Furthermore,no statistical analysis could be performed, since the absolute values were not completely reliable.

It is recommended to validate and improve the SO_4^{2-} correction for further research. It is recommendable to use SO_4^{2-} measuring equipment which can measure SO_4^{2-} in a higher range, so a smaller dilution factor is required. As well, other techniques for measuring the SO_4^{2-} concentration might be considered, for example sending the samples to specialized labs. Even though the SO_4^{2-} concentrations were not fully accurate, the research on the influence of pH, concentration and temperature is still very reliable and evident. Since the dilutions and concentration measurements of the same streams were all performed in the same way, in the same batch, with the same dilution factor, the relative trend became very evident. Therefore, the conclusions drawn from this report are still highly trustworthy. Additionally, the ammonium concentrations were found to be consistent with expected concentrations resulting in negligible errors.

Relative humidity
Relative humidity was not taken into account in this research, but this external condition can influence the performance stability of the membrane [44]. The incubator used for the temperature experiments automatically adapted the relative humidity in the room. Since the relative humidity therefore varied between different experiment, this could have impacted the results.

pH adjustification by H_2SO4 and NH_4OH
The pH of the $(NH_4)_2SO_4$ diluate was adjusted by the addition of H_2SO4 and NH_4OH. For the pH experiment, this resulted in differences in total volume of the diluate. On top of that, this resulted in variances in the amount of NH_4^+ ions present for the experiments with pH 6 - 10 diluates. The experiments with diluate pH 2 - 5 differed in the amount of SO_4^{2-} ions present in the diluate. Therefore, the experiments in the low pH spectrum were compared and the experiments within the high pH range were compared separately. The volume increase for the experiments (Table C.2) was considered not to be of influence.

Mass correction
Since the volumes of the solutions were based on their mass, a correction had to be performed for the mass of salt added in solution. Both initial diluate solution and initial ERS solution were corrected for the mass of the added salt. For the volumes at t=150 (temperature experiments) of t = 180 minutes, the assumption was made with a correction of 35 gram for the acid volume, 10 gram for the base mass 5 (or 55, 105, 155, 205) gram for the diluate solution and 71 gram for the ERS solution. This spread of salt over the solutions was based on the percentagewise distribution of NH_4^+ and SO_4^{2-} over the solutions. A more accurate way for determination of salt distribution can be performed by EC measurements which can provide the concentration and density of the solutions. However, this correction can only be

used in the case of only 1 salt present, which and is therefore not applicable in this case. Therefore, the described assumption is currently the most reliable correction for these type of experiments, but can slightly influence the results.

Hydraulic/Set-up optimization
The pH experiments showed an average volume loss of 3.6 % v/v, the average loss of the concentration experiments 2.0% v/v and for the temperature experiments, there was an average volume loss of 8.0 % v/v. Since the volume loss of the experiments did not increase with temperature, the explanation can be found in the hydraulic set-up of the temperature experiments. The less optimized set-up in the incubator apparently resulted into more losses, which impacts the recoverability of the ions during the experiments. However, since the set-up was the same for all temperature experiments, the set-up does not influence the comparison between different temperatures.

5.7.2 Practical implementation limitations

Energy consumption
For the electrochemical energy consumption only the applied power supply energy consumption was taken into account. Other power needs for pumping or heating/cooling the water were not taken into consideration but will contribute significantly to the total power consumption.

Membrane lifetime
The lifetime of the membranes for proper water treatment was not investigated during this research. Even though the membranes are produced with a lifetime in the order or years, literature supports on the fact that extreme conditions like high temperature can be of influence on the physio-chemical properties of the membrane and on its lifetime [44]. Before implementation of BPMED in such extreme conditions, the impact on the functionality and durability of the membrane should be assessed.

5.8 Strengths of this study

Extensive research on functionality and underlying principles
This research provides an extensive overview and fundamental background on the efficiency of BPMED treatment of ammonium sulfate rich industrial wastewater with extreme characteristics. Energy consumption and removal efficiency were examined, as well as purity and final concentrations of NH_4^+ and SO_4^{2-} in the base and acid, respectively. Combining all these parameters, convincing directions can be provided for optimal use of BPMED in for treatment with these extreme conditions. Additionally, underlying fundamentals could be identified by this extensive data collection, providing direction for more research on BPMED functionality.

Industrially competing
This research provides data suggesting the competitiveness of BPMED treatment for ammonium removal with current treatment technologies. The ammonium removal efficiency (up to 95%) and electrochemical energy consumption (between 22.7 and 5.49 $MJ * kg^{-1}_{NH_4^+}$) resulted in a NH_4+ current efficiency of at least 48% were found to be competitive with current BPMED ammonium removal systems for less extreme wastewater treatment [36]. Furthermore the base and acid produced could be sold or re-used in the system which would increase financial incomes or lower expenses on chemicals.

In line with ambition towards a more green/circular economy
The BPMED technology was found to be a treatment technology for ammonium sulfate rich water which commits towards green ambitions. The most important characteristics contributing to a greener process are:

- BPMED showed to have compatible energy consumption
- The improved functionality of BPMED with increased temperature might result in less energy needed for cooling down the water
- Little to no chemicals need to be added
- Smaller green house gas emissions than conventional nitrogen removal techniques

6 Conclusions and Recommendations

6.1 Conclusions

This research successfully demonstrated the usefulness of Bipolar Membrane Electrodialysis as a technique for treating ammonium sulfate-rich water streams with extreme characteristics. The technology was found to be capable of both ammonium and sulfate removal while producing high purity sulfuric acid and ammonium hydroxide, even under varying pH conditions, at high temperature up to 40°C and at high ammonium sulfate concentrations up to 250 g/L, which answers the main research question:

What is the influence of high temperature, high concentration and pH on the ammonium and sulfate removal efficiency and the purity of the generated sulfuric acid and ammonium hydroxide by scrubber effluent treatment with Bipolar Membrane Electrodialysis?

Research sub question 1: *What is the influence of pH on BPMED treatment of ammonium sulfate-rich scrubber effluent?*

Diluate solutions of 50 g/L ammonium sulfate with a pH ranging between 2 and 10 were tested with the BPMED technology. Looking into the low pH range (pH between 2 and 5), the ammonium removal at pH 2 was found to be lower than at pH 3, 4 and 5. In the diluate with pH 2, H^+ and NH_4^+ ions competed for transportation over the membrane, resulting in a lower NH_4^+ current efficiency and a higher electrochemical energy consumption for a diluate with pH 2. The competition between NH_4^+ and H^+ ions resulted in less efficient removal of ammonium for a lower pH. For sulfate, the removal from the diluate increased slightly with increasing pH due to presence of HSO_4^- ions in a low pH diluate, which complicates SO_4^{2-} removal. The purities of acid and base were found to be nearly unaffected by the pH with a 86 % H_2SO_4 solution and a 96 % NH_4OH solution produced with an initial diluate pH of 5. Both absolute ammonium and sulfate removal were higher with higher pH (in the high pH range: pH 6-10) of the diluate solution. Therefore the NH_4^+ current efficiency was found to slightly increase, with a decreasing electrochemical energy consumption. Even though the electrochemical energy consumption decreased, enhanced water splitting at both the CEM and AEM were most likely the source of a higher total energy consumption during 180 minutes for higher pH. This was compensated by higher ammonium transportation with high pH due to less H^+ competition, a more substantial concentration gradient and a higher ammonia fraction resulting in dissolved ammonia diffusion and volatilization for the diluate with pH 10. The increased SO_4^{2-} removal is not completely understood yet and should therefore be researched in more detail. The purity of the acid lowered and the purity of the base increased with increasing pH.

The competition between H^+ ions and NH_4^+ ions observed at low pH, made the diluate with pH 2 show sub optimal removal efficiencies and energy use. In the high pH range, the increased ammonia diffusion at high pH resulted in lower purity of the produced acid and a relatively smaller ammonium removal. For industrial implementation, the use of diluate at pH higher than 2 is recommended.

Research sub question 2: *What is the influence of the ammonium sulfate concentration on BPMED treatment of ammonium sulfate-rich scrubber effluent?*

BPMED technology was found to be able to treat waters with concentrations up to 250 g/L ammonium sulfate. With increasing ammonium sulfate concentrations, the NH_4^+ current efficiency was found

to increase from 54% for 50 g/L ammonium sulfate initial concentration to 74% for 250 g/L. This increase in ammonium removal efficiency is a consequence of the imperfection of the membranes, resulting in ammonia diffusion and co-ion leakage. The removal of SO_4^{2-} ions slightly decreased, which is most likely associated with $(NH_4)SO_4^-$ ion pair formation, resulting in a lower activity of the SO_4^{2-} ions. The purity of the acid and base decreased slightly, which confirmed the ammonia diffusion from the base towards the acid with increasing concentration. A higher concentration led to higher concentration gradients which resulted in less concentration polarization and a lower total energy consumption. It can be beneficial to stop BPMED treatment before all ammonium sulfate is removed, looking into the increased energy consumption and ammonia diffusion towards the end of the experiment. Research on the duration creating the optimal removal efficiency with the optimal acid and base purity should be researched further.

Research sub question 3: *What is the influence of temperature on BPMED treatment of ammonium sulfate-rich scrubber effluent?*

With increasing temperature, both ammonium and sulfate removal increased (82% and 87% respectively for 20°C and 90% and 94% for 40°C). The electrochemical energy consumption decreased with increasing temperature and the current efficiency slightly increased (57.5% for 20°C and 61% for 40°C) showing that less energy was needed for the transportation of the same amount of NH_4^+. Less proton leakage with increasing temperature results in less competition between H^+ and NH_4^+ ions and thereby resulted in a higher NH_4^+ removal efficiency. The increased ammonia fraction with increasing temperature resulted in bigger NH_4^+ losses due to dissolved ammonia diffusion and volatilization. Removal of SO_4^{2-} increased due to less proton leakage with higher temperature and due to more ammonium diffusion from diluate to acid, forcing the SO_4^{2-} to leave the diluate as well. The purity of both acid and base lowered with increasing temperature due to ammonia diffusion. In conclusion, the optimal operating temperature depends on the requirements: for higher removal with smaller energy consumption, a temperature up to 40°C is recommended. However, for the highest H_2SO4 and NH_4OH purity, a temperature of 20°C or 25°C is recommended. It should however be highlighted that the use of the BPMED technology at high temperatures (40°C) should be performed with caution. The membranes were found to show smaller NH_4^+ removal efficiencies and an increased energy consumption after exposure to 40°C, most likely due to structural damages to the membrane.

The findings of this research provide the theoretical background and confirmation on laboratory scale for the successful implementation of BPMED for treating stripper/scrubber effluent with the simultaneous production of a pure acid and base. With this energetically competitive technique, a circular nitrogen removal process can be created due to in situ generation of the sulfuric acid. On top of that, the proven functionality of BPMED under extreme conditions creates opportunities in other wastewater treatment processes.

6.2 Recommendations

6.2.1 Non-model wastewater

For this research, synthetic waters containing pure ammonium sulfate were used. Although scrubber effluent is expected to be pure, the next step would be to introduce raw wastewater. In non-artificial industrial wastewater, more different molecules can be present. Those could affect the functioning of the BPMED, for example by scaling or fouling the membranes or by interfering with the NH_4^+ and SO_4^{2-} ions.

Furthermore, the combination of a low pH, high temperature and high concentration wastewater solution was not tested during this research. However, the effluent of the industrial stripper/scrubber system has a combination of those characteristics, which might affect the functionality and is therefore recommendable to be tested.

6.2.2 Recommendations for scientific community

Several assumptions in this research should be verified or be investigated in more detail.

- First of all, the methodology for sulfate concentration determination should be improved. Literature describing sulfate concentrations measurements revealed the difficulty with obtaining accurate sulfate measurements in the laboratory [96]. To provide more insights in the absolute removal, the improvement of the sulfate concentration measurement is crucial. First of all, the origin of the error should be identified. Consequently, other methods for sulfate concentration measurements should be compared. Test tubes based of other brands might be of interest, the accuracy of the IC should be re-investigated or samples should be send to external laboratories specialized in sulfate concentration testing.

  A higher accuracy of sulfate concentration testing makes statistical tests possible. Proofing the effect of influence of a varying pH, concentration and temperature in a significant way would require more repetitions of the experiments.

- As became clear from the set-up development, the ERS stream, which was not evaluated and tracked during prior research, potentially influences the removal efficiency of sulfate. A look into the role of the ERS on the experiments should be done by varying ERS concentrations, the type of salt dissolved in the ERS and the pH of the solution.

- As discussed in section 5.7, the volumes and the amount of NH_4^+ and SO_4^{2-} ions differed for the pH experiments. For investigating the effect of pH on SO_4^{2-} removal in the low pH range, it is recommended to acidify the initial diluate solution with an acid composed of another anion than SO_4^{2-}. Similarly. for research on the effect of high pH on NH_4^+ removal, increasing the pH with a base without NH_4^+ is recommended. It should be noted that the newly introduced anions and cations might interfere within the process.

- More research should be performed on some unexplained phenomena observed during this research:

  1. Why was there increased sulfate removal for higher pH? The higher leakage with higher concentrations (in this case of NH_4^+) might result in higher SO_4^{2-} removal, but more explanations are likely to exist.

  2. Validation of the hypothesized reasoning for improved NH_4^+ removal and lowered SO_4^{2-} removal with increasing concentration is required. Is dissolved ammonia diffusion passing the imperfect

membranes the only reason for higher NH_4^+ removal? And what is the exact role of $(NH_4)SO_4^-$ ions on the SO_4^{2-} removal efficiency?

3. To get better insights in the movement of ions during the temperature experiments, it is recommended to test the permselectivity for ions at different temperatures. By measuring the ratio between fluxes the currently provided explanations might be confirmed.

- Ammonia diffusion from base to acid was found to rise mostly towards the end of the experiment. Research should be performed on the fact whether this diffusion is mostly gradient driven or time driven. By defining the origin of the ammonia diffusion, this could be lowered in the future.

- The impact of sulfate ions on BPMED treatment should be investigated further. Ammonium removal was researched before, although at lower concentrations. Less research was performed on the removal of sulfate, the phenomena behind it and the influence of the sulfate on the removal of the present cation. It is advisable to check the impact of the sulfate ion on the removal efficiency by replacing the sulfate ion with other (smaller) anions.

- More concentration measurements over time would be recommended. In this research, the ammonium and sulfate concentrations for only 4 experiments with differences in temperature were evaluated over time. However, a more definite answer on the chemical phenomena behind the results could be provided for the experiments on pH and concentration influence by evaluation of the various concentrations in all streams over time.

- In this study, a 3-compartment stack was used, resulting in the production of both acid and base. Literature states that electrodialysis with three compartments gives better current efficiencies compared to a two compartment configuration [69]. However, a two-compartment stack can be beneficial for the purity of the produced acid and base [23]. Therefore, depending on the application, investigation on the functionality of a 2-compartment BPMED stack is recommended.

- Literature suggests that scaling is proportional to the average electric current, implying that the scaling problem can be controlled by reducing the applied current [67]. Since scaling results in flux drop, less wastewater could be treated within the same period of time [97]. It is recommendable to look into the effect of current on formation of scale, especially before long-term industrial implementation.

- As explained in section 5.7, an assumption for mass correction was performed for the addition of salt to solution. Since this method is based on empirical data, it is recommended to find a more proven way of measuring the volume. One example can be the determination of volume by equipment like a measuring cylinder.

- Currently, theoretical explanations were mostly given trying to prove the experimental observations. It is highly recommended to look for/develop a simple model which can map the ionic flows and transportation of volume. In literature, some attempts were made to model electrodialysis, but not for this specific application [98, 99]. Based on empirical data as obtained in this research, a model can be build, which might simplify identification of processes in further research. Furthermore, a model showing electricity use and total costs of the process would facilitate large-scale application.

6.2.3 Recommendations for industrial partners -process optimization

For industrial companies treating enormous amounts of ammonium sulfate rich waters, the following recommendations are provided:

- The produced sulfuric acid with a purity of circa 85% with a pH of 1 could be added to the stripper system, realizing the required decrease in pH. Further purification/concentration steps might be required. The re-use of sulfuric acid would create the desired circular system for ammonium removal.

- The produced ammonium hydroxide solution (circa 95%) could be purified after which it can be sold to industrial partners. Ammonium hydroxide can be used as a cleaning agent and sanitizer in many household and industrial cleaners. Furthermore, ammonium hydroxide is used in the manufacture of products such as fertilizer, plastic, rayon and rubber [31, 32].

- The initial inflowing diluate stream for the BPMED, which is the effluent of the scrubber system, has a temperature of circa 70 °C. For using the BPMED, the temperature should be lowered to at least 40 °Celsius. Since the energy consumption at high temperature was lower and the removal efficiency of both ammonium and sulfate increased, less cooling of the scrubber effluent would be beneficial and cost less energy (to 40 °C instead of 20 °C).

- In this research, the PC 100D bipolar membrane stack was used, which is made for the production of organic acids. However, this type of membrane is not optimized for the production of H_2SO4 and SO_4^{2-}. There might be that other (selective) membranes available that perform even better for this purpose. On top of that, there is continuous improvement and development on the materials used in the membranes. The use of proton permselective cation exchange membranes might decrease proton leakage and is therefore highly recommended [54].

- Mapping the integrity and durability of the membranes is important before implementation on industrial scale. The extreme exposure conditions under which the BPMED would have to function for treating the effluent of a stripper/scrubber were tested only during small, limited duration experiments. However, practically these membranes would be exposed to extreme conditions for much longer times, which might affect the functionality of the membranes. The need for frequent replacement of the membranes would not be desirable. Useful life time of membranes under process conditions is generally in the range of a couple of years [4]. Membranes stability tests are in any case recommended during long time use.

- For the scope of this research, batch experiments were performed. Though, within an industrial system, a plug flow or continuous system is more likely. Therefore research on the influence of the type of system on the BPMED process and its functionality is recommended. The impact of a continuous system should be investigated on labscale first. Computational models might be of used for this as well. By knowing the impact of the type of system, the set-up might be adjusted or improved.

- More research is recommended on the evolution of concentrations over time. During this research it was found that in batch experiments the ammonia diffusion from base to acid (resulting in an decrease in purity of both acid and base) was happening mostly towards the end of the experiment. Since ammonia diffusion is an undesired process, it might be interesting to stop the BPMED process earlier. Nowak et al state that the performance of BPM decreases with concentration of acid and base [26]. Besides, Zhang et al. state that the current efficiency is decreasing with increasing sulfuric acid production in acid stream [25]. The sulfuric acid production in the acid stream was found to be higher towards the end of the experiment, which might be another reason for an earlier stop of the BPMED process.

- It is worth investigating the treatment of other types of streams with extreme characteristics with BPMED, since the technology was found to function under extreme conditions and therefore creates the theoretical foundation for many more desalination applications.
- A market research should be done to better understand the interest in a circular H_2SO4 system for ammonia recovery. Furthermore, a better understanding should be gained on the NH_4OH market, looking into potential purchasers and required purities.
- Before the implementation of BPMED in industrial ammonium sulfate streams with extreme characteristics it is crucial to provide a cost-benefit overview. Research should be done on the costs for implementation, but also on the savings that are made on treatment due to energy savings and smaller purchase costs on chemicals. Since these costs (reductions) are fully depend on the size and type of industry, an estimation in costs and cost savings is out of scope for this project.

6.2.4 Recommendations for policy makers

The BPMED has a proven record for treatment of ammonium rich wastewater streams. The current nitrogen crisis shows the urgency for the development and utilisation of innovations like these in order to minimize nitrogen losses in the environment. Therefore, the recommendations for policy makers are:

- Subsidize innovations in the field of BPMED technology.
- Look into other processes in which BPMED treatment can be useful as well.

References

[1] Byoflex.nl. Byoflex. URL https://byosis.com/systems/byoflex.

[2] H. Strathmann. Electrodialysis, a mature technology with a multitude of new applications. *Desalination*, 264(3):268–288, 2010. ISSN 00119164. doi: 10.1016/j.desal.2010.04.069. URL http://dx.doi.org/10.1016/j.desal.2010.04.069.

[3] T. Rottiers, K. Ghyselbrecht, B. Meesschaert, B. Van der Bruggen, and L. Pinoy. Influence of the type of anion membrane on solvent flux and back diffusion in electrodialysis of concentrated nacl solutions. *Chemical Engineering Science*, 113:95–100, 2014.

[4] H. Strathmann. *Ion-exchange membrane separation processes*. Elsevier, 2004.

[5] L. Y. Stein and M. G. Klotz. The nitrogen cycle. *Current Biology*, 26(3):R94–R98, 2016. ISSN 09609822. doi: 10.1016/j.cub.2015.12.021. URL http://dx.doi.org/10.1016/j.cub.2015.12.021.

[6] W. J. Mattson. Herbivory in Relation to Plant Nitrogen Content. *Annual Review of Ecology and Systematics*, 11(1):119–161, 1980. ISSN 0066-4162. doi: 10.1146/annurev.es.11.110180.001003.

[7] V. Smil. Global Population and the Nitrogen Cycle. *Scientific American*, 277(1):76–81, 1997. ISSN 0036-8733. doi: 10.1038/scientificamerican0797-76.

[8] A. R. Townsend and R. W. Howarth. Fixing the global nitrogen problem. *Scientific American*, 302 (2):64–71, 2010. ISSN 00368733. doi: 10.1038/scientificamerican0210-64.

[9] E. Stokstad. The nitrogen fix. *Science*, 353(6305):1225–1227, 2016. ISSN 10959203. doi: 10.1126/science.353.6305.1225.

[10] M. A. Sutton, C. M Howard, J. W. Erisman, G. Billen, A. Bleeker, P. Grennfelt, H. Van Grinsven, and B. Grizzetti. *The European nitrogen assessment: sources, effects and policy perspectives*. Cambridge University Press, 2011.

[11] J. W. Erisman, A. Bleeker, J. Galloway, and M. S. Sutton. Reduced nitrogen in ecology and the environment. *Environmental Pollution*, 150(1):140–149, 2007. ISSN 02697491. doi: 10.1016/j.envpol.2007.06.033.

[12] S. Okabe, M. Oshiki, Y. Takahashi, and H. Satoh. N2O emission from a partial nitrification-anammox process and identification of a key biological process of N2O emission from anammox granules. *Water Research*, 45(19):6461–6470, 2011. ISSN 18792448. doi: 10.1016/j.watres.2011.09.040. URL http://dx.doi.org/10.1016/j.watres.2011.09.040.

[13] B. Bates, Z. Kundzewicz, and S. Wu. *Climate change and water*. Intergovernmental Panel on Climate Change Secretariat, 2008.

[14] S. A. Saadabadi, A. Thallam Thattai, L. Fan, R. E.F. Lindeboom, H. Spanjers, and P. V. Aravind. Solid Oxide Fuel Cells fuelled with biogas: Potential and constraints. *Renewable Energy*, 134: 194–214, 2019. ISSN 18790682. doi: 10.1016/j.renene.2018.11.028. URL https://doi.org/10.1016/j.renene.2018.11.028.

[15] O. Grasham, V. Dupont, M. A. Camargo-Valero, P. García-Gutiérrez, and T. Cockerill. Combined ammonia recovery and solid oxide fuel cell use at wastewater treatment plants for energy and greenhouse gas emission improvements. *Applied Energy*, 240(February):698–708, 2019. ISSN 03062619. doi: 10.1016/j.apenergy.2019.02.029. URL https://doi.org/10.1016/j.apenergy.2019.02.029.

[16] IHS Chemical Economics Handbook. To make better decisions, you need to see the big picture. URL https://ihsmarkit.com/products/ammonia-chemical-economics-handbook.html#:~:text=During2020\OT1\textendash25,worldapparent,willcontinuetooutpaceconsumption.

[17] G. P. Robertson and J. M. Tiedje. Nitrous oxide sources in aerobic soils: Nitrification, denitrification and other biological processes. *Soil Biology and Biochemistry*, 19(2):187–193, 1987. ISSN 00380717. doi: 10.1016/0038-0717(87)90080-0.

[18] J. Gijs. Combined nitrification-denitrification processes. 15:109–117, 1994.

[19] Y. Jin, D. Wang, and W. Zhang. Effects of substrates on n 2 o emissions in an anaerobic ammonium oxidation (anammox) reactor. *SpringerPlus*, 5(1):1–12, 2016.

[20] S. P. Wei, F. van Rossum, G. Jan van de Pol, and M. K. H. Winkler. Recovery of phosphorus and nitrogen from human urine by struvite precipitation, air stripping and acid scrubbing: A pilot study. *Chemosphere*, 212:1030–1037, 2018. ISSN 18791298. doi: 10.1016/j.chemosphere.2018.08.154. URL https://doi.org/10.1016/j.chemosphere.2018.08.154.

[21] T. Franken. Bipolar membrane technology and its applications. *Membrane Technology*, 2000(125): 8–11, 2000. ISSN 09582118. doi: 10.1016/S0958-2118(00)80212-8.

[22] K. N. Mani. Electrodialysis water splitting technology. *Journal of Membrane Science*, 58(2): 117–138, 1991. ISSN 03767388. doi: 10.1016/S0376-7388(00)82450-3.

[23] G. Pourcelly. Electrodialysis with bipolar membranes: Principles, optimization, and applications. *Russian Journal of Electrochemistry*, 38(8):919–926, 2002. ISSN 10231935. doi: 10.1023/A:1016882216287.

[24] X. Tongwen. Electrodialysis processes with bipolar membranes (EDBM) in environmental protection - A review. *Resources, Conservation and Recycling*, 37(1):1–22, 2002. ISSN 09213449. doi: 10.1016/S0921-3449(02)00032-0.

[25] X. Zhang, W. Lu, H. Ren, and W. Cong. Sulfuric acid and ammonia generation by bipolar membranes electrodialysis: Transport rate model for ion and water through anion exchange membrane. *Chemical and Biochemical Engineering Quarterly*, 22(1):1–8, 2008. ISSN 03529568.

[26] M. Nowak, H. Jaroszek, and M. Turkowska. Conversion of waste sodium sulfate with bipolar membrane electrodialysis. *Membranes and Membrane Processes in Environmental Protection*, 119 (June):337–349, 2014.

[27] NijhuisIndustries. Nochemnar project proposal. 2019.

[28] Sulfuric acid - chembid. URL https://www.chembid.com/en/results/cluster/B/1/?q=sulfuricacid&gclid=Cj0KCQiAnKeCBhDPARIsAFDTLTL5faNlPx9WRkcL3RSEfvVm5_HxgeLbcdZfoef9NaoBOunG16z2HHAaAr3PEALw_wcB&filterCurrency=eur.

[29] Sulfuric acid market size, share, trends, opportunities forecast. URL https://www.verifiedmarketresearch.com/product/sulfuric-acid-market/.

[30] K. P. Resnik, J. T. Yeh, and H. W. Pennline. Aqua ammonia process for simultaneous removal of co2, so2 and nox. *International journal of environmental technology and management*, 4(1-2): 89–104, 2004.

[31] Ammonium hydroxide market - global industry analysis, size, share, growth, trends, and forecast 2017 - 2027. URL https://www.transparencymarketresearch.com/ammonium-hydroxide-market.html.

[32] KMG chemicals. Product safety summary sheet - ammonium hydroxide. 2014.

[33] Ammonia market size outlook: Industry forecast report, 2014-2025. URL https://www.grandviewresearch.com/industry-analysis/ammonia-market.

[34] Tanmay. Aqua ammonia market to witness the highest growth globally in coming years 2020-2025, Jan 2021. URL https://www.mccourier.com/aqua-ammonia-market-to-witness-the-highest-growth-globally-in-coming-years-2020-2025/.

[35] Alibaba ammonia solution. URL https://www.alibaba.com/product-detail/Ammonia-solution-Ammonium-Hydroxide-Ammonia-Water_60144671734.html?spm=a2700.7724857.normal_offer.d_title.72e7607ahY5ess.

[36] N. van Linden, G. L. Bandinu, D. A. Vermaas, H. Spanjers, and J. B. van Lier. Bipolar membrane electrodialysis for energetically competitive ammonium removal and dissolved ammonia production. *Journal of Cleaner Production*, 259:120788, 2020. ISSN 09596526. doi: 10.1016/j.jclepro.2020.120788. URL https://doi.org/10.1016/j.jclepro.2020.120788.

[37] M. Chen, F. Zhang, Y. Zhang, and R. J. Zeng. Alkali production from bipolar membrane electrodialysis powered by microbial fuel cell and application for biogas upgrading. *Applied Energy*, 103:428–434, 2013. ISSN 03062619. doi: 10.1016/j.apenergy.2012.10.005. URL http://dx.doi.org/10.1016/j.apenergy.2012.10.005.

[38] C. Huang and T. Xu. Electrodialysis with bipolar membranes for sustainable development. *Environmental Science and Technology*, 40(17):5233–5243, 2006. ISSN 0013936X. doi: 10.1021/es060039p.

[39] M. A. B. Ali, M. Rakib, S. Laborie, P. Viers, and G. Durand. Coupling of bipolar membrane electrodialysis and ammonia stripping for direct treatment of wastewaters containing ammonium nitrate. *Journal of Membrane Science*, 244(1-2):89–96, 2004. ISSN 03767388. doi: 10.1016/j.memsci.2004.07.007.

[40] J. Kroupa, J. Kinčl, and J. Cakl. Recovery of H2SO4 and NaOH from Na2SO4 by electrodialysis with heterogeneous bipolar membrane. *Desalination and Water Treatment*, 56(12):3238–3246, 2015. ISSN 19443986. doi: 10.1080/19443994.2014.980972. URL http://dx.doi.org/10.1080/19443994.2014.980972.

[41] H. S. Shin, J. Y. Jung, B. U. Bae, and B. C. Paik. Phase-separated anaerobic toxicity assays for sulfate and sulfide. *Water environment research*, 67(5):802–806, 1995.

[42] C. Namasivayam and M. V. Sureshkumar. Modelling thiocyanate adsorption onto surfactant-modified coir pith, an agricultural solid 'waste'. *Process safety and environmental protection*, 85(6): 521–525, 2007.

[43] Y. Marcus. Ionic radii in aqueous solutions. *Chemical Reviews*, 88(8):1475–1498, 1988.

[44] M. Marrony, R. Barrera, S. Quenet, S. Ginocchio, L. Montelatici, and A. Aslanides. Durability study and lifetime prediction of baseline proton exchange membrane fuel cell under severe operating conditions. *Journal of Power Sources*, 182(2):469–475, 2008. ISSN 03787753. doi: 10.1016/j.jpowsour.2008.02.096.

[45] D. Raucq, G. Pourcelly, and C. Gavach. Production of sulphuric acid and caustic soda from sodium sulphate by electromembrane processes. Comparison between electro-electrodialysis and electrodialysis on bipolar membrane. *Desalination*, 91(2):163–175, 1993. ISSN 00119164. doi: 10.1016/0011-9164(93)80055-R.

[46] A. D. McNaught and Oxford A. Wilkinson. Blackwell Scientific Publications. Iupac. compendium of chemical terminology. *Compendium of Chemical Terminology 2nd ed. (the "Gold Book")*, 1997.

[47] G. Provolo, F. Perazzolo, G. Mattachini, A. Finzi, E. Naldi, and E. Riva. Nitrogen removal from digested slurries using a simplified ammonia stripping technique. *Waste Management*, 69:154–161, 2017. ISSN 18792456. doi: 10.1016/j.wasman.2017.07.047. URL `https://doi.org/10.1016/j.wasman.2017.07.047`.

[48] M. Laureni, J. Palatsi, M. Llovera, and A. Bonmatí. Influence of pig slurry characteristics on ammonia stripping efficiencies and quality of the recovered ammonium-sulfate solution. *Journal of Chemical Technology and Biotechnology*, 88(9):1654–1662, 2013. ISSN 02682575. doi: 10.1002/jctb.4016.

[49] S. Guštin and R. Marinšek-Logar. Effect of pH, temperature and air flow rate on the continuous ammonia stripping of the anaerobic digestion effluent. *Process Safety and Environmental Protection*, 89(1):61–66, 2011. ISSN 09575820. doi: 10.1016/j.psep.2010.11.001.

[50] J. G. Speight. *Environmental organic chemistry for engineers*. Butterworth-Heinemann, 2016.

[51] Inamuddin and M. Luqman. *Ion exchange technology I: Theory and materials*. 2012. ISBN 9789400717008. doi: 10.1007/978-94-007-1700-8.

[52] T. Luo, S. Abdu, and M. Wessling. Selectivity of ion exchange membranes: A review. *Journal of membrane science*, 555:429–454, 2018.

[53] L. Bazinet, F. Lamarche, and D. Ippersiel. Bipolar-membrane electrodialysis: Applications of electrodialysis in the food industry. *Trends in Food Science and Technology*, 9(3):107–113, 1998. ISSN 09242244. doi: 10.1016/S0924-2244(98)00026-0.

[54] I. Raissouni, M. Marraha, and A. Azmani. Effect of some parameters on the improvement of the bipolar membrane electrodialysis process. *Desalination*, 208(1-3):62–72, 2007. ISSN 00119164. doi: 10.1016/j.desal.2006.03.584.

[55] T. Sata. Recent Trends in Ion Exchange Membrane Research. *Pure and Applied Chemistry*, 58(12): 1613–1626, 1986. ISSN 13653075. doi: 10.1351/pac198658121613.

[56] F. P. Cuperus and H. H. Nijhuis. Applications of membrane technology to food processing. *Trends in Food Science & Technology*, 4(9):277–282, 1993.

[57] Y. Kim. *Ionic separation in electrodialysis: analyses of boundary layer, cationic partitioning, and overlimiting current*. PhD thesis, 2010.

[58] H. Strathmann, J. J. Krol, H. J. Rapp, and G. Eigenberger. Limiting current density and water dissociation in bipolar membranes. *Journal of Membrane Science*, 125(1):123–142, 1997. ISSN 03767388. doi: 10.1016/S0376-7388(96)00185-8.

[59] N. van Linden, H. Spanjers, and Jules B. van Lier. Application of dynamic current density for increased concentration factors and reduced energy consumption for concentrating ammonium by electrodialysis. *Water Research*, 163:114856, 2019. ISSN 18792448. doi: 10.1016/j.watres.2019.114856. URL `https://doi.org/10.1016/j.watres.2019.114856`.

[60] S. Bhattacharya and S. T. Hwang. Concentration polarization, separation factor, and Peclet number in membrane processes. *Journal of Membrane Science*, 132(1):73–90, 1997. ISSN 03767388. doi: 10.1016/S0376-7388(97)00047-1.

[61] A. H. Galama, D. A. Vermaas, J. Veerman, M. Saakes, H. H.M. Rijnaarts, J. W. Post, and K. Nijmeijer. Membrane resistance: The effect of salinity gradients over a cation exchange membrane. *Journal of Membrane Science*, 467:279–291, 2014. ISSN 18733123. doi: 10.1016/j.memsci.2014.05.046. URL `http://dx.doi.org/10.1016/j.memsci.2014.05.046`.

[62] N. Berezina, N. Gnusin, O. Dyomina, and S. Timofeyev. Water electrotransport in membrane systems. Experiment and model description. *Journal of Membrane Science*, 86(3):207–229, 1994. ISSN 03767388. doi: 10.1016/0376-7388(93)E0075-U.

[63] Y. Lorrain, G. Pourcelly, and C. Gavach. Influence of cations on the proton leakage through anion-exchange membranes. *Journal of Membrane Science*, 110(2):181–190, 1996. ISSN 03767388. doi: 10.1016/0376-7388(95)00246-4.

[64] L. Han, S. Galier, and journal=Desalination volume=373 pages=38–46 year=2015 publisher=Elsevier Roux-de Balmann, H. Ion hydration number and electro-osmosis during electrodialysis of mixed salt solution.

[65] L. X. Dang. Solvation of ammonium ion. a molecular dynamics simulation with nonadditive potentials. *Chemical physics letters*, 213(5-6):541–546, 1993.

[66] G. Palinkas and K. Heinzinger. Hydration shell structure of the calcium ion. *Chemical physics letters*, 126(3-4):251–254, 1986.

[67] H. Guo, P. Yuan, V. Pavlovic, J. Barber, and Y. Kim. Ammonium sulfate production from wastewater and low-grade sulfuric acid using bipolar- and cation-exchange membranes. *Journal of Cleaner Production*, 285:124888, 2021. ISSN 09596526. doi: 10.1016/j.jclepro.2020.124888. URL `https://doi.org/10.1016/j.jclepro.2020.124888`.

[68] J. L. Gineste, G. Pourcelly, Y. Lorrain, F. Persin, and C. Gavach. Analysis of factors limiting the use of bipolar membranes: A simplified model to determine trends. *Journal of Membrane Science*, 112(2):199–208, 1996. ISSN 03767388. doi: 10.1016/0376-7388(95)00284-7.

[69] A. T. Cherif, J. Molenat, and A. Elmidaoui. Nitric acid and sodium hydroxide generation by electrodialysis using bipolar membranes. *Journal of Applied Electrochemistry*, 27(9):1069–1074, 1997. ISSN 0021891X. doi: 10.1023/A:1018438710451.

[70] Ammonia. URL `https://pubchem.ncbi.nlm.nih.gov/compound/Ammonia`.

[71] P. Thakur. *Advanced reservoir and production engineering for coal bed methane*. Gulf Professional Publishing, 2016.

[72] M. A. R. B. Ali and W. N. El-Sayed. Feed and bleed bipolar membrane electrodialysis process. *Mediterranean Journal of Chemistry*, 7(1):75–85, 2018. ISSN 20283997. doi: 10.13171/MJC71/01805210000-BENALI.

[73] M. Szczygiełda and K. Prochaska. Recovery of alpha-ketoglutaric acid from model fermentation broth using electrodialysis with bipolar membrane. *Separation Science and Technology*, 55(1): 165–175, 2020.

[74] S. M. Hosseini, S. S. Madaeni, and A. R. Khodabakhshi. The electrochemical characterization of ion exchange membranes in different electrolytic environments: Investigation of concentration and pH effects. *Separation Science and Technology*, 47(3):455–462, 2012. ISSN 01496395. doi: 10.1080/01496395.2011.615046.

[75] Ferial Nosratinia, Mehdi Ghadiri, and Hazhir Ghahremani. Mathematical modeling and numerical simulation of ammonia removal from wastewaters using membrane contactors. *Journal of Industrial and Engineering Chemistry*, 20(5):2958–2963, 2014.

[76] L. Fu, X. Gao, Y. Yang, F. Aiyong, H. Hao, and C. Gao. Preparation of succinic acid using bipolar membrane electrodialysis. *Separation and Purification Technology*, 127:212–218, 2014. ISSN 13835866. doi: 10.1016/j.seppur.2014.02.028. URL `http://dx.doi.org/10.1016/j.seppur.2014.02.028`.

[77] E. Gain, S. Laborie, Ph Viers, M. Rakib, G. Durand, and D. Hartmann. Ammonium nitrate wastewater treatment by coupled membrane electrolysis and electrodialysis. *Journal of Applied Electrochemistry*, 32(9):969–975, 2002. ISSN 0021891X. doi: 10.1023/A:1020908702406.

[78] M. D. Eisaman, L. Alvarado, D. Larner, P. Wang, B. Garg, and K. A. Littau. CO2 separation using bipolar membrane electrodialysis. *Energy and Environmental Science*, 4(4):1319–1328, 2011. ISSN 17545692. doi: 10.1039/c0ee00303d.

[79] Sulfate. URL `https://pubchem.ncbi.nlm.nih.gov/compound/Sulfate`.

[80] D. E. Husar, B. Temelso, A. L. Ashworth, and G. C. Shields. Hydration of the bisulfate ion: atmospheric implications. *The Journal of Physical Chemistry A*, 116(21):5151–5163, 2012.

[81] V. Blickle, T. Speck, C. Lutz, U. Seifert, and C. Bechinger. Einstein relation generalized to nonequilibrium. *Physical Review Letters*, 98(21):1–4, 2007. ISSN 00319007. doi: 10.1103/PhysRevLett.98.210601.

[82] E. Kniaginicheva, N. Pismenskaya, S. Melnikov, E. Belashova, P. Sistat, M. Cretin, and V. Nikonenko. Water splitting at an anion-exchange membrane as studied by impedance spectroscopy. *Journal of Membrane Science*, 496:78–83, 2015. ISSN 18733123. doi: 10.1016/j.memsci.2015.07.050. URL `http://dx.doi.org/10.1016/j.memsci.2015.07.050`.

[83] G. M. Geise, A. J. Curtis, M. C. Hatzell, M. A. Hickner, and B. E. Logan. Salt Concentration Differences Alter Membrane Resistance in Reverse Electrodialysis Stacks. *Environmental Science and Technology Letters*, 1(1):36–39, 2013. ISSN 23288930. doi: 10.1021/ez4000719.

[84] F. G. Wilhelm. *Bipolar Membrane Electrodialysis - Membrane Development and Transport Characteristics*. 2001. ISBN 9789036515276. URL `http://doc.utwente.nl/36287/`.

[85] L. Xiaoxiu, Z. Xiaoshan, M. Yujing, N. Anpu, and J. Guibin. Size fractionated speciation of sulfate and nitrate in airborne particulates in Beijing, China. *Atmospheric Environment*, 37(19):2581–2588, 2003. ISSN 13522310. doi: 10.1016/S1352-2310(03)00220-6.

[86] B. Elgquist and M. Wedborg. Stability of ion pairs from gypsum solubility degree of ion pair formation between the major constituents of seawater. *Marine Chemistry*, 3(3):215–225, 1975. ISSN 03044203. doi: 10.1016/0304-4203(75)90003-1.

[87] J. Pawliszyn. *Sampling and sample preparation in field and laboratory: fundamentals and new directions in sample preparation*, volume 37. Elsevier, 2002.

[88] E. J. Reardon. Dissociation constants of some monovalent sulfate ion pairs at 25° from stoichiometric activity coefficients. *The Journal of Physical Chemistry*, 79(5):422–425, 1975. ISSN 00223654. doi: 10.1021/j100572a005.

[89] G. Guigas and M. Weiss. Size-dependent diffusion of membrane inclusions. *Biophysical journal*, 91 (7):2393–2398, 2006.

[90] S. S. Zumdahl. *Lab Manual for Zumdahl/Zumdahls Chemistry*. Wadsworth Publishing Co Inc, 2012.

[91] T. Y. Cath, M. Elimelech, J. R. McCutcheon, R. L. McGinnis, A. Achilli, D. Anastasio, A. R. Brady, A. E. Childress, I. V. Farr, N. T. Hancock, J. Lampi, L. D. Nghiem, M. Xie, and N. Y. Yip. Standard Methodology for Evaluating Membrane Performance in Osmotically Driven Membrane Processes. *Desalination*, 312:31–38, 2013. ISSN 00119164. doi: 10.1016/j.desal.2012.07.005. URL `http://dx.doi.org/10.1016/j.desal.2012.07.005`.

[92] M. Tanaka, G. Girard, R. Davis, A. Peuto, and N. Bignell. Recommended table for the density of water between 0 °c and 40 °c based on recent experimental reports. *Metrologia*, 38(4):301–309, 2001. ISSN 00261394. doi: 10.1088/0026-1394/38/4/3.

[93] L. Korson, W. Drost-Hansen, and F. J. Millero. Viscosity of water at various temperatures. *Journal of Physical Chemistry*, 73(1):34–39, 1969. ISSN 00223654. doi: 10.1021/j100721a006.

[94] K. Yan, X. Hang, J. Liu, J. Luo, and Y. Wan. Preparation of Hypophosphorous Acid by Bipolar Membrane Electrodialysis: Process Optimization and Phosphorous Acid Minimization. *Industrial and Engineering Chemistry Research*, 58(47):21855–21863, 2019. ISSN 15205045. doi: 10.1021/acs.iecr.9b04710.

[95] M. A. Kelland. Effect of various cations on the formation of calcium carbonate and barium sulfate scale with and without scale inhibitors. *Industrial & Engineering Chemistry Research*, 50(9): 5852–5861, 2011.

[96] P. Harris, T. Scullion, S. Sebesta, and G. Claros. Measuring Sulfate in Subgrade Soil: Difficulties and Triumphs. *Transportation Research Record*, (1837):3–11, 2003. ISSN 03611981. doi: 10.3141/1837-01.

[97] A. Wang, S. Peng, Y. Wu, C. Huang, and T. Xu. A hybrid bipolar membrane. *Journal of Membrane Science*, 365(1-2):269–275, 2010. ISSN 03767388. doi: 10.1016/j.memsci.2010.09.016. URL `http://dx.doi.org/10.1016/j.memsci.2010.09.016`.

[98] Y. Wang, A. Wang, X. Zhang, and T. Xu. Simulation of electrodialysis with bipolar membranes: estimation of process performance and energy consumption. *Industrial & engineering chemistry research*, 50(24):13911–13921, 2011.

[99] Y. Tanaka. Development of a computer simulation program of batch ion-exchange membrane electrodialysis for saline water desalination. *Desalination*, 320:118–133, 2013.

Appendices

Appendix A Pump Calibration

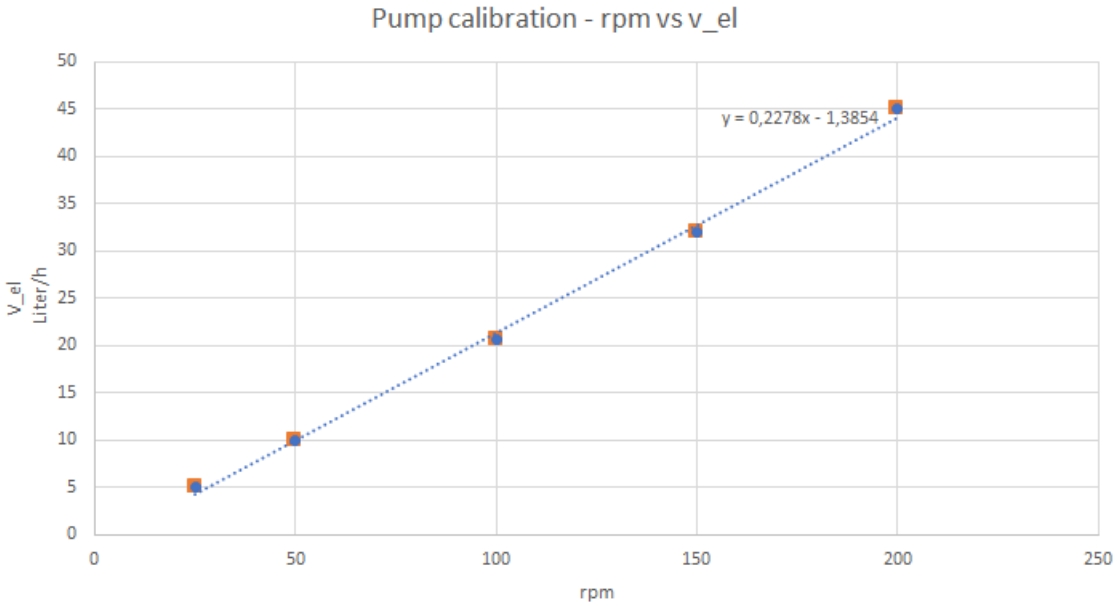

Figure A.1: Pump Calibration

Appendix B Experimental methods

B.0.1 H_2SO4 and NH_4OH addition to 50 g/L $(NH_4)_2SO_4$ solution for desired pH of solution

Table B.1: Adjustifications made to the initial 50 g/L $(NH_4)_2SO_4$ solution pH 5.3 to create the desired diluate pH

pH of Diluate 50 g/L	Added volume of 1M $H_2SO_4^{2-}$ solution	Added volume of 1M NH_4OH solution
2	12 mL	0 mL
3	1200	0 mL
4	150 µL	0 mL
5	10 µL	0 mL
6	0 µL	20 µL
7	0 µL	140 µL
8	0 µL	1300 µL
9	0 µL	12 mL
10	0 µL	110 mL

Table B.2: Adjustifications made to the initial 50, 100, 150, 200 and 250 g/L $(NH_4)_2SO_4$ solutions to realize a diluate pH of 4, used as diluate stream during the concentration experiments.

Concentration $(NH_4)_2SO_4$ in diluate (g/L)	Added volume of 1M $H_2SO_4^{2-}$ solution
50	150 µL
100	160 µL
150	220 µL
200	260 µL
250	300 µL

B.0.2 Measurement of concentration - IC or testkits comparison

Table B.3: Comparison between IC and testkits on their accuracy. Red values were under testrange or not present

Expected		Testkits		IC	
Ammonium (mg/L)	Sulfate (mg/L)	Ammonium (mg/L)	Sulfate (mg/L)	Ammonium (mg/L)	Sulfate (mg/L)
69,2	181,8	70	195	66,859	211,756
		71	195	66,815	211,976
		69	196		
		70	**195**	**66,8**	**211,9**
Ammonium (mg/L)	Sulfate (mg/L)	30	78	25,969	89,337
27,3	72,7	29	77	26,234	89,388
			75		
			77	**26,10**	**89,36**
Ammonium (mg/L)	Sulfate (mg/L)	59	14	58,241	0,414
57		56	14	58,085	0,428
		59			
		58		**58,2**	**0,4**

B.0.3 Duration of experiment

Table B.4: Ammoniumremoval after certain duration of the BPMED experiment, starting with 1 liter Diluate 50 g/L $(NH_4)_2SO_4$, 0.5 liter Acid 0.01 M $(NH_4)_2SO_4$, 0.5 liter Base 0.01 M $(NH_4)_2SO_4$ and 0.5 liter ERS 1 M Na_2SO_4.

Time running experiment (min)	Final concentration NH_4^+ in diluate (mg/L)	NH_4^+ removal from diluate
120	5116	63%
135	4196	70%
150	3360	76%
165	2220	84%
180	1244	91%
195	316	98%

Appendix C Set-up development

C.0.1 Acid and Base start concentrations

Table C.1: The 3 options as discussed. No correction was performed on the sulfate concentrations.

	Acid and Base 0,01 M $(NH_4)_2SO_4$		Acid 0,01 M $H_2SO_4^{2-}$ and Base 0,01 M		Acid 0,01 M $(NH_4)_2SO_4$ and Base 0,01 M NH_4OH	
	Mass percentage based on theoretical start concentrations		Mass percentage based on theoretical start concentrations		Mass percentage based on theoretical start concentrations	
	NH_4^+	SO_4^{2-}	NH_4^+	SO_4^{2-}	NH_4^+	SO_4^{2-}
Acid	24%	58%	24%	82%	23%	72%
Base	47%	0%	36%	0%	39%	0%
Diluate	34%	40%	35%	47%	35%	46%
ERS	0%		0%		0%	

C.0.2 PC 100 membrane or PC100D membrane

	NH_4^+	SO_4^{2-}	NH_4^+ removal
Acid	30%	63%	
Base	33%	3%	
Diluate	37%	46%	63%
ERS	7%	109%	

(a) Final percentage of NH_4^+ and SO_4^{2-} in the acid, base, diluate and ERS stream respectively for a PC 100 BPM (for sulfuric acid production) with CEEM and with ERS initial pH 2,25.

	NH_4^+	SO_4^{2-}	NH_4^+ removal
Acid	30%	65%	
Base	31%	3%	
Diluate	39%	45%	61%
ERS	7%	113%	

(b) Final percentage of NH_4^+ and SO_4^{2-} in the acid, base, diluate and ERS stream respectively for a PC 100 BPM (for sulfuric acid production) with CEEM and with ERS initial pH 5,7.

	NH_4^+	SO_4^{2-}	NH_4^+ removal
Acid	25%	60%	
Base	48%	0%	
Diluate	34%	42%	66%
ERS	0%	114%	

(c) Final percentage of NH_4^+ and SO_4^{2-} in the acid, base, diluate and ERS stream respectively for a PC 100D BPM (for organic acid production) with CEEM and with ERS initial pH 2,25.

	NH_4^+	SO_4^{2-}	NH_4^+ removal
Acid	21%	69%	
Base	46%	0%	
Diluate	36%	52%	64%
ERS	11%	109%	

(d) Final percentage of NH_4^+ and SO_4^{2-} in the acid, base, diluate and ERS stream respectively for a PC 100D BPM (for organic acid production) with CEEM and with ERS initial pH 5,7.

C.0.3 Anion Exchange End Membrane

Table C.2: Final percentage of NH_4^+ and SO_4^{2-} in the acid, base, diluate and ERS stream respectively for a PC 100D BPM (for organic acid production) with AEEM and with ERS initial pH 2.25.

	NH_4^+	SO_4^{2-}	NH_4^+ removal
Acid	25%	60%	
Base	48%	0%	
Diluate	34%	42%	66%
ERS	0%	114%	

Appendix D LCD Determination

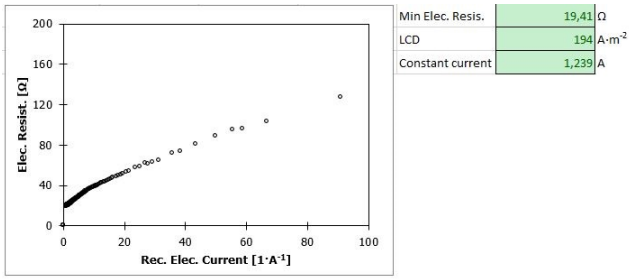

Min Elec. Resis.	19,41	Ω
LCD	194	A·m^{-2}
Constant current	1,239	A

(a) LCD determination experiment 1

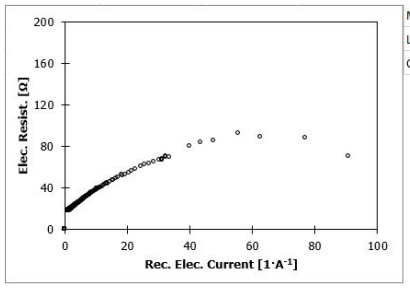

Min Elec. Resis.	17,52	Ω
LCD	196	A·m^{-2}
Constant Current	1,257	A

(b) LCD determination experiment 2

Figure D.1: Data determining the limiting current density used for the BPMED experiments

Appendix E 0 current Experiment

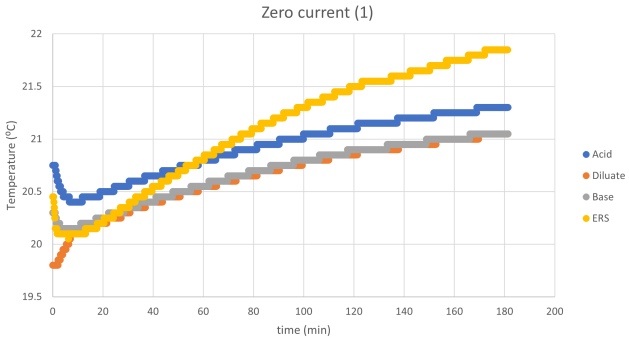

(a) Temperature development experiment 1

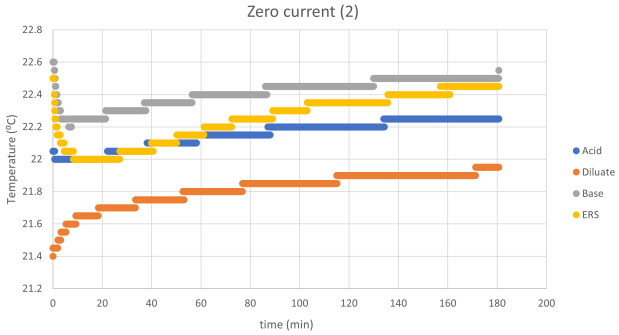

(b) Temperature development experiment 2

Figure E.1: Temperature development over time in solutions for experiments without applied current - blanco experiments

Table E.1: Ammonium and sulfate concentrations at t=0 and t=180 minutes for 2 experiments run without applying current for initial diluate of 50 g/L $(NH_4)_2SO_4$ pH 4 at room temperature. The sulfate concentrations were not corrected.

	Ammonium (mg/L) t = 0	Ammonium (mg/L) t = 180
Acid	407,5	473
Base	365	296
Diluate	13840	12400
ERS	0	46,5
	Sulfate (mg/L)t = 0	**Sulfate (mg/L) t = 180**
Acid	1560	2380
Base	1420	1600
Diluate	39000	33500
ERS	133000	117000

(a) Ammonium and sulfate concentrations at t=0 and t=180 minutes without applying current - experiment 1

	Ammonium (mg/L) t = 0	Ammonium (mg/L) t = 180
Acid	350	466
Base	357,5	346
Diluate	14280	13230
ERS	22,425	41
	Sulfate (mg/L) t = 0	**Sulfate (mg/L) t = 180**
Acid	1480	2380
Base	1420	1680
Diluate	36250	36250
ERS	116000	96000

(b) Ammonium and sulfate concentrations at t=0 and t=180 minutes without applying current - experiment 2

Appendix F Background temperature experiment

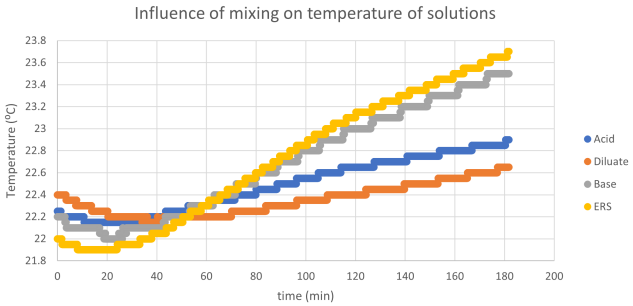

Figure F.1: Evolution of temperature in solutions that were being stirred by the magnetic stirrer only.

Appendix G Voltage development over time

G.1 Experiments on influence of concentration

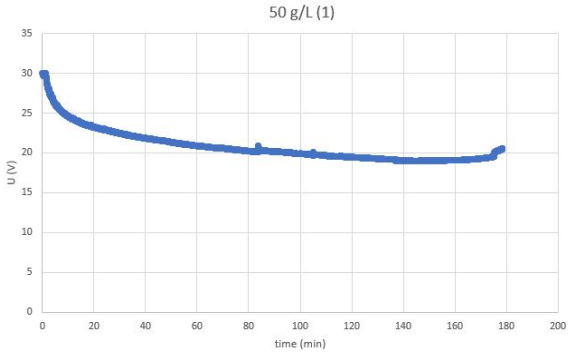

(a) Evolution of potential over time for 50 g/L $(NH_4)_2SO_4$ initial diluate solution with pH 4, duplicate 1.

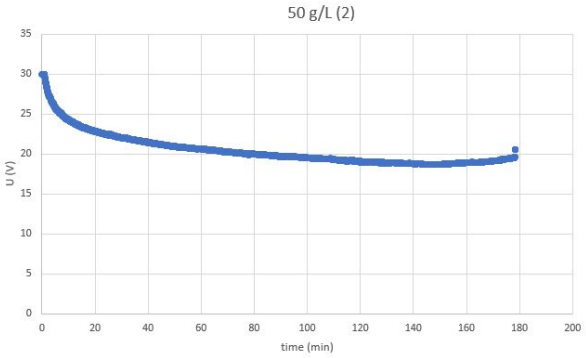

(b) Evolution of potential over time for 50 g/L $(NH_4)_2SO_4$ initial diluate solution with pH 4, duplicate 2.

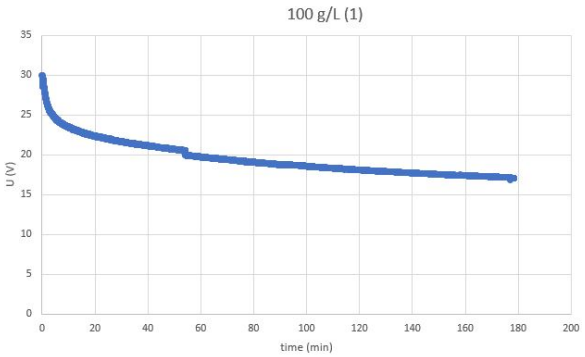

(c) Evolution of potential over time for 100 g/L $(NH_4)_2SO_4$ initial diluate solution with pH 4, duplicate 1.

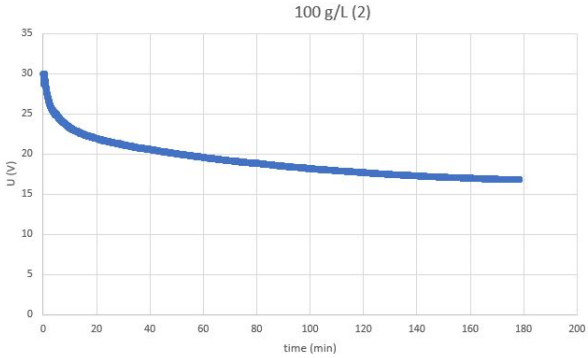

(d) Evolution of potential over time for 100 g/L $(NH_4)_2SO_4$ initial diluate solution with pH 4, duplicate 2.

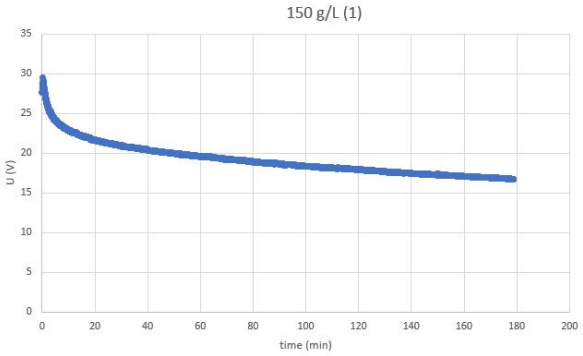

(e) Evolution of potential over time for 150 g/L $(NH_4)_2SO_4$ initial diluate solution with pH 4, duplicate 1.

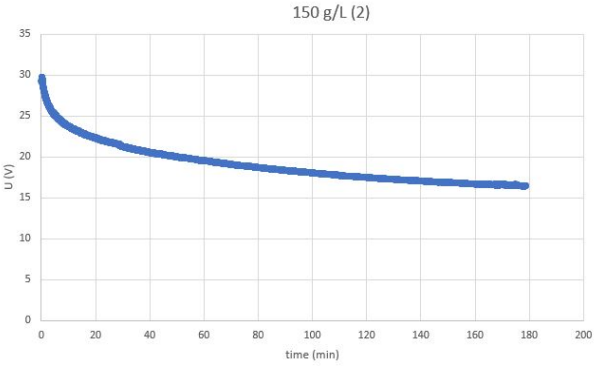

(f) Evolution of potential over time for 150 g/L $(NH_4)_2SO_4$ initial diluate solution with pH 4, duplicate 2.

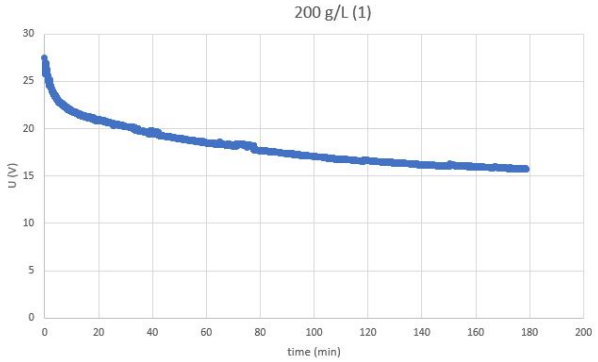

(a) Evolution of potential over time for 200 g/L $(NH_4)_2SO_4$ initial diluate solution with pH 4, duplicate 1.

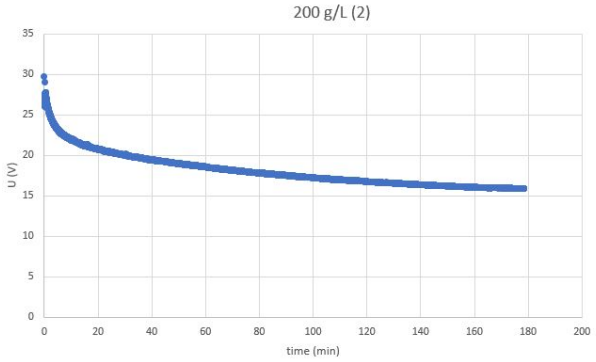

(b) Evolution of potential over time for 200 g/L $(NH_4)_2SO_4$ initial diluate solution with pH 4, duplicate 2.

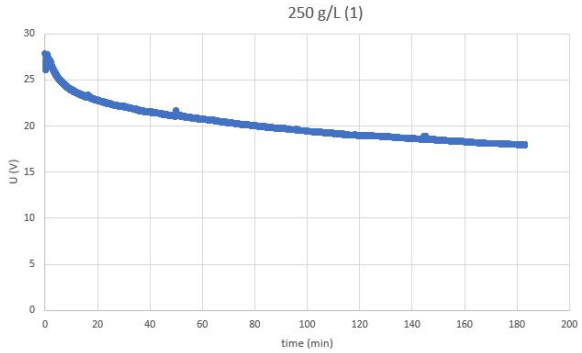

(c) Evolution of potential over time for 250 g/L $(NH_4)_2SO_4$ initial diluate solution with pH 4, duplicate 1.

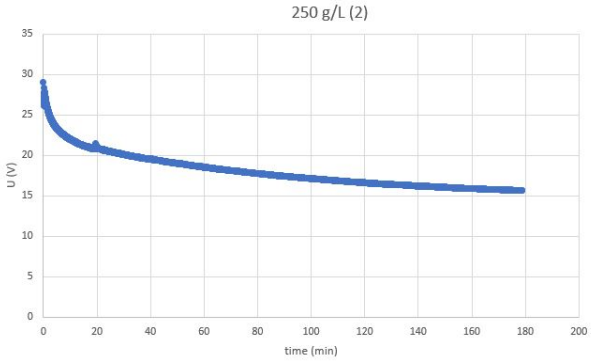

(d) Evolution of potential over time for 250 g/L $(NH_4)_2SO_4$ initial diluate solution with pH 4, duplicate 2.

G.2 Experiments on influence of temperature

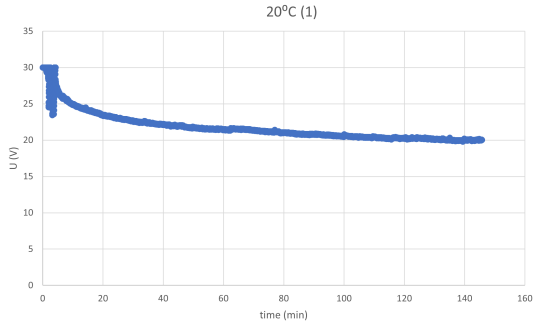

(a) Evolution of potential over time for 50 g/L $(NH_4)_2SO_4$ 293K initial diluate solution with pH 4, duplicate 1.

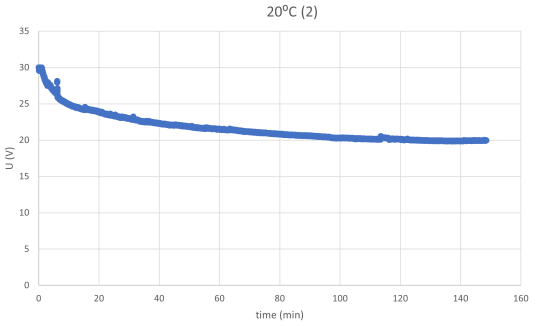

(b) Evolution of potential over time for 50 g/L $(NH_4)_2SO_4$ 293K initial diluate solution with pH 4, duplicate 2.

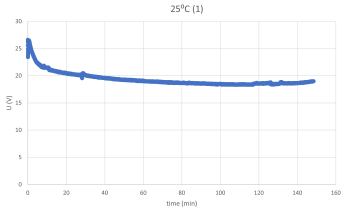

(c) Evolution of potential over time for 50 g/L $(NH_4)_2SO_4$ 298K initial diluate solution with pH 4, duplicate 1.

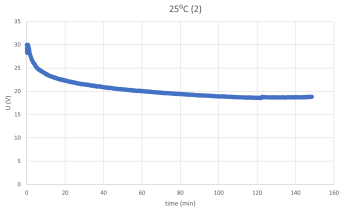

(d) Evolution of potential over time for 50 g/L $(NH_4)_2SO_4$ 298K initial diluate solution with pH 4, duplicate 2.

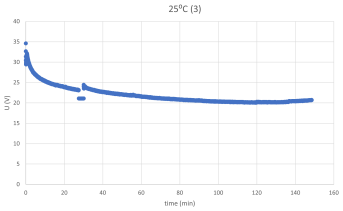

(e) Evolution of potential over time for 50 g/L $(NH_4)_2SO_4$ 298K initial diluate solution with pH 4, duplicate 3.

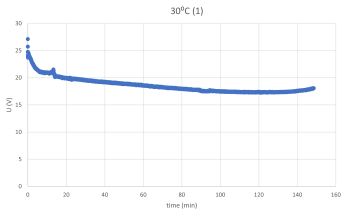

(f) Evolution of potential over time for 50 g/L $(NH_4)_2SO_4$ 303K initial diluate solution with pH 4, duplicate 1.

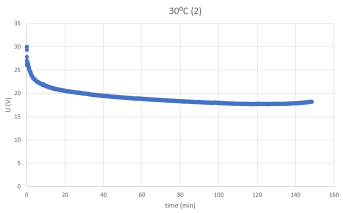

(g) Evolution of potential over time for 50 g/L $(NH_4)_2SO_4$ 303K initial diluate solution with pH 4, duplicate 2.

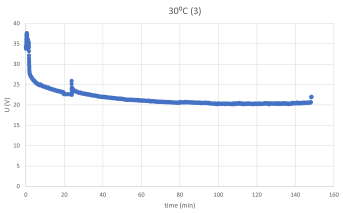

(h) Evolution of potential over time for 50 g/L $(NH_4)_2SO_4$ 303K initial diluate solution with pH 4, duplicate 3.

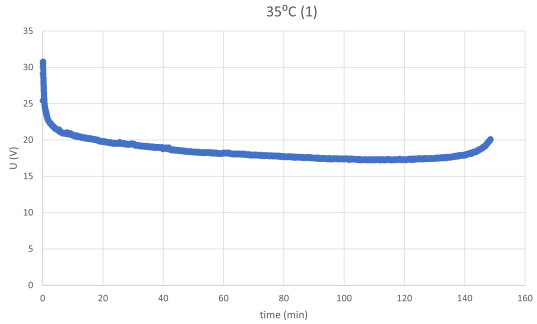

(a) Evolution of potential over time for 50 g/L $(NH_4)_2SO_4$ 308K initial diluate solution with pH 4, duplicate 1.

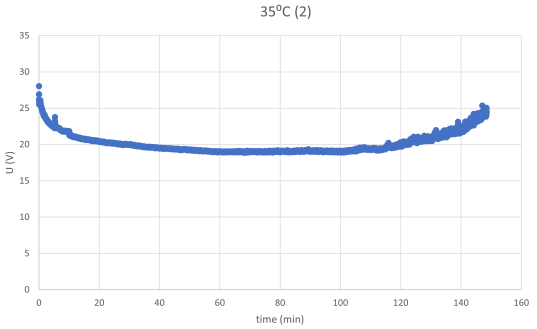

(b) Evolution of potential over time for 50 g/L $(NH_4)_2SO_4$ 308K initial diluate solution with pH 4, duplicate 2.

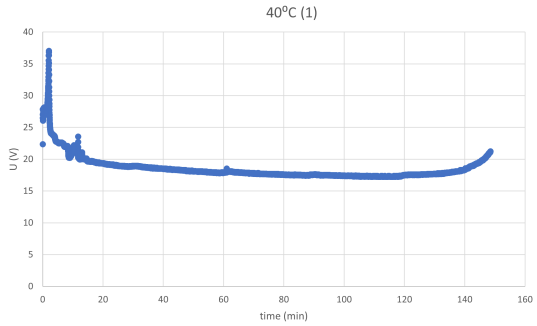

(c) Evolution of potential over time for 50 g/L $(NH_4)_2SO_4$ 313K initial diluate solution with pH 4, duplicate 1.

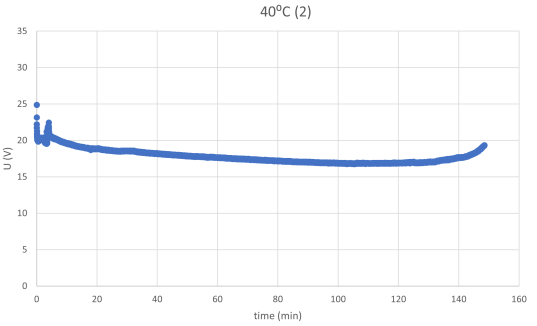

(d) Evolution of potential over time for 50 g/L $(NH_4)_2SO_4$ 313K initial diluate solution with pH 4, duplicate 2.

Appendix H pH and EC evolution

H.0.1 Influence of initial diluate pH - overview of pH and EC evolution over time of the acid, base, diluate and ERS streams

pH 2 (1)

Stream	Final pH	Final EC ($\mu S * cm^{-1}$)
Acid	0.81	$1.22 * 10^5$
Base	10.46	$5.92 * 10^3$
Diluate	2.36	$1.53 * 10^4$
ERS	1.75	$9.62 * 10^4$

pH 2 (2)

Stream	Final pH	Final EC ($\mu S * cm^{-1}$)
Acid	0.8	$1.24 * 10^5$
Base	10.46	$5.93 * 10^3$
Diluate	2.3	$1.62 * 10^4$
ERS	1.58	$9.85 * 10^4$

pH 3 (1)

Stream	Final pH	Final EC ($\mu S * cm^{-1}$)
Acid	0.86	$1.21 * 10^5$
Base	10.48	$6.25 * 10^3$
Diluate	2.48	$8.46 * 10^3$
ERS	1.76	$9.59 * 10^4$

pH 3 (2)

Stream	Final pH	Final EC ($\mu S * cm^{-1}$)
Acid	0.83	$1.19 * 10^5$
Base	10.5	$5.76 * 10^3$
Diluate	2.45	$8.88 * 10^3$
ERS	1.62	$9.32 * 10^4$

pH 4 (1)

Stream	Final pH	Final EC ($\mu S * cm^{-1}$)
Acid	0.87	$1.19 * 10^5$
Base	10.52	$5.82 * 10^3$
Diluate	2.54	$6.63 * 10^3$
ERS	1.88	$9.57 * 10^4$

pH 4 (2)

Stream	Final pH	Final EC ($\mu S * cm^{-1}$)
Acid	0.84	$1.22 * 10^5$
Base	10.51	$6.10 * 10^3$
Diluate	2.46	$6.32 * 10^3$
ERS	1.63	$9.33 * 10^4$

pH 5 (1)

Stream	Final pH	Final EC ($\mu S * cm^{-1}$)
Acid	0.84	$1.20 * 10^5$
Base	10.55	$5.82 * 10^3$
Diluate	2.5	$6.34 * 10^3$
ERS	1.78	$9.60 * 10^4$

pH 5 (2)

Stream	Final pH	Final EC ($\mu S * cm^{-1}$)
Acid	0.87	$1.16 * 10^5$
Base	10.55	$5.83 * 10^3$
Diluate	2.52	$5.49 * 10^3$
ERS	1.66	$9.33 * 10^4$

pH 6 (1)

Stream	Final pH	Final EC ($\mu S * cm^{-1}$)
Acid	0.83	$1.25 * 10^5$
Base	10.49	$6.89 * 10^3$
Diluate	2.44	$7.25 * 10^3$
ERS	1.78	$9.67 * 10^4$

pH 6 (2)

Stream	Final pH	Final EC ($\mu S * cm^{-1}$)
Acid	0.87	$1.21 * 10^5$
Base	10.5	$6.13 * 10^3$
Diluate	2.52	$5.85 * 10^3$
ERS	1.66	$9.38 * 10^4$

pH 7 (1)

Stream	Final pH	Final EC ($\mu S * cm^{-1}$)
Acid	0.9	$1.18 * 10^5$
Base	10.46	$5.97 * 10^3$
Diluate	2.51	$5.98 * 10^3$
ERS	1.78	$9.40 * 10^4$

pH 7 (2)

Stream	Final pH	Final EC ($\mu S * cm^{-1}$)
Acid		$1.19 * 10^5$
Base		$6.09 * 10^3$
Diluate		$4.80 * 10^3$
ERS	1.63	$9.21 * 10^4$

pH 8 (1)

Stream	Final pH	Final EC ($\mu S * cm^{-1}$)
Acid	0.94	$1.19 * 10^5$
Base	10.36	$7.64 * 10^3$
Diluate	2.59	$4.65 * 10^3$
ERS	1.78	$9.56 * 10^4$

pH 8 (2)

Stream	Final pH	Final EC ($\mu S * cm^{-1}$)
Acid	0.87	$1.23 * 10^5$
Base	10.42	$6.42 * 10^3$
Diluate	2.44	$8.41 * 10^3$
ERS	1.61	$9.34 * 10^4$

pH 9 (1)

Stream	Final pH	Final EC ($\mu S * cm^{-1}$)
Acid	1	$1.17 * 10^5$
Base	10.52	$6.46 * 10^3$
Diluate	5.46	$3.57 * 10^3$
ERS	1.76	$9.53 * 10^4$

pH 9 (2)

Stream	Final pH	Final EC ($\mu S * cm^{-1}$)
Acid	0.99	$1.19 * 10^5$
Base	10.38	$7.67 * 10^3$
Diluate	2.88	$5.21 * 10^3$
ERS	1.62	$9.29 * 10^4$

pH 10 (1)

Stream	Final pH	Final EC ($\mu S * cm^{-1}$)
Acid	1.89	$9.45 * 10^4$
Base	10.62	$7.05 * 10^3$
Diluate	11.55	923
ERS	1.97	$9.25 * 10^4$

pH 10 (2)

Stream	Final pH	Final EC ($\mu S * cm^{-1}$)
Acid	1.72	$9.47 * 10^4$
Base	10.65	$6.54 * 10^3$
Diluate	11.54	932
ERS	1.9	$8.80 * 10^4$

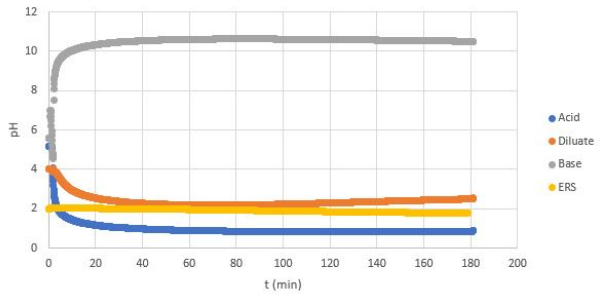

(a) Evolution of pH over time in the acid-, base-, and diluatestream for 50 g/L $(NH_4)_2SO_4$ initial diluate solution with pH 4, duplicate 1.

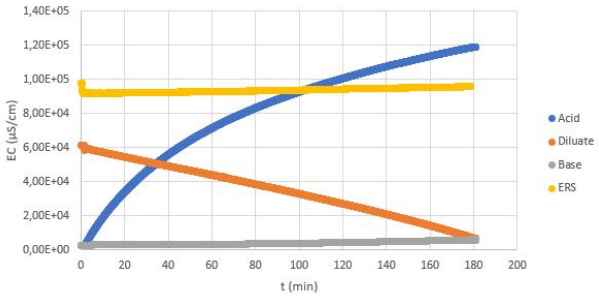

(b) Evolution of EC over time in the acid-, base-, and diluatestream for 50 g/L $(NH_4)_2SO_4$ initial diluate solution with pH 4, duplicate 1.

Figure H.1: EC and pH data for initial diluate concentrations pH 4

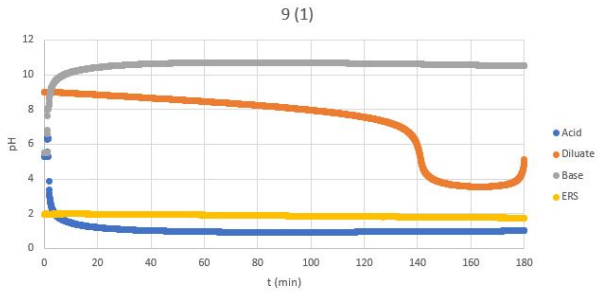

(a) Evolution of pH over time in the acid-, base-, and diluatestream for 50 g/L $(NH_4)_2SO_4$ initial diluate solution with pH 9, duplicate 1.

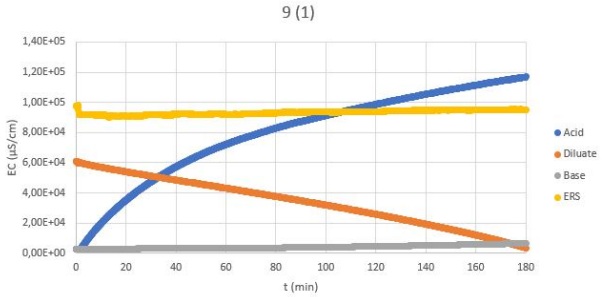

(b) Evolution of EC over time in the acid-, base-, and diluatestream for 50 g/L $(NH_4)_2SO_4$ initial diluate solution with pH 9 , duplicate 1.

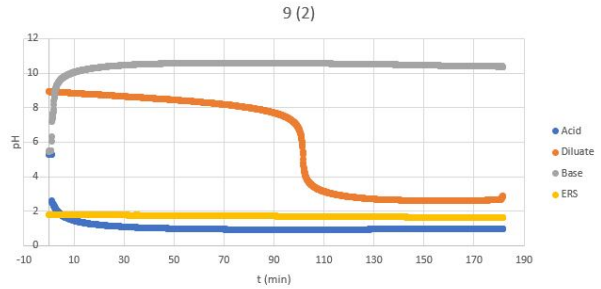

(c) Evolution of pH over time in the acid-, base-, and diluatestream for 50 g/L $(NH_4)_2SO_4$ initial diluate solution with pH 9, duplicate 2.

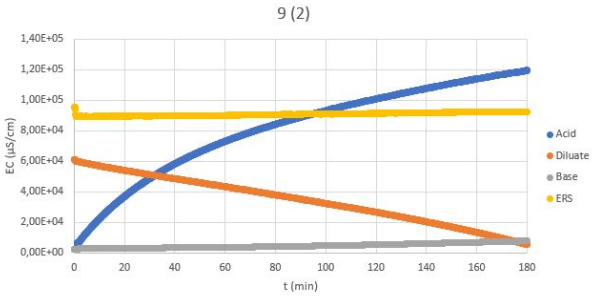

(d) Evolution of EC over time in the acid-, base-, and diluatestream for 50 g/L $(NH_4)_2SO_4$ initial diluate solution with pH 9, duplicate 2.

Figure H.2: EC and pH data for initial diluate concentrations pH 9

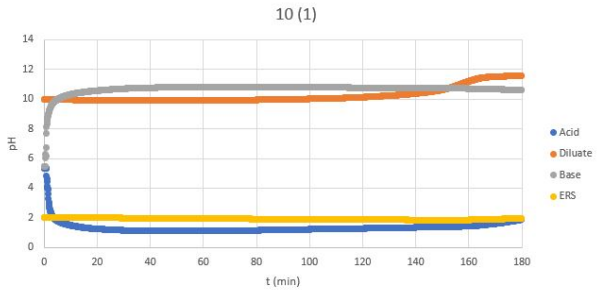

(a) Evolution of pH over time in the acid-, base-, and diluatestream for 50 g/L $(NH_4)_2SO_4$ initial diluate solution with pH 10, duplicate 1.

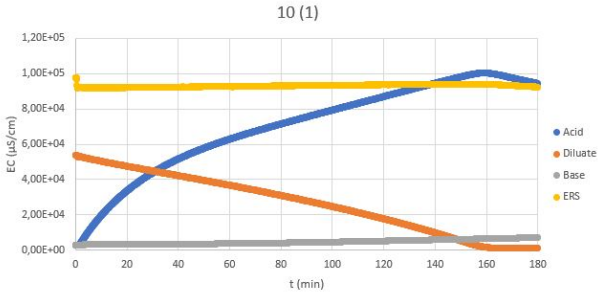

(b) Evolution of EC over time in the acid-, base-, and diluatestream for 50 g/L $(NH_4)_2SO_4$ initial diluate solution with pH 10, duplicate 1.

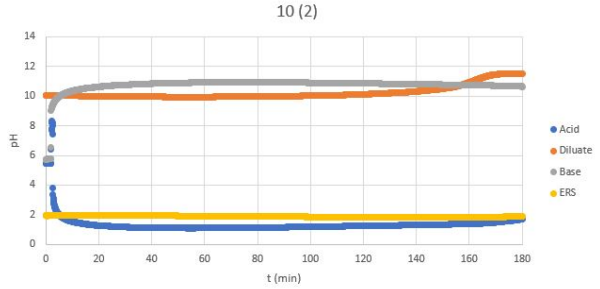

(c) Evolution of pH over time in the acid-, base-, and diluatestream for 50 g/L $(NH_4)_2SO_4$ initial diluate solution with pH 10, duplicate 2.

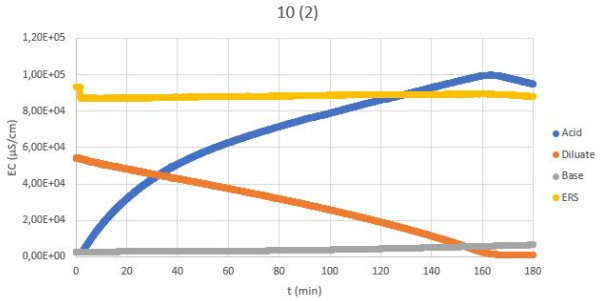

(d) Evolution of EC over time in the acid-, base-, and diluatestream for 50 g/L $(NH_4)_2SO_4$ initial diluate solution with pH 10, duplicate 2.

Figure H.3: EC and pH data for initial diluate concentrations pH 10

H.0.2 Influence of initial diluate concentration

50 (1) g/L $(NH_4)_2SO_4$

Stream	Final pH	Final EC ($\mu S * cm^{-1}$)
Acid	0.87	$1.19 * 10^5$
Base	10.52	$5.82 * 10^3$
Diluate	2.54	$6.63 * 10^3$
ERS	1.88	$9.57 * 10^4$

50 (2) g/L $(NH_4)_2SO_4$

Stream	Final pH	Final EC ($\mu S * cm^{-1}$)
Acid	0.84	$1.22 * 10^5$
Base	10.51	$6.10 * 10^3$
Diluate	2.46	$6.32 * 10^3$
ERS	1.63	$9.33 * 10^4$

100 (1) g/L $(NH_4)_2SO_4$

Stream	Final pH	Final EC ($\mu S * cm^{-1}$)
Acid	0.96	$1.15 * 10^5$
Base	10.39	$6.56 * 10^3$
Diluate	2.29	$6.46 * 10^4$
ERS	1.71	$9.52 * 10^4$

100 (2) g/L $(NH_4)_2SO_4$

Stream	Final pH	Final EC ($\mu S * cm^{-1}$)
Acid	0.98	$1.12 * 10^5$
Base	10.4	$7.00 * 10^3$
Diluate	2.41	$6.50 * 10^4$
ERS	1.58	$9.34 * 10^4$

150 (1) g/L $(NH_4)_2SO_4$

Stream	Final pH	Final EC ($\mu S * cm^{-1}$)
Acid	1.01	$1.12 * 10^5$
Base	10.42	$7.63 * 10^3$
Diluate	2.57	$1.06 * 10^5$
ERS	1.73	$9.56 * 10^4$

150 (2) g/L $(NH_4)_2SO_4$

Stream	Final pH	Final EC ($\mu S * cm^{-1}$)
Acid	1.03	$1.10 * 10^5$
Base	10.43	$7.52 * 10^3$
Diluate	2.67	$1.06 * 10^5$
ERS	1.6	$9.37 * 10^4$

200 (1) g/L $(NH_4)_2SO_4$

Stream	Final pH	Final EC ($\mu S * cm^{-1}$)
Acid	1.03	$1.13 * 10^5$
Base	10.36	$9.48 * 10^3$
Diluate	2.74	$1.35 * 10^5$
ERS	1.74	$9.53 * 10^4$

200 (2) g/L $(NH_4)_2SO_4$

Stream	Final pH	Final EC ($\mu S * cm^{-1}$)
Acid	1.04	$1.11 * 10^5$
Base	10.4	$8.54 * 10^3$
Diluate	2.82	$1.38 * 10^5$
ERS	1.62	$9.36 * 10^4$

250 (1) g/L $(NH_4)_2SO_4$

Stream	Final pH	Final EC ($\mu S * cm^{-1}$)
Acid	1.04	$1.13 * 10^5$
Base	10.42	$8.47 * 10^3$
Diluate	2.89	$1.64 * 10^5$
ERS	1.73	$9.59 * 10^4$

250 (2) g/L $(NH_4)_2SO_4$

Stream	Final pH	Final EC ($\mu S * cm^{-1}$)
Acid	1.06	$1.09 * 10^5$
Base	10.37	$9.74 * 10^3$
Diluate	3.1	$1.66 * 10^5$
ERS	1.61	$9.37 * 10^4$

H.0.3 Influence of initial diluate temperature

20°C (1)

Stream	Final pH	Final EC ($\mu S * cm^{-1}$)
Acid	0.94	$1.11 * 10^5$
Base	10.48	$5.21 * 10^3$
Diluate	2.32	$1.75 * 10^4$
ERS	1.81	$9.44 * 10^4$

20°C (2)

Stream	Final pH	Final EC ($\mu S * cm^{-1}$)
Acid	0.92	$1.14 * 10^5$
Base	10.56	$4.94 * 10^3$
Diluate	2.28	$1.86 * 10^4$
ERS	1.63	$9.28 * 10^4$

25°C (1)

Stream	Final pH	Final EC ($\mu S * cm^{-1}$)
Acid	1	$1.03 * 10^5$
Base	10.17	$6.27 * 10^3$
Diluate	2.48	$1.40 * 10^4$
ERS	1.86	$9.40 * 10^4$

25°C (2)

Stream	Final pH	Final EC ($\mu S * cm^{-1}$)
Acid	1	$1.02 * 10^5$
Base	10.23	$5.42 * 10^3$
Diluate	2.59	$1.35 * 10^4$
ERS	1.73	$9.09 * 10^4$

25°C (3)

Stream	Final pH	Final EC ($\mu S * cm^{-1}$)
Acid	1.02	$1.04 * 10^5$
Base	10.4	$5.02 * 10^3$
Diluate	2.43	$1.57 * 10^4$
ERS*	1.9	$9.38 * 10^4$

*Freshly made ERS solution

30°C (1)

Stream	Final pH	Final EC ($\mu S * cm^{-1}$)
Acid	1.04	$1.01 * 10^5$
Base	9.87	$8.66 * 10^3$
Diluate	2.67	$9.74 * 10^3$
ERS	1.9	$9.32 * 10^4$

30°C (2)

Stream	Final pH	Final EC ($\mu S * cm^{-1}$)
Acid	1.05	$9.80 * 10^4$
Base	10.7	$5.79 * 10^3$
Diluate	2.72	$1.20 * 10^4$
ERS	1.78	$8.92 * 10^4$

30°C (3)

Stream	Final pH	Final EC ($\mu S * cm^{-1}$)
Acid	1.18	$9.37 * 10^4$
Base	10.2	$2.53 * 10^3$
Diluate	8.77	$1.06 * 10^4$
ERS*	1.98	$9.33 * 10^4$

*Freshly made ERS solution

35°C (1)

Stream	Final pH	Final EC ($\mu S * cm^{-1}$)
Acid	1.12	$9.27 * 10^4$
Base	10.36	$6.26 * 10^3$
Diluate	5.21	$9.45 * 10^3$
ERS	1.98	$9.28 * 10^4$

35°C (2)

Stream	Final pH	Final EC ($\mu S * cm^{-1}$)
Acid	1.22	$8.54 * 10^4$
Base	9.99	$5.94 * 10^3$
Diluate	8.85	$8.18 * 10^3$
ERS*	2.07	$9.18 * 10^4$

*Freshly made ERS solution

40°C (1)

Stream	Final pH	Final EC ($\mu S * cm^{-1}$)
Acid	1.22	$8.45 * 10^4$
Base	9.91	$6.27 * 10^3$
Diluate	8.4	$7.73 * 10^3$
ERS	2.07	$9.11 * 10^4$

40°C (2)

Stream	Final pH	Final EC ($\mu S * cm^{-1}$)
Acid	1.2	$8.79 * 10^4$
Base	9.81	$6.36 * 10^3$
Diluate	8.21	$8.12 * 10^3$
ERS	2.01	$8.78 * 10^4$